DISSERTATION

Submitted to the

Combined Faculties of the Natural Science and Mathematics

of the Ruperto-Carola University of Heidelberg, Germany

for the degree of

Doctor of Natural Science

presented by

Master of Science Hanna Henrika Ahlgren

born in: Helsinki, Finland

Oral-examination:……...

TITLE

NMDA receptor mediated contribution to neuronal cell death - an *in vitro* evaluation.

Referees: Prof. Dr. Hilmar Bading

Prof. Dr. Christoph Schuster

Mammalle

Acknowledgements

During my PhD I have had the extraordinary opportunity to perform my work in three different laboratories and in two different countries. My first three years of PhD I also participated the Marie Curie Cortex PhD network that was a great experience and allowed me to meet talented fellow PhD students across the Europe. I want to thank everyone, friends and fellow scientist, who has contributed to my advancement and made this thesis possible.

I want to thank the following institutions for funding my PhD position and research: Marie Curie Cortex PhD network, The Letten foundation, European Research Council (ERC), Sonderforschungsbereich 488 (DFG) and Bernstein BCCN HD/MA (BMBF).

In Oslo University I want express my profound gratitude to Prof. Dr. Ole Petter who has been a very generous, and scientifically and professionally inspiring group leader and boss. I want to thank all my colleagues at Ottersen lab who contributed to advancement of this work, especially Dr. Elise Runden-Pran for introducing me to the organotypic slice cultures. M.Sc. Marianne Vaadal, M.Sc. Nadia Nabil Haj-Yasein, Dr. Jan Gunnar Sorbo, M.Sc. Kristi Henjum and Dr. Maria-Niki Mylonakou I want to thank for their warm and supportive friendship during rough waters. Furthermore, I am grateful for the generous hospitality Dr. Maria-Niki Mylonakou has shown. I want to thank M.Sc. Bjorg Riber, Karen Marie Gujord, Jorunn Knutsen for their warmness and for providing excellent technical assistance and Dr Johannes Helm always helping with all kind of problems. I want to thank all present and previous fellow scientists at Ottersen lab that contributed in creating a scientific, and additionally a pleasant, working atmosphere. Foremost, I want to express my deepest gratitude for the two persons whose support and belief in me made me reach my goal. Prof. Dr. Eric Rinvik is a remarkable person and professional who I have had have the great privilege to have not only as a supervisor but also as an honest, encouraging mentor and friend. Dr. Oivind Hvalby has always been a generous, fair and supportive supervisor who has made me feel comfortable in scientific issues.

I want to thank Dr. Avi Ring at FFI for collaboration and for a positive and encouraging attitude.

In Heidelberg University I want to express my foremost gratitude to Prof. Dr. Hilmar Bading for giving me the opportunity to work at his excellent group. I am

deeply grateful for his stimulating, positive supervision, shared with his vast scientific knowledge. I want to thank previous and present colleagues and friends at Bading lab and Ciccolini lab members for making me feel immediately welcome and sharing fun time outside lab, especially Dr. Daniela Mauceri who has shown generous hospitality also outside lab surroundings and Dr. Eckehard Freitag for his warm friendship. I want to thank the participants of the IZN tour 2011 for lots of fun and good times! I am deeply grateful to Dr. Ana Oliveira for all the scientific discussions and for her honest and supportive friendship at all times. I want to thank all lab members, previous and present, for helping me with scientific questions and supporting me to develop my scientific skills, creating a very inspiring working atmosphere. I want to thank everyone who has contributed to my advancement and made this thesis possible. I want to thank Dr. Peter Bengtson for thorough proof reading and commenting my thesis, M.Sc. Thekla Helmstedt and Dr. Bettina Buchtal for helping me with the German summary translation. I am grateful to Iris Bünzli-Ehret for providing excellent neuronal cultures.

I am extremely grateful to Prof. Dr. Peter Seeburg at Max Planck Institute for Medical Research, Heidelberg for helpful discussion and comments on my first manuscript.

I want to thank all my friends who have stayed in touch throughout my years of exile and visited me. I want to express my gratitude to M.A. Linda Loikkanen and M.D. Riikka Gunnar for their encouragement and for always being there in every aspect of life, and to M.Phil. Sarah (Kitaen) Keating for an inspiring and encouraging friendship. Dr. Gustavo Acuna I want to thank for his support during the writing process and for offering his straightforward perspective in issues troubling my mind.

Lastly, and most importantly, I want to thank my family with all the extended members and animals for always being there. My every visit home gave me the very much-needed calibration to normality. Especially I want to thank my mother, M. Sc. Iris Ahlgren, for her love and support and believing in me throughout the years.

TABLE OF CONTENTS

LIST OF FIGURES

CHAPTER 1 SUMMARY

Brain ischemia is one of the leading causes of death and disability in the world with enormous socioeconomic consequences annually, however to date, despite multiple studies, the only clinically available remedy is the thrombolytic tissue plasminogen activator (tPa). The development of new therapeutic interventions/strategies requires a deeper insight into the pathology, which can only come from better characterization of ischemic models and usage of appropriate parameters to evaluate neuronal damage.

The usage of a right model and cell death assay is essential for an effective translation to *in vivo* and clinical studies. Organotypical hippocampal slice cultures offer an *in vitro* model to study brain ischemia by induction of oxygen and glucose deprivation (OGD). In organotypic hippocampal slice cultures the interaction between neuronal and non-neuronal cells are well preserved and intrinsic connections of the hippocampal structure are largely maintained. However, there is scant data regarding the expression and functionality of *N*-Methyl-D-aspartate receptors (NMDARs) in such slice cultures. NMDARs, which are essential mediators of synaptic plasticity under normal physiological conditions, are during brain ischemia excessively activated due to glutamate overflow and mediate excitotoxic cell death. The aim of the first part of my thesis was thus to evaluate the expression of NR1, NR2A and NR2B and their contribution to excitotoxic cell death after exposure to NMDA or OGD in organotypical hippocampal slices cultures after 14 days *in vitro* (DIV14). OGD induced the typical ischemic injury damage as it is delayed and most pronounced in the hippocampus cornu ammonis (CA) 1 pyramidal neurons. This study revealed that NR1, NR2A and NR2B subunits were expressed at DIV14 and contributed to cell death, as shown by use of the NMDAR antagonist MK-801 (dizocilpine). Excitotoxic cell death induced by NMDA was antagonized by 10 μM MK-801, a dose that offered only partial protection against OGD-induced cell death. High concentrations of MK-801 (50–100 μM) were required to counteract delayed cell death (48–72 h) after OGD. The higher dose of MK-801 needed for protection against this delayed phase of OGD-induced death could not be attributed to down-regulation of NMDARs at the gene expression level. Additionally, I found that NR2B-subunits did not contribute to NMDA-or OGD-induced cell death at DIV14 and that NR2B possibly is post-translationally modified under normal physiological

conditions. My data indicate that NMDAR signaling is just one of several mechanisms underlying ischemic cell death and that prospective cytoprotective therapies must be directed to multiple targets.

Another important aspect to be taken in consideration in studies aimed to discover cytoprotective agents are the parameters used for evaluation. Most studies evaluate neuronal survival from nuclear damage, which reflects the final stage of cell death and lacks information about neuronal function. The aim of the second part of my thesis was to investigate more subtle changes in neurons prior to cell death by assessing dendritic damage and furthermore to characterize the functionality of these neurons using electrophysiological recordings. Dendritic damage, manifesting as focal swellings of dendrites (beadings), is an early morphological hallmark of neuronal damage and has been described in a variety of pathological conditions including brain ischemia. Protection against dendritic beading is likely to reduce later neuronal damage. NMDARs are involved in mediating also cell survival, not only cell death. Increased synaptic activity triggers Ca^{2+} influx via synaptic NMDAR receptors that activates a gene transcription dependent acquired neuroprotection program. Here I show that increased synaptic activity protects, in a transcription and partly nuclear calcium dependent manner, against dendritic damage. Increased synaptic activity induced gene program for acquired neuroprotection includes activating transcription factor 3 (ATF3). I show additionally that overexpression of ATF3 protects against NMDA-induced dendritic damage in line with its known protection against neuronal death. Furthermore, the protected dendrites are functional indicated by the restoration of synaptic transmission-dependent network activity within 48 h of an otherwise toxic NMDA insult. I conclude that ATF3 is a robust neuroprotective gene offering protection against acute neuronal injury and hence improving the functional outcome after neuronal damage.

CHAPTER 2 ZUSAMMENFASSUNG

Die zerebrale Ischämie ist weltweit eine der führenden Krankheits- und Todesursachen mit weitreichenden sozioökonomischen Auswirkungen. Trotz vielfacher Studien gibt es jedoch bis heute nur den trombolytischen Gewebe Plasminogen Aktivator (tPA) als klinisch verfügbares Heilmittel. Die Entwicklung neuer therapeutischer Interventionen/Strategien verlangt ein besseres Verständnis der Pathologie, die nur durch eine bessere Charakterisierung der Ischämiemodelle und entsprechender Parameter zur Beurteilung einer neuronalen Schädigung erlangt werden kann.

Die Verwendung des richtigen Modells und eine Bestimmung des Zelltods sind für eine wirksame Umsetzung in *in vivo* Bedingungen und klinischen Studien notwendig. Organotypische hippokampale Schnitt-Kulturen stellen ein *in vitro* Modell dar, um die Ischämie des Gehirns durch die Induktion des Entzugs von Sauerstoff und Glucose (OGD) zu studieren. In organotypischen hippokampalen Schnitt-Kulturen wird die Wechselwirkung zwischen neuronalen und nicht-neuronalen Zellen gut bewahrt und intrinsische Verbindungen der hippokampelen Struktur werden größtenteils aufrechterhalten. Jedoch gibt es gibt nur spärliche Daten bezüglich der Expression und der Funktionalität der N-Methyl-D-Aspartat-Rezeptoren (NMDAR) in solchen Schnitt-Kulturen. NMDAR, welche unter normalen physiologischen Bedingungen die wesentlichen Vermittler der synaptischer Plastizität sind, werden während einer Ischämie des Gehirns übermäßig durch eine Glutamat-Überschwemmung aktiviert und erzeugen einen exzitotoxischen Zelltod. Das Ziel des ersten Teils meiner Arbeit befasst sich mit der Bestimmung der Expression von NR1, NR2A und NR2B und deren Beitrag zum exzitotoxischen Zelltod nach Behandlung mit NMDA oder OGD in organotypischen hippokampalen Schnitt-Kulturen nach 14 Tagen *in vitro* (DIV14). OGD führte zu typisch ischämischen Verletzungen, da er verzögert und am ausgeprägtesten in den pyramidalen Neuronen im Hippocampus Cornu Ammonic (CA) 1 auftritt. Diese Studie zeigte, dass durch die Verwendung des NMDAR Antagonisten MK-801 (dizocilpine), NR1-, NR2A- und NR2B-Untereinheiten an DIV14 expremiert werden und zum Zelltod beitragen. Durch NMDA verursachter exzitotoxischer Zelltod wurde mit 10 µM MK-801 antagonisiert, einer Dosierung die gegen den OGD-veranlassten Zelltod nur teilweise Schutz bot. Um einem verzögertem Zelltod (48-72 Stunden) nach OGD entgegenzuwirken waren

hohe Konzentrationen von MK-801 (50-100 µM) erforderlich. Die höhere Dosierung von MK-801, welche für den Schutz für diese verzögerte Phase des OGD-induzierten Zelltodes erforderlich ist, konnte nicht einer Herunterregulation der NMDAR auf Genexpressionsebene zugeschrieben werden. Des Weiteren habe ich herausgefunden, dass NR2B-Untereinheiten nicht zu NMDA-oder OGD veranlassten Zelltod an DIV14 beitrugen und dass NR2B möglicherweise posttranslational unter normalen physiologischen Bedingungen modifiziert wird. Meine Daten deuten darauf hin, dass die NMDAR Signalwirkung nur eine von mehreren Mechanismen bei ischämischem Zelltod und zukünftigen zytoprotektive Therapien darstellt.

Ein wichtiger Aspekt, der bei Studien zur Entdeckung zytoprotektiver Wirkstoffe berücksichtigt werden sollte, ist die Auswahl der Parameter die zur Evaluierung der Daten verwendet werden. Die meisten Studien bewerten das Überleben von Neuronen anhand der Schädigung des Zellkerns, welches das Endstadium des Zelltods wiederspiegelt und Informationen über die neuronalen Funktion vorenthält. Das Ziel des zweiten Teils meiner Arbeit war es anhand von dendritischen Schäden die genauere Veränderungen in Neuronen vor dem Zelltod zu untersuchen. Des Weiteren wurde die Funktionalität dieser Neurone mit Hilfe von elektrophysiologischen Messungen charakterisiert. Dendritische Schädigung, die sich als eine fokale Schwellung der Dendriten (so genannte Beadings) äußert, ist ein frühes morphologisches Kennzeichen von neuronaler Schädigung und wurde bereits in einer Reihe von pathologischen Zuständen, einschließlich der zerebralen Ischämie, beschrieben. Der Schutz vor einer fokalen Schwellung der Dendriten führt wahrscheinlich zur Reduktion späterer neuronaler Schädigung. NMDAR sind nicht nur bei Prozessen des Zelltods beteiligt, sie spielen auch bei Prozessen die zum Überleben von Zellen führen eine Rolle. Erhöhte synaptische Aktivität erzeugt Kalzium Einstrom via synaptischen NMDA Rezeptoren, wodurch ein Gen transkripionabhängiges erworbenes Neuroprotektionsprogramm aktiviert wird. Hier zeige ich, dass eine erhöhte synaptische Aktivität in einer transkriptionsabhängigen und teilweise durch nukleären Kalzium bedingten Weise gegen dendritische Schädigung schützt. Genprogramme für eine erworbene Neuroprotektion, die durch erhöhte synaptische Aktivität induziert werden, schließen die Aktivierung des Transkriptionsfaktors 3 (ATF3) mit ein. Zusätzlich zeige ich, dass eine Überexpremierung von ATF3 gegen eine NMDA-induzierte dendritische Schädigung

schützt. Dies stimmt mit dem bereits bekannten Schutz gegen neuronalen Zelltod überein. Des Weiteren sind die geschützten Dendriten funktional, welches durch die Wiederherstellung der transmissionsabängigen Netzwerkaktivität innerhalb von 48 Stunden von einem ansonsten toxischen NMDA Insult angezeigt wird. Ich folgere daraus, dass ATF3 ein robustes, neuroprotektives Gen ist, welches einen Schutz gegen eine akute neuronale Verletzung bietet und somit das funktionale Ergebnis nach einer neuronalen Schädigung verbessert.

CHAPTER 3 INTRODUCTION AND AIMS

3.1 BRAIN ISCHEMIA

Stroke is the third most prevalent cause of death and the primary catalyst for acquired disabilities in developed countries, having extensive socioeconomic consequences annually (Albers et al., 2011; Goldstein et al., 2011; Green and Shuaib, 2006). Stroke is divided into two categories, ischemic and hemorrhagic, with ischemic stroke making up approximately 87% of all the cases (Doyle et al., 2008). Ischemic stroke results when a blood clot, either an embolus or a thrombosis, occludes a cerebral artery resulting in a transient or permanent reduction in local cerebral blood flow. The reduced blood flow limits the availability of oxygen and glucose that is needed to support the neuronal cellular homeostasis (Dirnagl et al., 1999). The only treatment for brain ischemia is intravenous tissue-type plasminogen activator therapy (tPA), which may dissolve the blood clot and restore local circulation. The draw-back of tPA is the narrow symptom onset-to-treatment interval (up to 4.5h) (Albers et al., 2011) and the lack of cytoprotective properties.

The ischemic brain region may be divided into two regions that are affected by the degree and the duration of ischemia: the core and the penumbra. The ischemic core area is characterized by a severely impaired blood flow and a fast irreversible neuronal damage and necrosis. The penumbra region lies between the core region and the unaffected brain region. Penumbra neurons have a partially preserved energy metabolism as nutrients and oxygen are supplied from collateral arteries (Hossmann, 1994). The ischemic core can spread into penumbra region by apoptotic signaling cascades. Neurons in the penumbra area are also subjected to peri-infarct depolarizations (PIDs), which are repetitive depolarizations caused by the released K^+ and excitatory amino acids from cells in the ischemic core. As the number of depolarizations increases, more energy is depleted enlarging the ischemic core. (Fig 1.) (Dirnagl et al., 1999; Dreier, 2011). Therefore, penumbra neurons are the main target for acute ischemic therapy.

Anaerobic metabolism and acidosis are hallmarks of brain ischemia due to the reduced oxygen accessibility. Neuronal energy production via anaerobic glycolysis produces an accumulation of lactate and H^+ (Katsura et al., 1994) causing the

extracellular and intracellular pH fall to 6.0-6.5 (Nedergaard et al., 1991; Silver and Erecinska, 1992).

Brain ischemia is also associated with oedema, an imbalance in the distribution of water in the injured brain. Cerebral ischemia initially produces cytotoxic oedema, which is characterized by a decrease of the extracellular space (Simard et al., 2007) and swelling of all types of brain cells, although the most prominent swelling occurs in the astrocytes (Amiry-Moghaddam and Ottersen, 2003). The blood-brain-barrier (BBB) is still intact during cytotoxic oedema (Klatzo, 1994), however, the subsequent vasogenic oedema (Klatzo, 1994) is characterized by increasing extracellular space and disrupted BBB due to severe alterations in endothelial functions.

Acute cell death, delayed cell death and cytotoxic oedema induced by brain ischemia do all have a common initiation point: excitotoxicity.

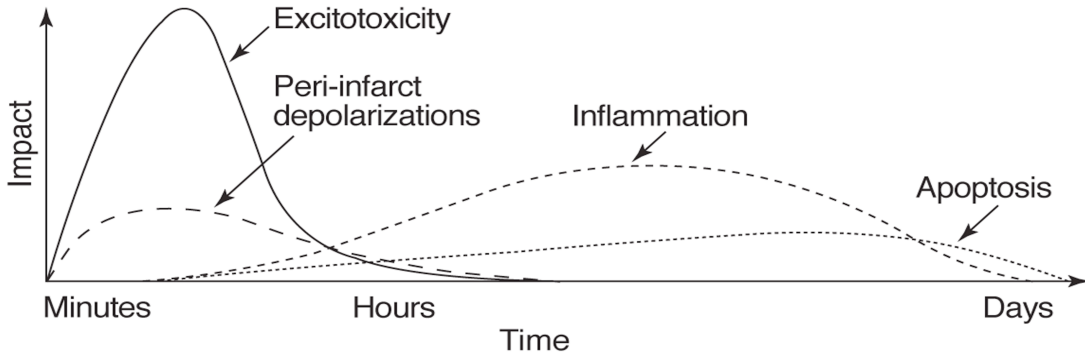

Figure 1. Ischemic events contributing to neuronal damage. The plot reflects the approximate impact of various phases of ischemia on the final brain damage outcome. The abscissa indicates time after an ischemic damage whereas the ordinate shows the impact of each damaging event on the final outcome. Excitotoxicity occurs during the first minutes after blood flow cessation but has the highest impact on neuronal damage by triggering acute necrosis, peri-infarct depolarizations and delayed responses as apoptosis. (Figure from Dirngal et al., 1999).

3.1.1 Excitotoxicity

In higher concentrations, glutamate, the most abundant excitatory neurotransmitter in the mammalian central nervous system, is toxic (Lucas and Newhouse, 1957). The term excitotoxicity, which refers to this glutamate toxicity, was introduced by Olney in 1969 (Olney, 1969). Excitotoxicity occurs in many neuropathological conditions, one of the most studied being glutamate toxicity taking

place in brain ischemia (Jorgensen and Diemer, 1982). Excitotoxicity elicits acute cell death and triggers molecular events leading to delayed cell death, and is assumed to account for much of the neuron loss during brain ischemia (Fig. 1) (Dirnagl et al., 1999). Acidosis and cytotoxic oedema take place concurrently, further exacerbating the excitotoxic damage.

Excitotoxicity is initiated by the lack of oxygen and/or glucose required for oxidative phosphorylation, causing a stop in adenosine triphosphate (ATP) production. The trans-plasmamembrane ion gradient is maintained by ATP dependent pumps and thus can no longer be maintained, resulting in loss of the membrane potential and in anoxic depolarization of neurons and glia (Katsura et al., 1994; Meldrum et al., 1985). Anoxic depolarization leads to a massive glutamate release (Lipton and Rosenberg, 1994; Meldrum et al., 1985), an overstimulation of the glutamanergic *N*-Methyl-D-aspartate receptors (NMDARs) and a subsequent increase in intracellular calcium (Ca^{2+}) (Arundine and Tymianski, 2003; Choi, 1987; Sattler et al., 1998). A reduced re-uptake of neurotransmitters from the extracellular space contributes further to the build up of extracellular glutamate concentration (Benveniste et al., 1984; Camacho and Massieu, 2006; Rossi et al., 2000). NMDAR activation also results in substantial intracellular sodium (Na^{+}) loading (Olney et al., 1986; Rothman, 1985) which is believed to contribute to acute neuronal injury (Arundine and Tymianski, 2003). An increased intracellular Ca^{2+} concentration activates damaging enzymes and down-stream neurotoxic cascades. Ca^{2+}-dependent enzymes like the protease calpain (Siman et al., 1989) and nitric oxide synthase (NOS) (Dawson et al., 1991) are activated. NOS activation results in production of oxygen free radical nitric oxide (NO) (Beckman and Koppenol, 1996; Iadecola, 1997). Over-production of NO and reactive oxygen species (ROS) have been shown to induce damage to cellular macromolecules, initiate acute necrosis and apoptosis (Dirnagl et al., 1999). Ca^{2+} accumulation in mitochondria and mitochondrial membrane depolarization results in augmented ROS production (Dugan et al., 1995). Moreover, Ca^{2+} accumulation in mitochondria induces the formation of mitochondrial permeability transition pore which promotes mitochondrial swelling and leakage (Kristian and Siesjo, 1998) resulting in cytochrome C release (Fujimura et al., 1998) which provides a trigger for apoptosis (Dirnagl et al., 1999). Thus, Ca^{2+} accumulation especially in mitochondria is considered deleterious (Stout et al., 1998). The

hippocampal pyramidal neurons of Cornu Ammonis (CA) display a selective vulnerability during ischemia that is believed to be due to an increased susceptibility of their mitochondria to Ca^{2+} overload (Stanika et al., 2010).

3.1.1.1 Dendritic damage

A morphological hallmark of acute excitotoxic neuronal damage is the dendritic damage, dendrotoxicity, that manifests itself as focal swellings (beadings) of the dendrites (Olney et al., 1979). Dendritic beading during brain ischemia (Hori and Carpenter, 1994; von Lubitz and Diemer, 1983) is thought to make neurons more susceptible for neuronal damage and may contribute to the development of delayed cell death (Petito and Pulsinelli, 1984).

Dendritic damage requires NMDAR activation (Hasbani et al., 2001b; Park et al., 1996). The initial beading requires the influx of Na^+, Cl^- and water (Hasbani et al., 1998; Ikegaya et al., 2001). Permanent damage requires a substantial intracellular Ca^{2+} increase (Faddis et al., 1997; Hasbani et al., 1998; Vander Jagt et al., 2008) and a breakdown of the mitochondrial membrane potential (Greenwood et al., 2007; Kintner et al., 2010). *In vitro,* formation of dendritic beadings can be induced by application of a glutamate receptor agonists (Faddis et al., 1997; Hasbani et al., 1998; Hasbani et al., 2001a; Ikegaya et al., 2001; Park et al., 1996) or by activating extrasynaptically localized NMDARs (Leveille et al., 2008). Formation of dendritic beadings are reversible with mild or sublethal excitotoxic stimuli (Faddis et al., 1997; Hasbani et al., 1998; Hasbani et al., 2001a; Ikegaya et al., 2001; Park et al., 1996). *In vivo,* dendritic beadings are observed in brain ischemia models where, depending on the length of the insult and the proximity to core area, distant penumbra dendrites recover to some extent (Enright et al., 2007; Sigler and Murphy, 2010; Zhang et al., 2005) whereas damaged dendrites hardly show any recovery (Murphy et al., 2008). However, neurons in the penumbra may well be subjected to a delayed ischemic damage. Dendritic beading is a morphological change that is associated with peri-infarct depolarization that is linked with the increase of ischemic core size (Dreier, 2011).

3.2 GLUTAMANERGIC N-METHYL-D-ASPARTATE RECEPTORS (NMDARs)

NMDARs are glutamate-gated ionotropic channels and are important mediators of synaptic plasticity both in the developing and in the mature brain (Aamodt and Constantine-Paton, 1999; Bliss and Collingridge, 1993; Malenka and Nicoll, 1999). NMDAR activation requires the simultaneous binding of both L-glutamate and its co-agonist glycine (Johnson and Ascher, 1987; Kleckner and Dingledine, 1988) as well as membrane depolarization to remove magnesium (Mg^{+})-ions, which block the pore at resting membrane potentials (Nowak et al., 1984). NMDAR mediated postsynaptic responses have slow activation and deactivation kinetics in comparison to other ionotropic glutamate receptors (Johnson and Ascher, 1987; Stern et al., 1992). NMDARs are permeable for Ca^{2+}, Na^{+} and potassium (K^{+}) ions and in contrast to other ionotropic glutamate receptors they have a high Ca^{2+} permeability (Burnashev et al., 1995). NMDARs activity is modulated via allosteric binding sites by protons (H^{+}), zinc (Zn^{2+}) and polyamines (Paoletti, 2011).

Functional NMDARs are probably heterotetrameric (either diheteromeric or triheteromeric) composed of two mandatory NR1 subunits and either two NR2 subunits (A-D) or a combination of NR2 and NR3 (A-B) subunits (Luo et al., 1997; Monyer et al., 1994; Sheng et al., 1994; Ulbrich and Isacoff, 2008). The NR1 subunits contain the glycine-binding site and the NR2 subunits contain the glutamate-binding site (Furukawa et al., 2005). The NR1 subunits are expressed in all central neurons (Moriyoshi et al., 1991) and exhibit eight different splice variants (NR1-1a-b, 2a-b, 3a-b, 4a-b) that differ in the C-terminal (Hollmann et al., 1993; Sugihara et al., 1992). NR2A and NR2B are predominantly expressed in the forebrain with particularly high expression in hippocampal pyramidal cells. The NR2 subunits differ in their expression profile during development: the NR2B-subunits are expressed already prenatally, whereas NR2A-subunits gradually appear after birth. For either of the two subunits the expression peaks around P20 (Monyer et al., 1994; Sheng et al., 1994; Watanabe et al., 1992). The NR2 subunits determine the functional and pharmacological properties of NMDARs (Paoletti, 2011; Traynelis et al., 2010).

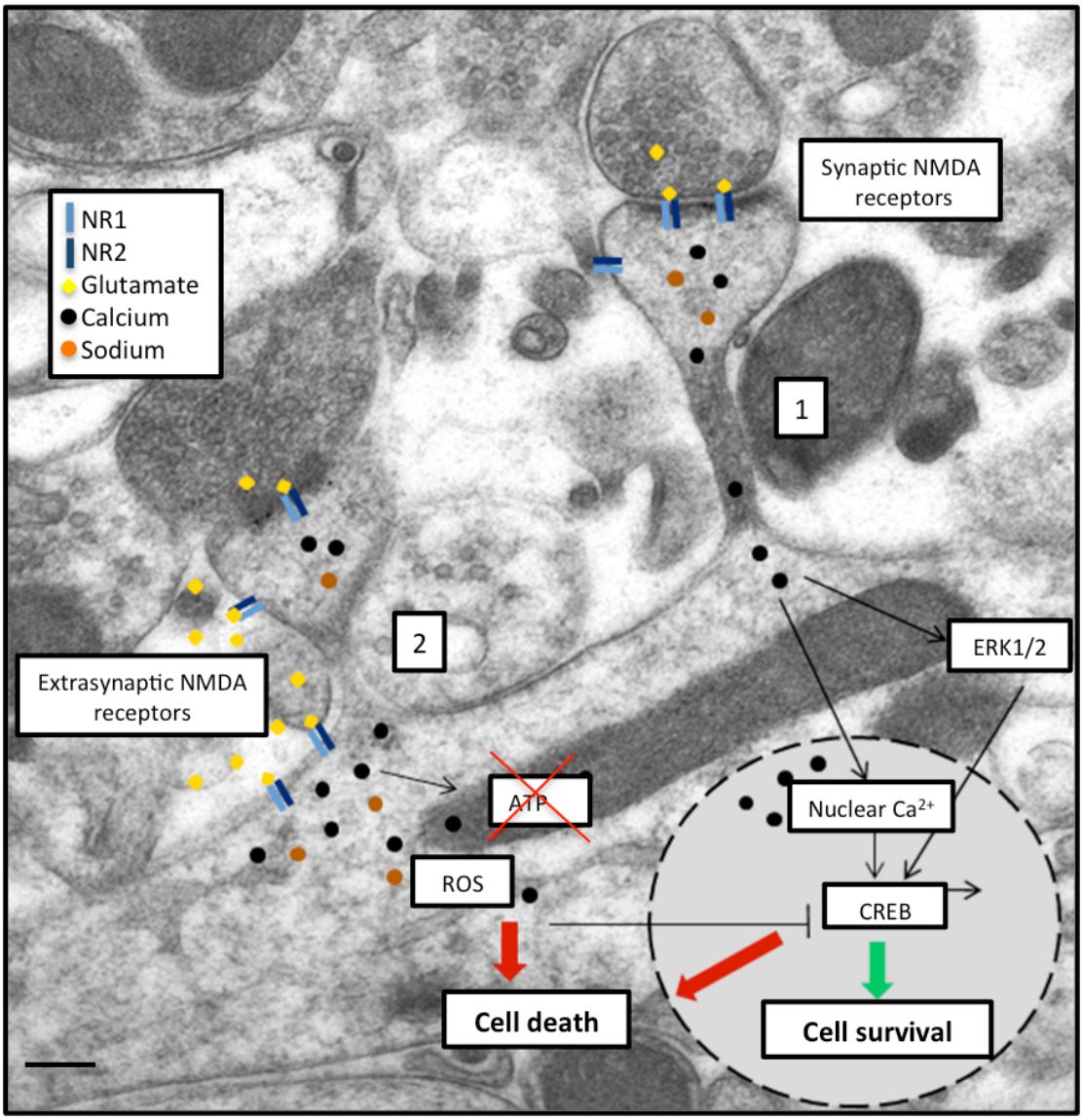

Figure 2. An overview of acquired neuroprotection through synaptic NMDARs and some features of the excitotoxic cell death through extrasynaptic NMDARs. 1. Nuclear Ca^{2+} transients evoked by synaptic NMDAR stimulation regulate CREB-dependent gene transcription via nuclear calcium and Ras-extracellular-signal regulated kinase (ERK) 1/2 signaling pathway. Activation of both pathways ensures a prolonged CREB phosphorylation and long-term neuroprotection against harmful stimuli such as ischemia. 2. Anoxic depolarization during ischemia leads to an excessive glutamate release, subsequent extrasynaptic NMDAR activation and intracellular Ca^{2+} and Na^{+} overload, resulting in neuronal dysfunction and death. Ca^{2+} influx in mitochondria results in ROS production and the collapse of the ATP-production. Furthermore, activation of extrasynaptic NMDAR blocks CREB-mediated neuroprotection. Immunogold particles label for the postsynaptic density protein 95 (PSD95). Scale bar 100 nm.

NMDARs are predominantly located on dendrites at both extrasynaptic and synaptic sites (Groc et al., 2009; Harris and Pettit, 2007; Petralia et al., 2010; Thomas

et al., 2006). A receptor is classified as extrasynaptic if located on the perisynaptic annulus (within 100nm from postsynaptic density (PSD)), on the spine shaft, on the dendritic shaft or on the cell body (Petralia et al., 2010). The amount of extrasynaptic and synaptic NMDARs varies with developmental stage; in younger animals the extrasynaptic receptors represent 2/3 of the surface population and in older animals 1/3 of the population (Groc et al., 2006; Tovar and Westbrook, 1999). NR2B subunits are reported to be more abundant at extrasynaptic locations (Martel et al., 2009; Tovar and Westbrook, 1999), although the regulation of subunit distribution at subcellular locations is not fully resolved (Kohr, 2006).

3.2.1 NMDAR contribution to neuronal cell death

As mentioned above, NMDARs play a crucial role during neurodegeneration occurring as a result of ischemic cell death. NMDAR-mediated responses in ischemic cell death signaling are assumed to depend on receptor localization (extra synaptic versus synaptic) and/or NR2 subunit composition (NR2A versus NR2B). NMDARs located at extrasynaptic sites are activated when there is sufficient glutamate spill over (Sattler et al., 2000; Stanika et al., 2009) and are thought to activate signaling cascades that promote cell death (Hardingham and Bading, 2010; Hardingham et al., 2002; Zhang et al., 2007) (Fig 2). Of the NR2 subunits, the NR2B-subunit has been shown in several studies to mediate cell death (Brewer et al., 2007; Liu et al., 2007; Martel et al., 2009; Stanika et al., 2009; Zhou and Baudry, 2006), and in some cases especially NR2B-subunits located at extrasynaptic sites (Hardingham et al., 2002; Sinor et al., 2000). However, others have reported that both 2A and 2B NMDAR subunits are able to promote of cell survival as well as cell death (Martel et al., 2009; Stanika et al., 2009). In contrast, synaptic NMDARs activate signaling cascades and genes promoting cell survival (Hardingham and Bading, 2010; Hardingham et al., 2002; Zhang et al., 2007) (Fig. 2).

3.2.2 Ca^{2+} regulated acquired neuroprotection via synaptic NMDARs

Ca^{2+} entry through synaptic NMDA receptors activates neuroprotective mechanisms either in a nuclear Ca^{2+}-dependent manner, activating or repressing transcription of various genes, or via phosphotidylinositide 3'-OH kinase (PIK3)-AKT pathway which is independent of the on-going gene transcription (Hagenston

and Bading, 2011; Hardingham, 2009; Hardingham and Bading, 2010). Gene transcription dependent neuroprotection is mainly mediated by the transcription factor cyclic-AMP response element (CRE) binding protein (CREB) (Hardingham et al., 2002).

Activation of CREB is regulated by the nuclear Ca^{2+}/calmodulin-dependent protein kinase (CaMK) pathway and the Ras-extracellular-signal regulated kinase (ERK) 1/2 pathway, mediating fast acting responses and slow but long-lasting responses respectively (Hardingham et al., 2001a, b; Wu et al., 2001). CREB activation by the CaM kinase pathway is initiated by Ca^{2+} translocation to the nucleus and binding to calmodulin forming a Ca^{2+}/calmodulin complex, initiating the subsequent activation of CaMKIV and phosphorylation of CREB at serine 133 (Chawla et al., 1998; Matthews et al., 1994). CREB phosphorylation by the Ras-ERK1/2 pathway is mediated by p90 ribosomal S6 protein kinase 2 (RSK2) (Xing et al., 1996) and nuclear located mitogen- and stress-activated protein kinases (MSK) 1/2 (Arthur et al., 2004). Activation of CREB-dependent transcription in neuronal cells depends on the recruitment of co-activator CREB binding protein (CBP) (Chrivia et al., 1993; Hardingham et al., 1999) upon phosphorylation at serine-301 (Impey et al., 2002) presumably by CaMKIV (Chawla et al., 1998).

Nuclear Ca^{2+} regulates a pool of genes, termed activity-regulated inhibitors of death (AID) that make neurons more resilient against damage both *in vitro* and in animal models of neurodegeneration (Zhang et al., 2009). AID genes appear to protect neurons by a common process that boosts mitochondrial resistance against cellular stress and toxic insults (Lau and Bading, 2009a; Leveille et al., 2008; Zhang et al., 2007; Zhang et al., 2009). Some of the AID genes are potential CREB target genes such as activating transcription factor 3 (ATF3) (Zhang et al., 2011; Zhang et al., 2007; Zhang et al., 2009).

3.2.2.1 Activating transcription factor 3 (ATF3)

ATF3 is a member of the ATF/CREB family of basic region-leucine zipper domain (b-ZIP) transcription factors with a calculated molecular mass of 22 kDa (Hai et al., 1989). The leucine zipper domain is responsible for ATF3 dimerization while the basic-region domain of ATF3 is a deoxyribonucleic acid (DNA)-binding domain that binds to promoters (Liang et al., 1996) with the consensus sequence

TGACGTCA (Lin and Green, 1988). ATF3 heterodimers either activates or represses gene transcription depending on the promoter context (Hai et al., 1999) while ATF3 homodimer generally functions as a repressor and moreover, by creating a negative feedback loop can repress its own promoter activity (Wolfgang et al., 1997; Wolfgang et al., 2000). ATF3 is an early immediate gene with low expression in most quiescent cells, but is upregulated in response to various stress and injury conditions (Hai and Hartman, 2001; Hai et al., 1999), in response to inflammatory reactions (Gilchrist et al., 2006; Suganami et al., 2009) and in various tumors (Janz et al., 2006; Pelzer et al., 2006; Yin et al., 2008).

In the nervous system ATF3 has been documented to be upregulated following excitotoxic insult (Zhang et al., 2011), simulated brain ischemia (MCAO: middle cerebral artery occlusion) (Ohba et al., 2003; Song et al., 2011), simulated brain seizure (kainate injection) (Francis et al., 2004), peripheral nerve injury (Isacsson et al., 2005; Seijffers et al., 2006; Tsujino et al., 2000), optic nerve injury (Takeda et al., 2000) and nerve growth factor (NGF) depletion (Mayumi-Matsuda et al., 1999). Due to its specific expression in response to nerve injury, ATF3 is generally used as a marker for such (Hai et al., 1999; Takeda et al., 2000; Tsujino et al., 2000). Its expression seems to attribute to a beneficial outcome. ATF3 has been found to protect against NGF-deprivation (Nakagomi et al., 2003) and kainate- (Francis et al., 2004) and MCAO-induced (Zhang et al., 2011) neuronal cell death. Furthermore, in nerve injury ATF3 is considered to contribute to nerve regeneration as ATF3 promotes myelinisation, and neurite outgrowth both *in vivo* and *in vitro* (Nakagomi et al., 2003; Seijffers et al., 2006; Seijffers et al., 2007). In the nervous system, few ATF3 target genes involved in recovery and survival have been identified so far. Many ATF3 target genes may well themselves be transcription regulators as the induction of ATF3 is fast and transient.

3.3 ORGANOTYPIC SLICE CULTURES – AN *IN VITRO* MODEL TO STUDY NEURONAL CELL DEATH

To address a specific question in a study an important decision is to choose the right experimental model. *In vitro* preparations are often used for initial testing of a working hypothesis as they, despite being a simpler model than an *in vivo* model, offer the benefit to execute experiments faster and in a more controlled environment.

However, it is important to select the right *in vitro* model to conduct the investigation because different models offer distinct advantages. There are three major *in vitro* preparations used for the study of neuronal damage *in vitro*: acute slices, organotypic slices and dispersed neuronal cultures.

Hippocampal organotypic slice cultures are often used to investigate brain ischemia. Hippocampal organotypic slices can be cultivated either by the roller drum technique introduced by Gähwiler (Fig. 3) (Gahwiler, 1981, 1984; Gahwiler et al., 1997; Laake et al., 1999; Runden-Pran et al., 2005) or as interface cultures grown on a semi-porous membrane, commonly known as Stoppini cultures (Stoppini et al., 1991). The interactions between neuronal and non-neuronal cells are sustained and intrinsic connections of the hippocampus *in situ* are largely maintained (Gahwiler, 1984; Stoppini et al., 1991). The structural organization of the hippocampal formation is relatively well preserved in organotypic slice cultures (Gahwiler, 1981, 1984; Stoppini et al., 1991; Zimmer and Gahwiler, 1984), containing components of the hippocampus proper consisting of Cornu Ammonis (CA) 1, 2, and the dentate gyrus (DG) including dentate hilus and subgranular zone and in addition the subiculum (Andersen 1975). Organotypic slices are prepared from young animals, usually postnatal day (P) 5-7, and cultivated for two weeks before experimental manipulations. The cultivation period results in correct maturation of synaptic connections, and moreover, gives time for the slices to recover from the dissection procedure. Preparations from younger animals result in cell migration, and preparations from older animals exhibit anoxic cell death in the central part of the slice. During cultivation, the typically 300-400 µm thick slices maintained by the roller drum technique flatten to a monolayer of 50 µm whereas Stoppini cultures have a thickness of 100 µm (Gahwiler, 1984; Gahwiler et al., 1997; Stoppini et al., 1991).

Hippocampal organotypic slice cultures are particularly sensitive to ischemia and display a distinct pattern of cell death, delayed and being most pronounced in the CA1 region (Kirino, 1982; Kirino et al., 1984; Schmidt-Kastner and Freund, 1991). Due to the relatively well-preserved cytoarchitecture *in vitro,* the characteristic cell death pattern of hippocampal sub-regions is easily observed. Ischemic cell death in organotypic slices is achieved by oxygen and glucose deprivation (OGD) and by NMDA or glutamate bath application (Runden et al., 1998; Runden-Pran et al., 2005; Rytter et al., 2003).

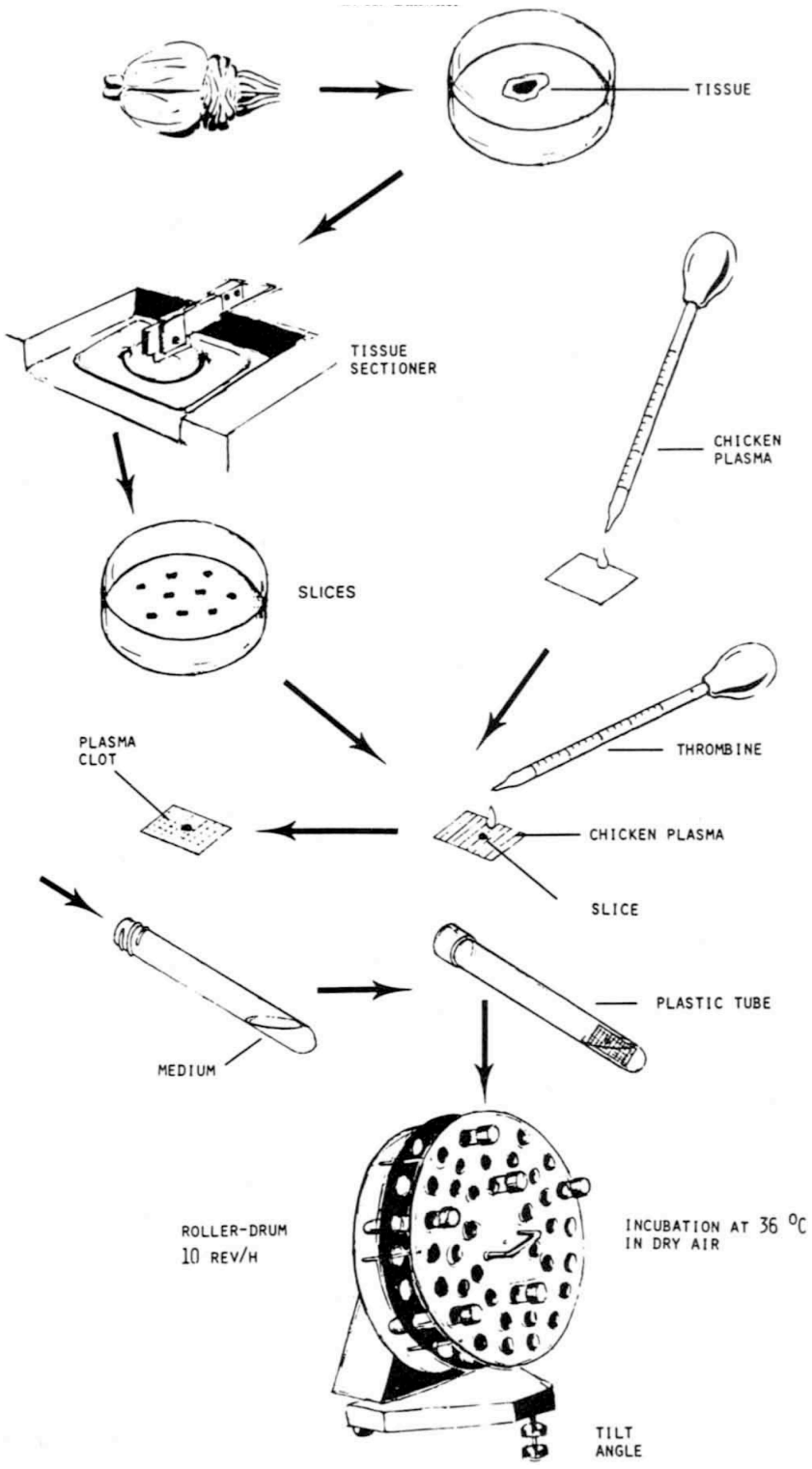

Figure 3. Roller drum cultivation procedure of organotypic hippocampal slice cultures. After dissection, slices are clotted with plasma and thrombin on a glass cover slip and grown in individual tubes for 2 weeks before experimental manipulations (figure from Gahwiler et al., 1984).

Cell death can be evaluated with light microscopy using DNA binding fluorescent dyes like propidium iodide (PI) (Laake et al., 1999). Slice cultures grown with the roller drum technique are more accessible for imaging studies as they are grown directly on glass cover slips (Gahwiler et al., 1997) and are thinner than Stoppini cultures. A drawback is the variability of cell death between batches of cultures. Slight changes in the duration of hypoxia can lead to pronounced variations in cell death in both CA1 and CA3. Another drawback relates to the fact that slices grown with the roller drum technique are attached to the coverslip by a drop of plasma clotted with thrombin (Fig. 3). This clot may limit the cellular uptake of drugs and therefore usually higher drug concentrations are needed to obtain a biological response.

Organotypic cultures provide a way to investigate a particular molecular mechanism or an isolated cellular event as the observed effect must reflect a direct influence on the cells and cannot be due to a change in blood flow. In *in vivo* situations this is sometimes very difficult to achieve due to the complexity of cellular networks and their interactions as well as the problems produced by the blood-brain-barrier. This also offers more accessibility for blocking a singular event or cascades of events by drugs. Another advantage, as in other *in vitro* platforms, is the possibility to control variable external factors such as temperature, oxygen, ionic ambient and nutrient availability. Organotypic slice cultures offer a compromise model between the simplified, but more stable, dissociated cell cultures and the *in vivo* situation

3.3 AIMS

3.3.1 Study I

Pharmacological studies have established that NMDARs contribute to cell death in organotypic slice cultures (Bonde et al., 2005; Kristensen et al., 2001; Martinez-Sanchez et al., 2004; Newell et al., 1995), and acute brain slices (Zhou and Baudry, 2006) when exposed to simulated ischemia *in vitro*. However, in organotypic slice cultures, there are no evaluations comparing the NMDA-evoked and OGD-evoked cell death and the contribution of the NMDARs to these distinct stimuli for inducing dell death. Furthermore, given the distinct developmental profile of NMDAR subunits, one cannot assume, a priori, that slices harvested from new-born rats and grown isolated from all extrinsic or intrinsic input from other brain regions

display the same complement of receptors as seen in mature animals used for *in vivo* stroke models. Therefore, in the current study I first aimed to characterize the NMDAR expression in organotypic slices compared to the *in situ* situation and, secondly, to evaluate the contribution of NMDARs in NMDA- and OGD induced cell death at days *in vitro* (DIV) 14, an age at which organotypic slices are often used for experiments.

In this study, MSc Kristi Henjum performed experiments for figure 3, 4B and 6. Parts of this study have been published in: Ahlgren, H., Henjum, K., Ottersen, O.P., and Runden-Pran, E. (2011). **Validation of organotypical hippocampal slice cultures as an ex vivo model of brain ischemia: different roles of NMDA receptors in cell death signalling after exposure to NMDA or oxygen and glucose deprivation**. Cell and tissue research *345*, 329-341.

3.3.2 Study II

Dendritic beading is an early morphological hallmark of neuronal damage in brain ischemia thought to make neurons more prone for delayed ischemic damage. Therefore, protection against dendritic beading is likely to reduce later neuronal damage. As most synaptic contacts are located on the dendrites, a protection strategy capable of also maintaining the synaptic transmission is essential**.** Increased synaptic activity which controls a gene program for acquired neuroprotection including ATF3 (Zhang et al., 2011) offers a possible protection strategy. In this study, I aimed first to establish and characterize the excitotoxic parameters that induce dendritic damage that precedes neuronal cell death in dissociated hippocampal cultures. Second, I wanted to investigate if increased synaptic activity offers protection against dendritic damage, and if so, to identify if activity regulated genes are involved, particularly ATF3 which is known to be neuroprotective.

In this study, Andrea Hellwig performed electron microscopy (EM) images (Fig. 2C) and Dr. H. Eckehard Freitag performed microelectrode array (MEA)-measurements (Fig. 1D, E and Fig 5). Iris Bunzli-Ehert prepared dissociated hippocampal cultures. Parts of this study have been included in a manuscript in preparation: Ahlgren, H.[1], Freitag, H.E.[1], Hellwig, A.[1], Ottersen, O.-P.[2], Bading, H.[1*] **ATF3-overexpression protects against dendritic injury and facilitates the recovery of synaptic transmission after neuronal damage.** [1]Department of

Neurobiology, Interdisciplinary Center for Neurosciences IZN, INF 364, University of Heidelberg, 69120 Heidelberg, Germany. [2]Center for Molecular Biology and Neuroscience and Department of Anatomy, Institute of Basic Medical Sciences, University of Oslo, 0317 Oslo, Norway.

Manuscript in preparation

CHAPTER 4 MATERIAL AND METHODS

4.1 DISSOCIATED HIPPOCAMPAL PRIMARY CULTURES

Hippocampal neuron cultures from postnatal day 0 (P0) C57Black mice were prepared and maintained as described previously (Bading and Greenberg, 1991), except that the growth medium was supplemented with B27 (Invitrogen/BRL) and 1 % rat serum. Neurons were plated on poly-D-lysine (2 µg/cm^2)/laminin-coated 12 mm coverslips or 35-mm plastic dishes (Nunc) or plastic 96-well microplate (Perkin Elmer). For MEA recordings neurons were plated on MEA dishes containing a grid of 60 planar electrodes (Multi Channel Systems, Reutlingen, Germany) as described previously (Arnold et al., 2005; Soriano et al., 2006). On day *in vitro* (DIV) 3, 2.4 µM cytosine d-arabinofuranoside (ARA-C) (Sigma) was added to each dish to prevent proliferation of non-neuronal cells. On DIV8, growth medium was replaced with transfection medium (TM) (Bading et al., 1993), consisting of a salt–glucose–glycine (SGG) solution and minimum Eagle's medium (9:1; v/v) plus sodium selenite 10 µg/ml, insulin 15 µg/ml, transferrin 8.25 µg/ml, and penicillin-streptomycin 0.5 %. SGG contains (in mM): NaCl 114, $NaHCO_3$ 26, KCl 6.3, $MgCl_2$ 1, $CaCl_2$ 2, Hepes 10, glycine 1, glucose 30, sodium pyruvate 0.5, Phenol Red 0.2 %. All experiments were performed on DIV13-15 if not otherwise noted. The following chemicals were used: bicuculline (Bic) (Enzo LifeScience), Actinomycin D (Applichem), 2-amino-5-phosphonovaleric acid (APV) and NMDA (Sigma), tetrodotoxin (TTX) (Biotrend, Cologen, Germany) and dizocilpine (MK-801) (Tocris, Bioscience) and Hoechst 33258 (Serva).

4.1.1 DNA constructs and transfection of hippocampal neurons

Hippocampal neuronal cultures were DNA-transfected 36-72 h prior to experiments using Lipofectamine 2000 (Invitrogen) at a concentration of 5 µl/ml in TM without penicillin streptomycin. The total DNA concentration was 1.6 µg/µl and for co-transfection 2 µg/µl. The Lipofectamine/DNA mixture was left on the cells for 2.5 h before being replaced with TM. Transfection efficiency was 0.1-0.5 % of the cell population. Co-transfection efficacy was 100 % determined by counting the percentage of co-localized enhanced green fluorescent protein (EGFP) positive and Flag positive neurons by immunocytochemical staining with mouse monoclonal Anti-

Flag M2 antibody 1:4000 (Sigma-Aldrich). The following DNA plasmids were used: EGFP containing a 1.3 kbp fragment of the mouse CaMKII promoter (a gift from Ali Cetin and Peter Seeburg, Max Planck Institute for Medical Research, Heidelberg, Germany), mitochondrial targeted mCherry under CaMKII promoter (generated by Dr. David Lau), ATF3-Flag under cytomegalovirus enhancer (CMV)/chicken beta-actin hybrid promoter (CBA) (Zhang et al., 2007; Zhang et al., 2009).

4.1.2 Recombinant adeno-associated viruses (rAVVs) and infection of hippocampal neurons

At DIV7 neuronal cultures were infected by exposure to viral particles for either 3 h ((rAAV-CKII-mCherry-nuclear localised signal (NLS)), rAAV-mCherry-calmodulin ((CaM)-binding peptide (CaMBP4)) or overnight (rAAV-CMV-mCherry-NLS, rAAV-Flag-ATF3) in TM. Infection efficiency (co-localization with Hoechst 33258) was ~ 80 % for rAAV-mCherry-NLS, rAAV-mCherry-CaMBP4 and rAAV-Flag-ATF3 (determined with mouse monoclonal anti-Flag M2 antibody 1:4000, (Sigma)). Co-transfection-infection efficacy was (80-90 %) determined by counting the percentage of co-localized EGFP positive and anti-Flag or mCherry positive neurons. The following viruses were used: rAAV-CMV-mCherry-NLS, rAAV-CMV-ATF3-Flag, rAAV-CKII-mCherry-NLS and rAAV-mCherry-CaMBP4. The ATF3 and NLS rAAV protein expression cassette contains a CMV/CBA promoter, a woodchuck hepatitis virus post-translational regulatory element (WPRE) and a bovine growth hormone polyA signal. rAAV-ATF3 carried a flag-tag and mCherry-NLS carried a myc-tag. The rAAV protein expression cassette for mCherry-CaMBP4 and mCherry-NLS expression contains a 1.3 kbp fragment of the mouse CaMKII promoter (kindly provided by A. Cetin and P. Seeburg, Max Planck Institute for Medical Research, 69120 Heidelberg, Germany), the woodchuck hepatitis virus posttranslational regulatory element (WPRE) and a bovine growth hormone polyA signal (Zhang et al., 2007; Zhang et al., 2009).

4.1.2.1 rAAV

The vectors used for construct and package of rAAVs have been described previously (Klugmann et al., 2005). Mosaic serotypes rAAV1/2 were produced by co-transfecting human kidney cell line 293 (HEK293) (ATCC) via the calcium phosphate

precipitation method. HEK293-cells were grown in 25 ml high-glucose-containing (4.5 g/l) Dulbecco's Modified Eagle Medium (DMEM; Life Technologies/Invitrogen) medium supplemented with 1 % sodium pyruvate (Life Technologies/Invitrogen) 10 % fetal calf serum (FCS) (Life Technologies/Invitrogen), 1 % non-essential amino acids (Life Technologies/ Invitrogen), 100 units/ml penicillin and 100 µg/ml streptomycin (Sigma-Aldrich) at 37 °C in a 5 % carbon dioxide (CO_2) humidified atmosphere. Medium was changed for each 15-cm-diameter HEK-cells plate (60-70% confluent) 2-3 h prior a transfection with Iscove`s Modified Dulbecco Medium (IMDM; Life Technologies/Invitrogen) containing 5 % fetal bovine serum without antibiotics. Packaging of chimeric serotypes rAAV1/2 transducing vectors was carried out with 25 µg of a mini-adenovirus helper plasmid pFΔ6, 6.25 µg of AAV2 helper plasmid pRV1, 6.25 µg of AAV1 helper 4 plasmid pH21 together with 12.5 µg of the rAAV plasmid containing the respective construct of interest for each 15-cm culture dish. The medium was replaced with fresh DMEM containing 10 % fetal bovine serum and antibiotics after 18-22 h transfection. Sixty-65 h after transfection HEK-cells were washed once with pre-warmed PBS, harvested, pelleted (5 min at 800 × g), re-suspended in 100 mM NaCl and 10 mM Tris-HCl (pH 8.0), lysed with 0.5 % sodium deoxycholate monohydrate (Sigma-Aldrich) and 50 U/ml Benzonase® Nuclease (Sigma- Aldrich) for 1 hour at 37 °C, finally pelleted (at 4 °C for 15 min at 3000 × g) and frozen over-night at -20 °C prior purification of highly purified rAAV1/2 vector with heparin affinity HiTrapTM Heparin HP Columns (GE Healthcare). The rAAV1/2 vector stocks were concentrated with Amicon® Ultra-4 Centrifugal Filter Units (Millipore) and the integrity of viral particles were routinely checked by SDS- PAGE (10 % resolving gel).

4.1.3 NMDA toxicity assay for dendritic damage and cell death

Hippocampal neurons grown on coverslips and transfected with EGFP were challenged for 10 min at 37 °C with different NMDA concentrations: 2.5, 5, 10, 20 and 30 µM. Stimulations were performed in 4-well plates. All experiments were ended by washing three times with TM. After washout of NMDA cells were either fixed immediately with 4 % paraformaldehyde supplemented with 4 % sucrose or incubated for a further 2, 4 or 24 h at 37 °C before fixation. After fixation, nuclei

were stained with Hoechst33285 before mounting coverslips onto microscope slides in Mowiol.

In experiments with increased synaptic activity, neurons were treated with 50 µM Bic for 15-16 h prior to an NMDA challenge. Bic is a γ-aminobutyric acid receptor type A ($GABA_AR$) blocker and Bic induces recurrent synchronous network bursting. Bicculline was dissolved in dimethylsulfoxide (DMSO) and the final concentration of DMSO did not exceed 0.05 %. In experiments with Actinomycin D (10 µg/ml) the drug was added 30 min prior to Bic. In experiments both with Actinomycin D and CaMBP4-infected neurons Bic treatment was terminated by transferring coverslips to TM containing 1 µM TTX for 4 h before adding NMDA in order to halt all electrical activity and to only observe transcription mediated responses.

4.1.3.1 Dendritic morphology evaluation

The hippocampal neurons were evaluated for dendritic damage immediately after NMDA stimulation or after 2 h or 4 h recovery. Evaluation after 24 h recovery was impossible as most of the damaged dendritic processes were dissolved. The dendritic damage was assessed by counting 15 EGFP positive neurons for every coverslip (2 coverslips per condition) for each experiment at a light microscope (Leica DM IRBE) with 40× magnification. Dendrites were classified as swollen if more than one spherical beading was visualized along the dendritic arbor. Analysis was done blind to the treatment group of each coverslip. Normalization of data was done by taking into consideration the basal damage of each neuronal preparation and the maximum damage after NMDA treatment, i.e. values were normalized against the minimum (lowest percentage of damaged dendrites) and maximum (highest percentage of damaged dendrites). When acquired, statistical analyses were done with one-way ANOVA followed by Bonferronis post hoc test. Data are presented as mean and standard error of the mean (±SEM) from at least three independent cell preparations.

4.1.3.2 Cell death quantification

The hippocampal neurons were evaluated for cell death immediately after NMDA stimulation or after 24 h recovery. Cell death was assessed by observing

morphological abnormalities on nuclei characteristic of apoptotic death as previously described (Hardingham et al., 2002; Papadia et al., 2005; Zhang et al., 2011; Zhang et al., 2007; Zhang et al., 2009). The percentage of hippocampal neurons with shrunken cell bodies and large round chromatin clumps was determined by counting Hoechst 33258-stained nuclei in 20 visual fields for every condition in each experiment at a light microscope (Leica DM IRBE) with 40× magnification. Hoechst 33285 is a nuclear dye binding to DNA.

4.1.4 ATP measurement

Neurons were plated on a 96-well plate and infected at DIV7. Prior to experiments, TM medium was changed to CO_2-independent salt–glucose–glycine (SGG; 140.1 mM NaCl, 5.3 mM KCl, 1 mM $MgCl_2$, 2 mM $CaCl_2$, 10 mM HEPES, 1 mM glycine, 30 mM glucose, and 0.5 mM sodium pyruvate). Neurons were left to stabilize for 15 min prior adding 20 µM NMDA for 10 min. The NMDA challenge was terminated by washing neurons three times with SGG. ATP levels were measured immediately after simulation and were performed with a luminescence based ATP detection assay; ATPlite 1 step (Perkin Elmer) accordingly manufacturer's instructions. All experiments were performed at RT.

4.1.5 Quantitative reverse transcriptase polymerase chain reaction (qPCR) - Sample collection, RNA isolation, cDNA synthesis and qPCR

RNA from hippocampal cultures was isolated with RNeasy Total RNA isolation kit (Qiagen, Roche) and DNAse treatment with RNase-free DNase set (Qiagen) according to manufacturer's instructions. Two µg of total RNA with the A_{260}/A_{280} ratio 1.95-2.2 was converted further into cDNA using High Capacity cDNA Reverse Transcription kit (Applied Biosystems). qPCR was performed on an ABI7300 thermal cycler using universal QRT-PCR master mix with following TaqMan Gene Expression Assays (Applied Biosystems): *Slc9a1* (NHE-1, Mm00444270_m1), *AQP4* (Mm00802131_m1), *Slc12a5* (KCC2, Mm00803929_m1), *Slc12a2* (NKCC1, Mm00436554_m1), *Gusb* (Mm00446953_m1), *TRPV4* (Mm00499025_m1) and *TRPM7* (Mm00457998_m1). Gene Ct-values were normalized to GusB as endogenous control gene. Statistical analyses were done with

Student's t test for independent samples. Data are presented as mean ±SEM from at least three independent cell plating.

4.1.6 Immunocytochemistry

Hippocampal neurons were fixed in warm 4 % paraformaldehyde supplemented with 4 % sucrose for 10-15 min at RT, thereafter were permeabilised with Triton-X-100 (0.3 % for 10-15 min) in PBS-Tween (0.1 %). After permeabilisation, neurons were incubated with 50 mM glycine to reduce background un-specificity and non-specific binding sites were blocked with PBS containing 2 % BSA and 10 % NGS. Neurons were incubated overnight at 4°C with primary antibodies diluted in 2 % BSA. Next day, primary antibody was collected and neurons were washed repeatedly with PBS before incubated with secondary antibody for 45 min-1 h at RT. HOECHST 33258 (Serva) was used for nuclear staining and coverslips were mounted on microscope slides in Mowiol**.** The following primary and secondary antibody were used in this study: mouse monoclonal anti-Flag M2 antibody 1:4000 (Sigma-Aldrich) and goat anti-mouse 594 1:750 (Invitrogen). Secondary antibody was centrifuged for 6 min at 13 000 rpm before use.

4.1.7 Confocal imaging

Hippocampal neurons were imagined using a confocal laser-scanning microscope TCS SP2 (Leica) equipped with an inverted fluorescence microscope DM IRE2 (Leica) and Leica confocal scan software. For live imaging experiments a HCX PL APO 63×1.4 NA oil immersion fluorescence objective (Leica) with 4x zoom was used and for all other confocal imaging experiments a HCX PL APO 40×1.25 NA oil immersion fluorescence objective was used. All immunocytochemistry images were obtained with sequential acquisition setting at a resolution of 1024 x 1024 pixels. Each image shown represents a z series projection of images taken at 0.5 µm intervals.

4.1.7.1 Confocal live imaging

All live imaging experiments were performed at 22-24 °C. Hippocampal neurons plated on coverslips were transferred into a custom-made metal perfusion chamber (LIS) connected to a peristaltic pump (BioRad) with the perfusion speed

adjusted to 1 min/ml. The chamber was filled with CO_2-independent SGG (140.1 mM NaCl, 5.3 mM KCl, 1 mM $MgCl_2$, 2 mM $CaCl_2$, 10 mM HEPES, 1 mM glycine, 30 mM glucose, and 0.5 mM sodium pyruvate) (Bading et al., 1993) and mounted on the microscope stage. One EGFP positive neuron was chosen per visible field. Z-stacks with optical sections of 0.3µm spanning the whole dendritic branch were collected every 5 min over a time period of 30 min. EGFP was excited by 488 nm laser line at ~ 5- 10 % of maximal intensity and emitted light was collected at 504-524 nm and mCherry was excited by 594 nm laser line at ~ 15-25% of maximum intensity and emission was collected at 600-620 nm. For EGFP and mCherry double-transfected parallel scans were performed. All images were acquired at a resolution of 512 x 512 pixels. The imaging protocol was as follows: 8 min baseline imaging, 10 min drug application, 12 min imaging after drug washout (including 5 min washing) (Fig. 2A). Drugs, either NMDA solely or in the presence of MK-801 (20 µM), were directly applied to the chamber with a pipette. NMDA sensitivity varies in hippocampal cell cultures between preparations (Tauskela et al., 2001) and was taken in account as we were investigating single cell responses. Inherent NMDA sensitivity was predetermined separately for each preparation on a control 'test' culture and NMDA concentrations were then adjusted accordingly, typically to 20 µM, to induce dendritic beading. Exposure for genetically manipulated neurons was the same as those for parallel control neurons. Images were saved as 8-bit TIFF-files and for data analysis z-stack images were made into projections. Dendritic area of 40 µm secondary or tertiary branch dendrite was marked and measured with open source software ImageJ at each collected time-point and normalized with the area volume prior the NMDA-treatment. Statistical analysis was done by comparing dendritic area values of ATF3 over-expressing group to dendritic area values of control group at each respective time point by repeated measure (RM) two-way ANOVA followed by Bonferronis post hoc test. Data are presented as mean ±SEM from six independent cell preparations.

4.1.8 Transmission Electron Microscopy (TEM)

Hippocampal neuronal cultures grown on coverslips were challenged with NMDA (10, 20, 30 µM) for 10 min at 37 °C. After washout of NMDA neurons were fixed with 2 % glutaraldehyde in 0.1 M sodium phosphate buffer, pH 7.4 and washed

with 0.1 M sodium phosphate buffer. Neurons were post-fixed with 1 % OsO4/1.5 % $K_4[Fe(CN)_6]$, contrasted en bloc with uranyl acetate, dehydrated with a graded dilution series of ethanol, and embedded into glycid ether 100- based resin. Ultrathin sections were cut with a Reichert Ultracut S ultramicrotome (Leica Microsystems) and contrasted with uranyl acetate and lead citrate (Reynolds, 1963). Sections were examined in an electron microscope (EM 10 CR; Carl Zeiss NTS) at an acceleration voltage of 60 kV.

4.1.9 Hippocampal networks and microelectrode array (MEA) recordings

MEA recordings were done as described previously (Arnold et al., 2005; Soriano et al., 2006)**.** Briefly, recordings were acquired with an MEA-60 amplifier board (10 Hz–35 kHz, gain 1200, sampling frequency 20 kHz, Multi-Channel Systems). The distance between the electrodes on the MEA dishes was 200 µm and the electrode diameter was 30 µm. From DIV10 to DIV13 recordings of spontaneous network activity were acquired for 5 min once per day, drug application was done at div14. Before NMDA application, network activity was recorded for 3 min. Cultures with spontaneous bursting activity were excluded. Hippocampal neurons were treated for 10 min with 20 µM NMDA which was washed away by changing the medium three times. Cultures were put back into the incubator and 3 min recordings were repeatedly performed at different time points (0.5 h, 1 h, 2 h, 4 h, 24 h, 48 h and 72 h). Analysis was done with Neuroexplorer (NEX Technologies, http://www.neuroexplorer.com). Statistical analysis was done by comparing rAAV-Flag-ATF3 culture values to control culture area values (non-infected and rAAV-mCherry-NLS) at each respective time point by two-way ANOVA followed by Bonferronis post hoc test. Data are presented as mean ±SEM from four independent cell plating's.

4.1.10 Solutions

Phosphate-buffered saline (PBS) (1M)

NaCl	8.0 g
KCl	0.2 g
Na_2HPO_4	1.44 g

KH_2PO_4	0.24 g

pH adjustment to 7.4 with HCl

H_2O was added to a final volume of 1 liter

Mowiol 4-88 mounting medium

Glycerol	6.0 g
Mowiol 4-88 (Merck)	2.4 g
H_20	6.0 ml
Tris (0.2 M, pH 8.5)	12.0 ml

Resolving gel 10 %

30 % acrylamide solution (Roth)	13.8 ml
10 % ammonium persiflage (APS)	200 μl
TEMED (Merck)	20 μl
4 x Lower Tris-buffer	10 ml

H_2O was added to a final volume of 40 ml

4.2 ORGANOTYPIC SLICE CULTURES WITH ROLLER DRUM METHOD

4.2.1 Preparation and maintenance of organotypic hippocampal slice cultures

Organotypic hippocampal slice cultures were prepared as previously described (Runden et al., 1998). P5 or P6 days old Wistar rats (M&B, Taconic, Denmark) were sacrificed by decapitation and both hippocampi were quickly dissected under aseptic conditions. The hippocampi were then cut into 350-375 µm thick transverse slices with a McIlwain tissue chopper and immediately transferred for separation into Gey's balanced salt solution (GBSS) (1.5 mM $CaCl_2$, 5 mM KCl, 0.22 mM KH_2PO_4, 1 mM Mg_2 Cl, 0.3 mM Mg_2SO_4, 137 mM NaCl, 2.7 mM $NaHCO_3$, 1 mM Na_2 HPO_4, 5.6 mM D-glucose) supplemented with 5 mg/ml glucose. Hippocampal slices with intact subregions and fimbria were individually placed onto glass cover slips (Kindler Gmbh, Freiburg, Germany) in a droplet of chicken plasma. Thrombin (from bovine plasma, Merck KGA, Germany) diluted in GBSS/ultra-pure H_20 was added in order to attach the slice to the cover slip by clot formation. The slices were then transferred to flat-sided culture tubes (Nunc, Nalge Nunc International Nagerville, USA)

containing 750 µl culture media composed of 50 % Basal medium Eagle (with Hanks' salts, BME, BioConcept, Switzerland), 25 % Hanks' balanced salts (HBSS, GIBCO), 25% horse serum (GIBCO) and supplemented with 100 U/ml Penicillin G, 100 µg/ml streptomycin (Invitrogen or GIBCO), 1 mM L-glutamine and 20 mM glucose and cultivated in a roller drum on a rotator (Bellco Biotechnology, NJ, USA) tilted at an angle of 5º, rotating with a speed of ~8 r.p.h. in an incubator at 36 ºC. The culture medium was changed after a week and the cultures were grown for two weeks prior to experiments. Efforts were made to reduce the number of experiments in accordance with the European Communities Council directive 86/609/EEC. Culture media were from GIBCO (Life Technologies, Paisley, Scotland) and other chemicals used were from Sigma-Aldrich (Norway) unless otherwise indicated.

4.2.2 Oxgen-glucose deprivation (OGD)

OGD was induced as previously described (Laake et al., 1999) with some modifications (Rytter et al., 2003). Prior to an experiment (OGD or NMDA-treatment), the slice cultures were incubated overnight with propidium iodide (PI) (5 µg/ml dissolved in (0.001 %) DMSO) added to the culture medium. Slice cultures showing a distinct uptake of PI in the pyramidal cell layer were excluded. PI is a fluorescent dye that binds to nucleic acid in cells with a damaged cell membrane, and is used as an indicator of cell death (Laake et al., 1999; Noraberg et al., 1999). During an experiment, PI was included in all solutions used unless stated otherwise. On the experimental day, the slice cultures were 60 min pre-incubated in culture medium with MK-801 or solvent alone. After pre-incubation, the slice cultures in the OGD group were washed once with ischemic cerebral spinal fluid (iCSF) (0.3 mM $CaCl_2$, 70 mM NaCl, 5.25 mM $NaHCO_3$, 70 mM KCl, 1.25 mM NaH_2PO_4, 2 mM $MgSO_4$, 20 mM sucrose, pre-bubbled with an anoxic gas mixture (80% N_2, 10% H_2 and 10% CO_2) pH 6.5-6.8). The slice cultures were then transferred to an anaerobic incubator with custom made modifications (Electrotec workstation, mini, Sweden) with the same gas mixture and a temperature set to 36 ºC. Traces of oxygen were removed by a palladium catalyst, and stable anaerobic conditions were monitored with an oxygen indicator solution. In the anaerobic incubator the slice cultures were washed once more with iCSF before adding either iCSF solely or the NMDA-receptor antagonist MK-801 (10, 50, 100 µM) diluted in iCSF and placed for 15min in a roller drum on a

rotator (Bellco Biotechnology, NJ, USA) (see above). After the ischemic insult the slice cultures were removed from the anaerobic incubator, washed twice with culture medium and incubated for up to 72h with either culture medium or culture medium supplemented with MK-801 at the same concentrations as above. The control slice cultures (no OGD) were washed twice with artificial cerebral spinal fluid (aCSF) (2 mM $CaCl_2$, 125 mM NaCl, 25 mM $NaHCO_3$, 2.5 mM KCl, 1.25 mM NaH_2PO_4, 2mM $MgSO_4$, 20 mM glucose, pH ~7.4) and incubated throughout the experiment with aCSF in a standard aerobic incubator. At the end of an experiment the control slices were also washed twice with culture medium, added fresh culture medium and evaluated for cell death at defined time-points up to 72h without further change of media (as roller drum slice cultures normally get new media only once a week). For evaluation of development of cell death, recordings were made up to 144h after OGD.

4.2.3 NMDA toxicity assay

NMDA-induced cell death was achieved by incubating the slice cultures with aCSF and NMDA (150 µM) for 15 min in a standard aerobic incubator. Pre-selection of viable slice cultures, pre-incubation with MK-801 (10, 50, 100 µM), control slices and the termination of the experiments were performed according to the OGD-protocol described above. The slice cultures were evaluated for cell death at defined time-points up to 72 h after exposure with no further change of media.

4.2.4 Cell death quantification

Quantification of cell death was performed as described previously (Runden-Pran et al., 2005). Cell death was assessed by measuring the PI-fluorescence before OGD or NMDA (0 h) and at different time-points (24 h, 48 h, and 72 h) following OGD or NMDA treatment. Slice cultures were examined with an inverted Olympus IMT2 microscope with a 4× objective and 2.5× ocular and images were captured with a C4880-96 cooled CCD camera driven by manufacturer's software (Hamamatsu HiPic 4.2.1). PI-fluorescence was induced with light from a 100W mercury lamp, attenuated with a grey-filter, and passed through a rhodamine filter cube (Olympus IMT2-DMG). Illumination, integration time and camera gain were set to fully exploit the 12-bit intensity range of the imaging system without saturating it and were kept throughout the experiment nominally constant for all images at each time-point. Each

series of recording was started by recording a dark current image with the chosen integration time and camera gain, but with a closed light path (camera temperature −30°C). Also a shading correction image was recorded from a preparation of PI dissolved in DMSO (2.5 mg/ml). Shading correction was performed to correct for spatially non-uniform sensitivity of the complete imaging system. PI fluorescence was evaluated with the image processing software analySIS (Soft Imaging Software, Münster, Germany). For semi-quantitative analysis, freehand regions of interest (ROIs) were created around the DG and the CA3 and CA1 hippocampal subfields of each slice culture. All analysis was performed blind to the treatment group. The mean grey-values for each ROI (per unit area) were calculated from the fluorescence intensity, and imported into the SPSS statistical software (SPSS, Inc.). We have earlier shown that there is a good correlation between the number of dead cells and the PI fluorescence intensity (Laake et al., 1999). The auto-fluorescence and unspecific accumulation of PI in the tissue were corrected by subtracting the grey-values from the images at 0h from the grey-values of the same cultures at 24 h, 48 h, and 72 h after OGD or NMDA treatment, i.e. each slice was normalized to itself using this method. The statistical analyses were performed with non-parametric Kruskall-Wallis test; comparison of differences between all groups; and non-tailed non-parametric Mann-Whitney U-test; for comparison of paired groups. Data are presented as means ± S.E.M.; $P < 0, 05$ was considered statistically significant.

4.2.5 Immunoblotting

4.2.5.1 Sample collection of organotypic slice cultures and tissue

For comparative developmental immunoblot analysis of protein expression levels the whole hippocampal formation was studied at postnatal day (P) 6, 12, 19, and 26, whereas slice cultures were studied at corresponding developmental stages: days in vitro (DIV) 0 (at the same day the slice was prepared), 7, 14 and 21. Slice cultures from four to five different animals (n = 4-5) were pooled at each time-point and immediately snap frozen in liquid nitrogen. Whole hippocampi from two rat pups (n=2) at each time point as well as whole hippocampi and cortex from adult mouse and rat were dissected in ice-cold GBSS buffer and snap frozen in liquid nitrogen. Forebrain tissue from adult NR2A$^{-/-}$ and NR2B$^{\Delta f}$ knock out (KO) mice and their wild

type (WT) mice was collected immediately after preparation of acute hippocampal slices and snap frozen in liquid nitrogen. NR2B conditional KO mice were generated with the Cre/loxP system to target NR2B gene deletion in principal neurons of the postnatal brain ($NR2B^{\Delta Fb}$). The NR2B exon 9 was flanked by loxP sites ($NR2B^{2lox}$ mice) and GABAergic interneurons are spared as they do not express α-CaMKII promoter-driven Cre (Sakimura et al., 1995; von Engelhardt et al., 2008).

4.2.5.2 Sample preparation of organotypic slice cultures and tissue

Pooled slice cultures were homogenized with a tip sonicator on ice in radioimmunoprecipitation assay (RIPA)-lysis buffer containing 0.1 % SDS, 1 % Triton-X-100, 0.5 % DOC (deoxycholic acid), 50 mM Tris (pH 7.4), 150 mM NaCl, 5 mM EDTA, protease inhibitor cocktail (Roche). Rat pup hippocampi were homogenized on ice in RIPA-lysis buffer (1mg tissue/10µl lysis buffer) with a pestle. After homogenization, samples were centrifuged for 20 min at 14 000 rpm at 4 ºC to remove all cell debris and insoluble material. The supernatant was collected into new tubes and the total protein concentration was determined with detergent-compatible DC-Kit (Bio-Rad) measured at 622 nm by microplate reader (Bio-Rad Benchmark). Samples were diluted to a final concentration of 1 µg/µl in 6x sample loading buffer (1× sample loading buffer contained 1.7 % SDS, 60 mM Tris-HCl pH 6.8, 5 % glycerol, 100 mM dithiothreitol (DTT) and a trace amount of bromophenol blue).

4.2.5.3 SDS-PAGE with pre-cast gradient gels, protein transfer and immunostain

Twenty µg of protein were applied per well on a pre-cast Tris-HCl 4-20% gradient gel (Criterion, Bio-Rad) and separated under denaturating conditions (120V ~ 2h), where after transferred onto a 0.2 µm polyvinylidene difluoride (PVDF) (BioRad) membranes (100V 40 min). PVDF membranes were incubated for 1-2 h in blocking buffer (5 % non-fat milk in Tris buffered saline (137 mM NaCl, 20 mM Tris, pH 7.6) containing 0.05 % Tween (TBS-T)) and then overnight at 4 °C with primary antibodies against: rabbit-anti-NR1 aa 909-938 (AB9864 Chemicon 1:800, 0.03-0.16 µg/ml), mouse-anti-NR1 aa 660-811 (556308 BD Pharmingen 1:800, 0.6 µg/ml), rabbit-anti-NR2A (AB1555P Chemicon 1:300, 0.67 µg/ml), rabbit-anti-NR2B (NB300-106 Novus Biological 1:300, 0.67 µg/ml) and rabbit-anti-β-actin (A2066 Sigma-Aldrich 1:500, 1.4 µg/ml). Membranes were rinsed 3x TBS-T and incubated

with secondary antibodies; either with peroxidase-labelled anti-rabbit or anti-mouse (SigmaAldrich) for 1-1.5 h. After washes with TBS-T and the membranes were incubated for 10 min with Enhanced Chemi-Fluoresence (ECF)-substrate (Amersham Biosciences) to produce a fluorescent signal which was scanned on a Typhoon 9410 scanner (Amersham Biosciences) (at 532 nm).

4.2.6 Quantitative reverse transcriptase PCR (qPCR) - Sample collection, RNA isolation, cDNA synthesis and qPCR

Slice cultures from four to five different animals were collected at different time points after OGD (1 h, 3 h, 4 h and 24 h), pooled together and stored in RNAlater (Ambion) at -20 ºC. The RNA isolation was performed with RNeasy RNA isolation kit (Qiagen) and the DNAse treatment with RNase-free DNase set (Qiagen) according to the manufacturer's instructions. The RNA concentration was quantified using NanoDrop (NanoDrop Technologies, Wilmington, USA) UV spectrometry, and RNA with the A_{260}/A_{280} ratio 1.9-2.1 was converted further into cDNA (0.04 µg RNA/µl reaction) using High Capacity cDNA Archive Kit (Applied Biosystems). The expression of different NMDAR subunits was measured using TaqMan assays: Rn01436034_m1 (NR1, all splice variants), Rn01424654_m1 (NR2A) and Rn00680474_m1 (NR2B) (Applied Biosystems) and standardized to rGAPDH (Rn99999916_s1) control, on a 7900 HT Fast Real-Time PCR System (Applied Biosystems).

CHAPTER 5 RESULTS

5.1 VALIDATION OF ORGANOTYPIC HIPPOCAMPAL SLICE CULTURES AS AN *IN VITRO* MODEL TO STUDY NMDA MEDIATED CELL DEATH

5.1.1 Expression profile of NR1, NR2A and NR2B subunits of the NMDARs in organotypic slice cultures is comparable to that *in situ*

The most commonly expressed NMDARs in the mammalian CNS are composed of two NR1 subunits and either NR2A and/or NR2B (Kohr, 2006). NR2A and NR2B subunits are expressed differently during development: the NR2B-subunit already from the early developmental stages, whereas NR2A starts appearing postnatally (Monyer et al., 1994; Sheng et al., 1994; Watanabe et al., 1992). I set out to investigate whether the expression and subunit profile of NMDAR subunits in slice cultures are comparable with those *in situ*. Protein expression levels of each subunit were assessed at different *days in vitro* (DIV0, DIV7, DIV14 and DIV21). Extracts from rat organotypic slice cultures were compared with extracts obtained from rat hippocampi dissected from animals at postnatal days 6, 12, 19 and 26 (P6, P12, P19 and P26). Organotypic slice cultures were prepared from P6 rat pups (corresponding to DIV0 *in vitro*) and grown for two weeks till DIV14. DIV0 material corresponds to slice cultures that were collected at the day of the preparation following 6 h recovery at 37 °C. I found that protein levels of the NR1, NR2A and NR2B subunits in slice cultures from DIV7 to DIV21 (corresponding to P14 and P26 *in situ*) were strikingly similar to the ones *in situ* (Fig. 4A-C). The NR1 and NR2B subunits were strongly expressed throughout development *in situ* (Fig. 4A, C) while the NR2A subunit displayed a gradual up-regulation (Fig. 4B). The most striking *in vitro* result was the pronounced reduction of protein levels for all the NMDAR subunits at the day the slices were prepared (DIV0; cf. levels at P6). The expression of the NR1 subunit was investigated with two antibodies recognizing two different epitopes. The BD Pharmingen NR1 antibody recognizes an extracellular epitope common to all NR1 splice variants, while the Chemicon NR1 antibody recognizes an intracellular epitope common to four different splice variants found at high concentrations in hippocampus (Collingridge and Watkins, 1994). Both antibodies produced similar NR1 expression patterns and protein levels both in the *in vitro* and *in situ* material (Fig. 4A).

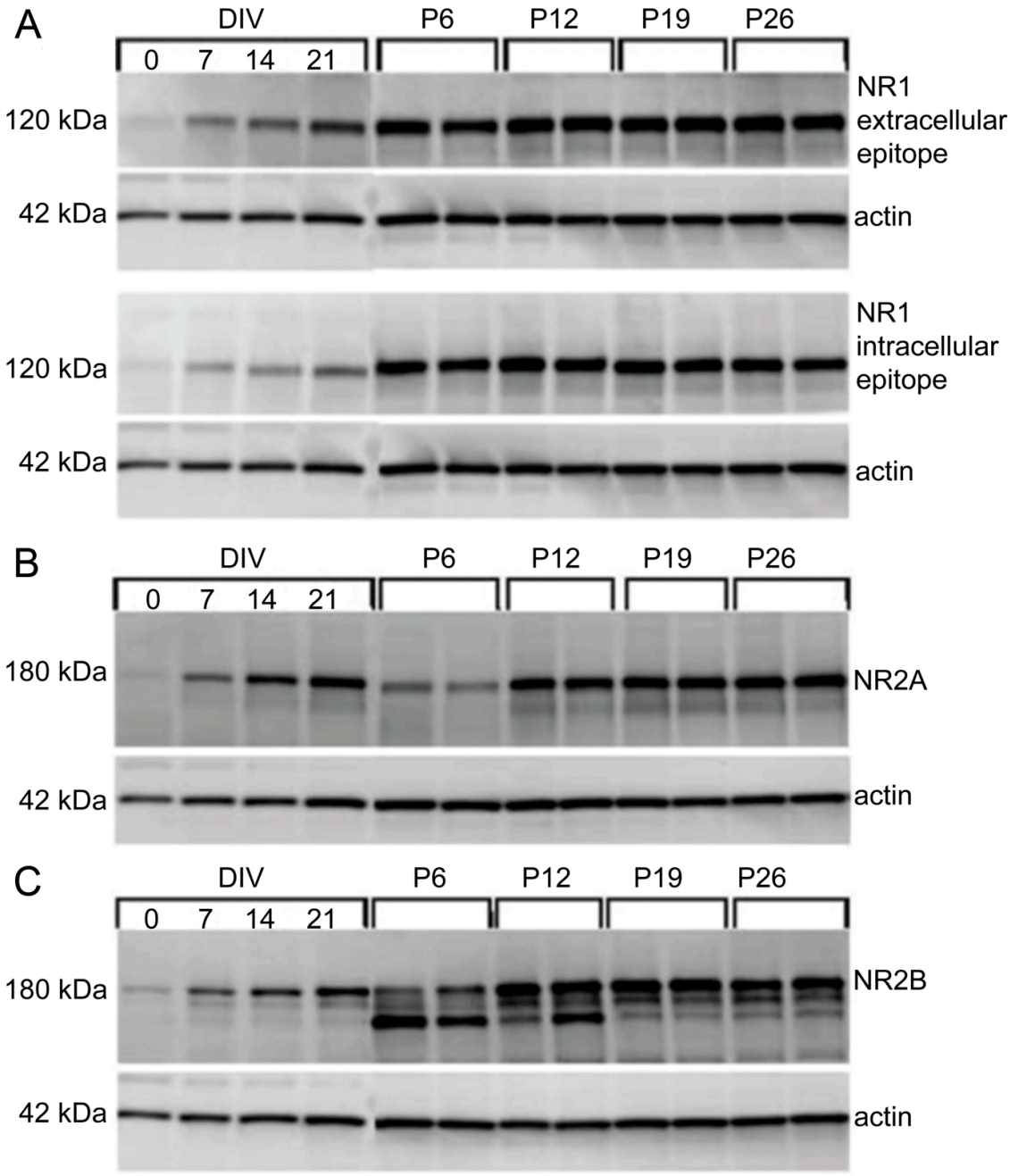

Figure 4. NMDA receptor subunit expressions *in vitro* and *in situ* – developmental comparison between rat hippocampal organotypic cultures and rat pup hippocampi. ***A-C***, Representative Western blots of extracts from organotypic hippocampal slice cultures at different days *in vitro* (DIV) (0, 7, 14 and 21) and extracts from rat hippocampi at corresponding postnatal days (P) (6, 12, 19 and 26). Blots were labelled with antibodies against an extracellular epitope of the NR1 subunit (***A***, upper panel) an intracellular epitope of the NR1 subunit (***A,*** lower panel), the NR2A subunit (***B***) and the NR2B subunit (***C***). β-actin was used as a loading control. Material *in vitro* consisted of n = 4-5 animals per group (4-5 slices from 4-5 animals pooled together per group) and *in situ* n = 2 animals per group.

Characteristic for the *in situ* situation, and weakly for *in vitro*, was the appearance of three high molecular weight (MW) bands for NR2B. The relative density of these bands changed as a function of age, with the lowest MW band at ~140 kDa being predominant at P6 (Fig. 1C) and the highest band at ~180 kDa being predominant at P19 and P26 (Fig. 4C). Antibody specificity for the NR2 subunits was tested in adult mice with either global deletion of the gene encoding NR2A (*NR2A*$^{-/-}$) or with conditional deletion of the gene encoding NR2B (*NR2B*$^{\Delta fb}$).

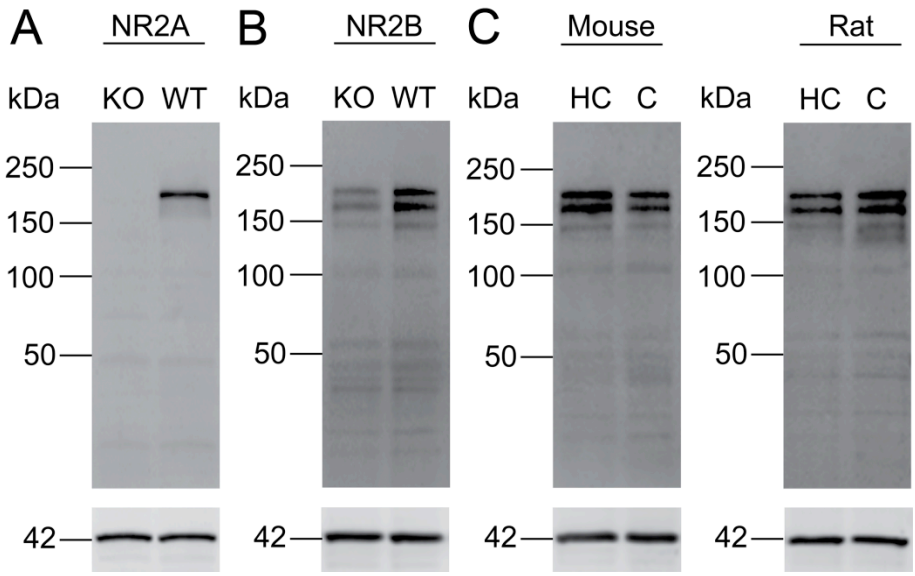

Figure 5. Western blots confirming the specificity of NR2 subunit antibodies. ***A,*** Representative blot of NR2A subunit antibody tested on forebrain material from adult NR2A knock out mice (KO) and their control littermates (WT). ***B*****,** Representative blot of NR2B subunit antibody tested on forebrain material from adult conditional forebrain-specific NR2B knock out mice (KO) and their control littermates (WT). ***C***, Representative blot of NR2B subunit antibody tested on hippocampal (HC) and cortical (C) material from adult wild type mice and rat.

The NR2A signal was abolished in the NR2A KO material (Fig. 5A). For NR2B a residual signal remained in tissue from the *NR2B*$^{\Delta fb}$ mice, probably reflecting NR2B in GABAergic interneurons (Sakimura et al., 1995; von Engelhardt et al., 2008) (Fig. 5B). A mosaic expression pattern (Clark et al., 1994), including a residual signal, can often be observed in conditionally modified knock out mice. Each of the three high-MW bands for NR2B was attenuated (Fig. 5B), indicating that they represent *bona fide* NR2B immunoreactivity.

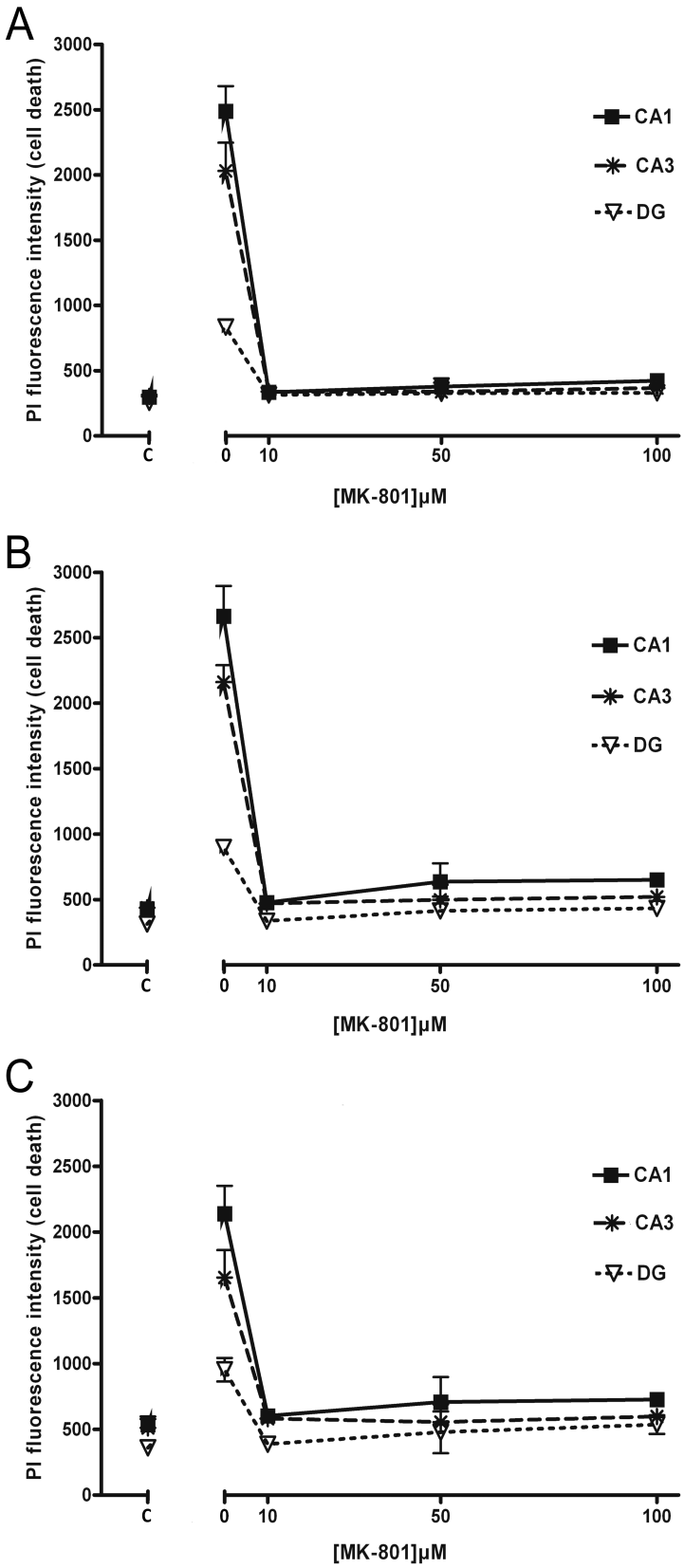

Figure 6. NMDA-induced excitotoxic cell death in organotypic slice cultures - an effect blocked by MK-801. ***A-C*****,** Cell death induced by NMDA (150 µM 15 min) in presence or absence of the NMDA receptor antagonist, MK-801 at the concentrations

indicated. Cell death was assessed by propidium iodide (PI) fluorescence intensity in the different hippocampal sub-regions (CA1, CA3 and dentate gyrus (DG)). Cell death was assessed 24 h (***A***), 48 h (**B**) and 72 h (**C**) after NMDA treatment. $p < 0.05$ for all hippocampal sub-regions at each time-point in the presence of MK-801 compared with solely NMDA. Data are presented as mean ± standard error of the mean (SEM). $n \geq 4$ for all groups.

The three bands obtained with the NR2B antibody (see Fig. 4) were reproduced in extracts from hippocampus and cerebral cortex of both WT mice and rats (Fig. 5C), ruling out the possibility of species or regional differences. Taken together, despite the initial reduction of protein levels at DIV0, at DIV14 organotypic cultures displayed a similar protein expression profile of the NMDAR subunits as *in situ* and thus are representative for the *in vivo* situation. I conclude that organoptypic slice cultures display a representative model to study NMDAR mediated responses.

5.1.2 NMDARs expressed in organotypic hippocampal slice cultures induce excitotoxic cell death at DIV14

NMDARs are important in mediating both neuronal survival and death (Hardingham and Bading, 2010). I next wanted to test whether NMDARs expressed in slice cultures were functional in inducing cell death. I exposed slice cultures to high concentrations (150 µM) of NMDA to induce excitotoxicty in presence or absence of the open channel blocker MK-801. This approach allows blockage of only the activated NMDARs (Fig. 6). We observed NMDA-induced cell death in all hippocampal sub-regions. The cell death was antagonized by MK-801 at all applied concentrations (10, 50, or 100 µM) in all sub-regions at all-time points (24, 48, and 72 h) after the NMDA exposure (Fig. 6A-C). I concluded that endogenous NMDARs in slice cultures at DIV14 are functional and capable of inducing excitotoxic cell death.

5.1.3 OGD-induced cell death is only partially prevented by NMDAR blockade in organotypic hippocampal slice cultures

Classical OGD-induced cell death in hippocampus is characterized by selective neuronal death in the CA1 region appearing 48 to 72 h after recovery from a 10 to 15 min ischemic insult (Kirino, 1982; Kirino et al., 1984). To gain a similar temporal pattern of cell death in organotypic hippocampal slice culture model I mimicked the changes in ion distribution observed during anoxic depolarization *in vivo* (Hansen, 1985) and modified the iCSF-medium used in OGD-experiments by

reducing the pH, [Na^+], [Ca^{2+}] and increasing [K^+] (Rytter et al., 2003). The reduced extracellular Ca^{2+} concentration (0.3 mM) offered a sufficient extracellular Ca^{2+}-gradient to support excitotoxcity as previously reported (Noraberg, 2004; Rytter et al., 2003). The observed OGD-induced cell death was delayed, appearing around 24 h post-OGD and increasing until 72 h post-OGD. The effect was most pronounced in the vulnerable CA1 region (Fig. 7A, B).

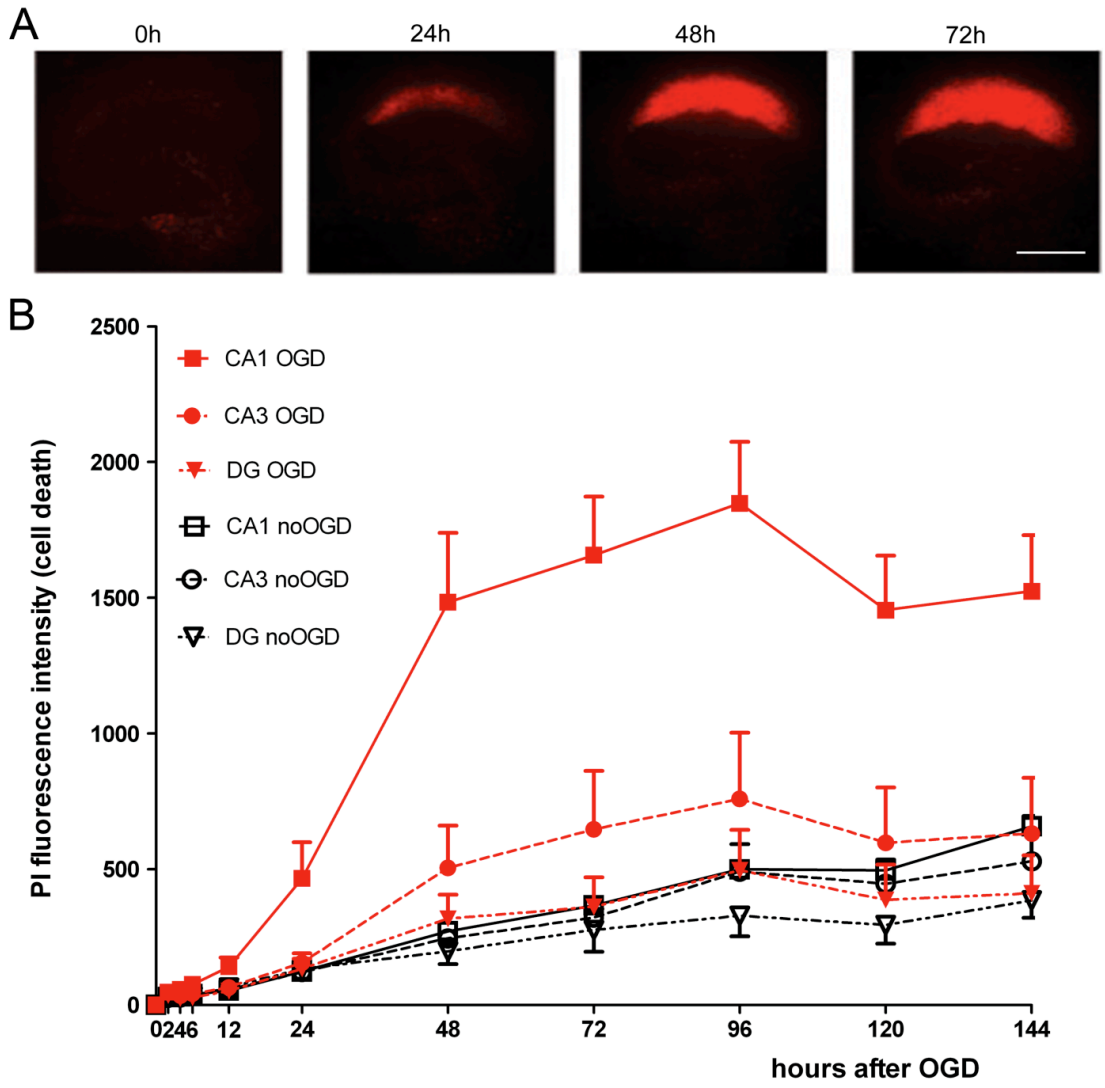

Figure 7. OGD induces delayed cell death induced in organotypic hippocampal slice cultures. ***A,*** Representative images of PI labelling in the CA1 region at the indicated times after OGD treatment. Scale bar 0.5 mm. ***B,*** Quantification of cell death for different hippocampal sub-regions at the indicated times after OGD treatment. The drop in the curves between 96 and 144 hours is probably due to PI-fluorescence bleaching. OGD was induced by incubation in glucose deprived ischemic cerebral spinal fluid (iCSF) in an anaerobic chamber. Cell death was measured in the different sub-regions (CA1, CA2 and DG) by PI-fluorescence intensity. Data presented as mean ± SEM., n= 4 (4-10 slices per group).

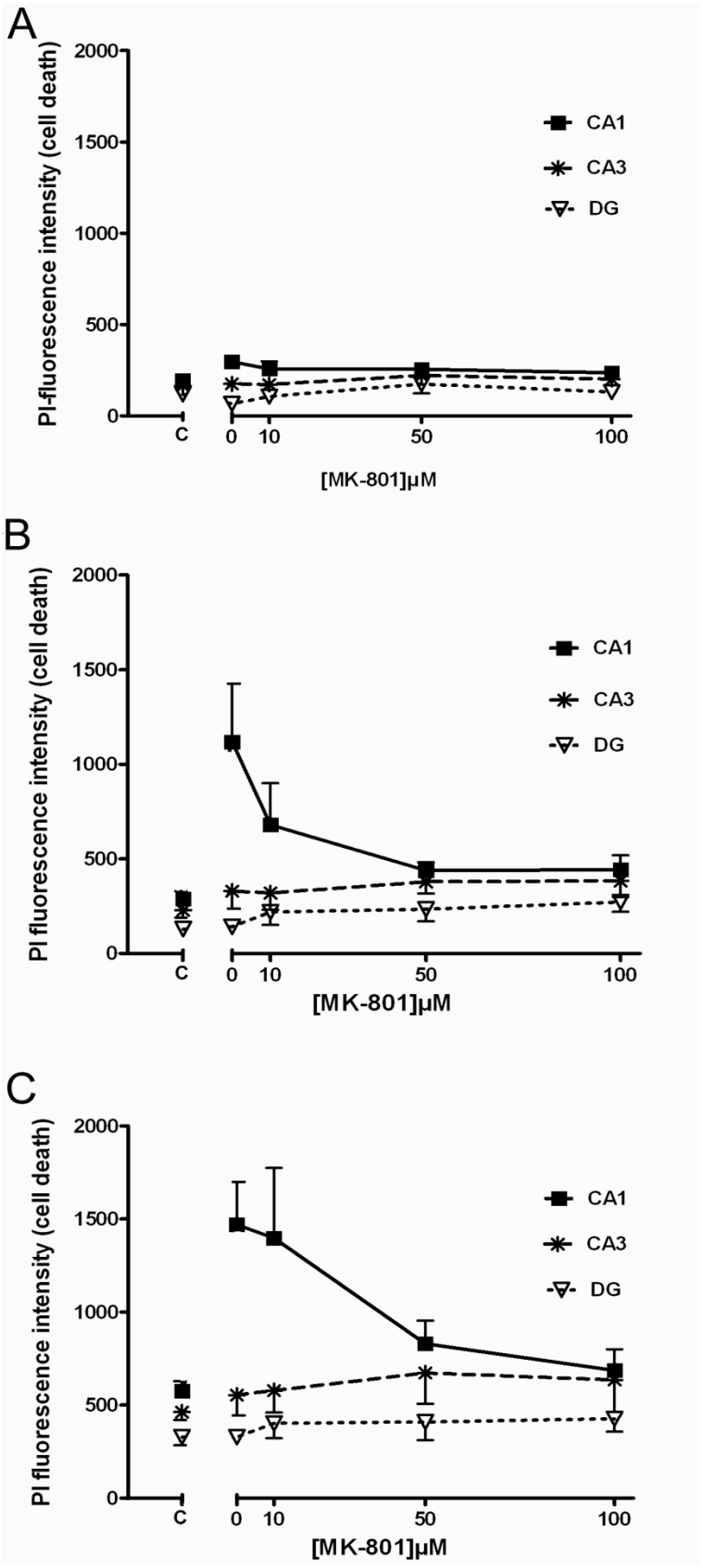

Figure 8. OGD induced cell death is partially blocked by MK-801. ***A-C*****,** Cell death induced by OGD in presence or absence of the NMDA receptor antagonist, MK-801 at concentrations indicated in the hippocampal subregions (CA1, CA3 and

DG) was assessed by propidium iodide (PI) fluorescence intensity at 24 h (***A***), 48 h (**B**) and 72 h (**C**) after the OGD insult. $p < 0.05$ for all hippocampal sub-regions at 48 h post-OGD in the presence of 50 and 100 µM MK-801 and $p < 0.05$ for or all hippocampal sub-regions at 72 h post-OGD in the presence of 100 µM MK-801. Data are presented as mean ± SEM. $n \geq 5$ for all groups.

Next the involvement of NMDARs in OGD-induced cell death was investigated. OGD was applied in presence or absence of the (+) MK-801 stereoisomer, which blocks with similar IC_{50} values both NR2A and NR2B containing NMDARs. The (+) isomer is more pH stable than the (-) MK-801 stereoisomer (Dravid et al., 2007), a property which is critical as during OGD the pH drops approximately 1-unit to ~ 6.5-6.8 by use of iCSF to mimic pH changes occurring during ischemic conditions *in vivo* (Nedergaard et al., 1991).

The MK-801 concentration needed to obtain neuroprotection increased with time after the insult (Fig. 8B, C). Protection against cell death was obtained with MK-801 at 50 µM and 100 µM (48 h post-OGD) (Fig. 8B) or 100 µM (72 h post-OGD) (Fig. 8C). MK-801 at 10 µM failed to offer significant protection (Fig. 8). These results suggest that blocking only NMDARs at delayed cell death does not offer complete protection.

5.1.4 The excitotoxic effects of NMDA and OGD are not additive

Although the (+) MK-801 stereoisomer in contrast to (-) MK-801 is pH stable (Dravid et al., 2007) we wanted to ascertain that the low efficacy did not reflect pH-mediated inhibition of NMDAR responses (Tang et al., 1990). Therefore, the slice cultures were exposed to OGD in iCSF in the presence of NMDA (200 µM). NMDA was found to induce excitotoxic cell death with similar potency under conditions of OGD with its associated lowered pH (Fig. 9) and under control conditions with physiological pH (Fig. 6). Exposure to OGD induced the same extent of cell death as NMDA alone; however, the development of cell death was delayed and produced similar amount of cell death at 48 h and 72 h. These data indicate that the low efficacy of MK-801 is not due to proton block of the NMDARs as NMDA induced excitotoxic cell death with the same potency regardless of whether the pH was reduced or physiological (Figs. 6, 9).

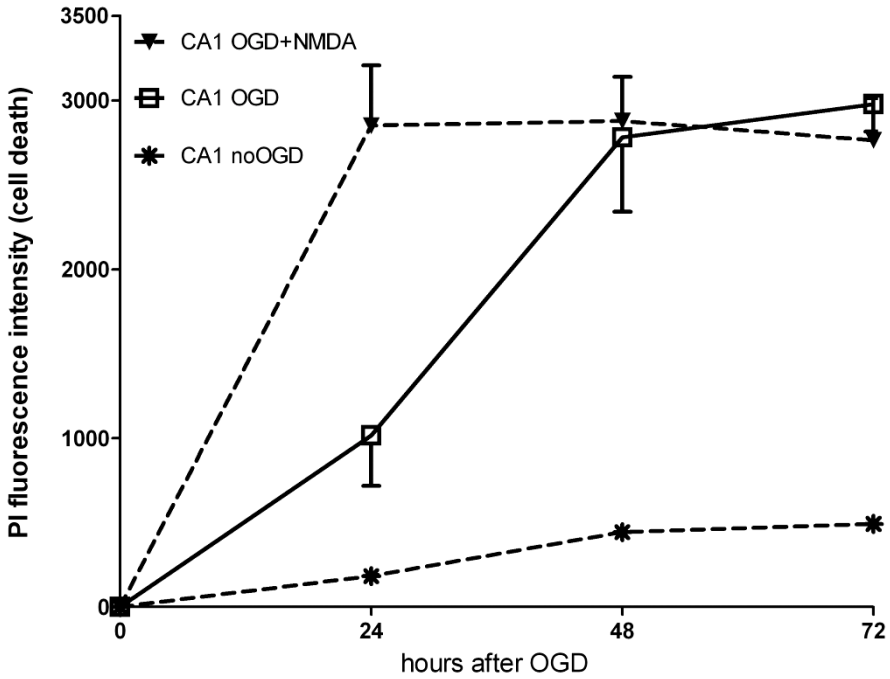

Figure 9. NMDA induces a similar extent of cell death at ischemic low pH and at physiological pH. The time course of NMDA-induced cell death at low pH (6.8) and at physiological pH (7.4). OGD was induced by incubation in glucose deprived ischemic cerebral spinal fluid (iCSF) in an anaerobic chamber in presence or absence of NMDA (200 µM). Cell death was measured in the different subregions (CA1, CA2 and DG) by PI-fluorescence intensity. Data are presented as mean ± SEM., n = 4.

5.1.5 No significant changes in mRNA levels of NR1, NR2A or NR2B after OGD

Previous reports on organotypic hippocampal slice cultures have described an immediate down-regulation of all NMDAR subunit mRNA levels after OGD, with partial recovery after 3 h (Dos-Anjos et al., 2009). I next investigated whether an early down-regulation of NMDAR expression during the acute response could explain the observed reduced protection of MK-801 against cell death at extended time-points (i.e., 72 h; see Fig. 8). I compared NR1, NR2A and NR2B mRNA expression levels at different time points (1, 3, 4 and 24 h) after OGD with corresponding control groups. I found that NO OGD controls showed stable mRNA levels over the 24 h period (Fig. 10A) and moreover, none of the NMDAR subunits displayed statistically significant changes in mRNA levels at 1 h, 3 h, 4 h or 24 h post-OGD (Fig. 10B). I concluded that OGD does not produce acute down-regulation of NMDAR expression, and additionally, oragnotypic slice cultures offer a reliable model to study gene expression changes post-OGD based on stable control values**.**

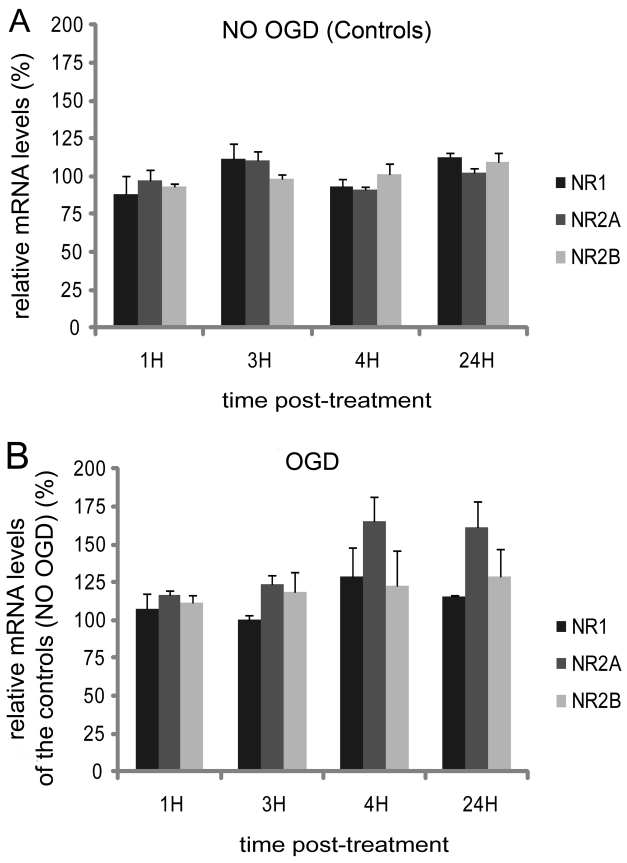

Figure 10. No evidence of NMDAR mRNA down regulation after OGD. ***A, B,*** Graphs show the quantification from TaqMan real-time PCR of mRNA isolated from organotypic slices subjected to OGD (iCSF) (**B**) or to control treatment (aCSF; i.e., NO OGD) (**A**). The graphs represent results from one experiment in three individual runs. NO OGD groups are normalized to the average of NO OGD controls**.** (***A***). The OGD groups are standardized to the NO OGD control at each respective time-point (***B***). NMDAR Ct-values were relative to the housekeeping gene, GAPDH and normalized to the control group for each time point. For each data point slices from 4-5 animals pooled together. Data are presented as mean ± SEM.

5.1.6 No NR2 subunit difference in mediating neuronal cell death.

NR2B subunits in particular have been implicated in neuronal cell death during brain ischemia (Liu et al., 2007). I wanted to examine whether blocking of NR2B-containing NMDARs offer a better protection against OGD- and NMDA-induced cell death. OGD and NMDA cell death assays were preformed in presence of the non-competitive NR2B blocker Ro 25-6981. Ro 25-6981 was bath applied at 0.5 µM, a concentration that block NR2B subunit-containing NMDARs selectively (Mutel et al., 1998), and has been reported to protect against ischemic cell death (Liu et al., 2007). An additional higher concentration of Ro 25-6981 (2.5 µM) was tested in OGD-experiments due to the observed higher dose dependency of MK-801 in delayed cell death. I found no protective effect by blocking NR2B subunit containing NMDARs at the two concentrations, neither in NMDA-induced nor in OGD-induced cell death assays (Fig. 11A, B, C).

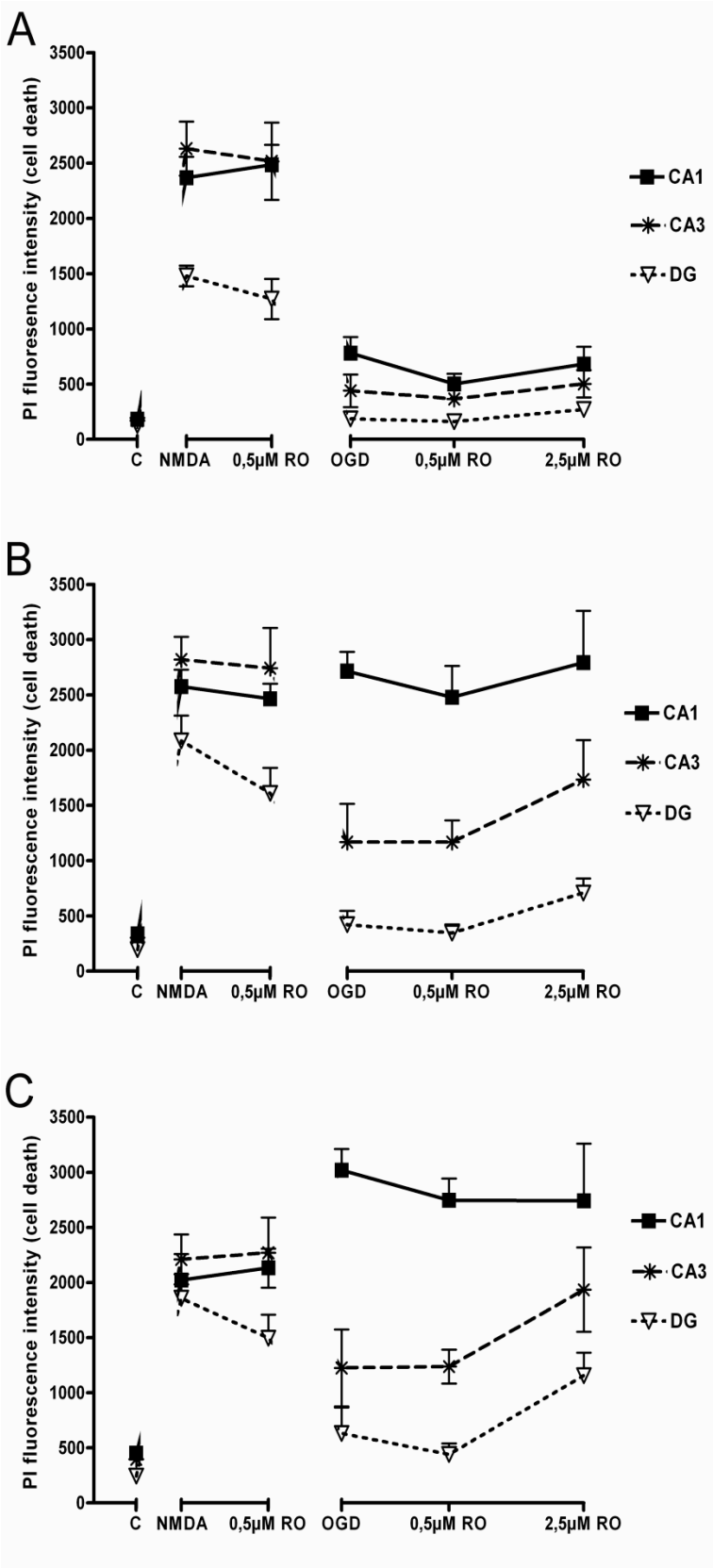

Figure 11. No protection offered by a NR2B subunit specific inhibitor during NMDA and OGD induced cell death in organotypic slice cultures.

Graphs show cell death induced either by NMDA or OGD in the presence or absence of the NR2B receptor antagonist, Ro 25-6981 in concentrations as indicated. Cell death in the different hippocampal sub-regions (CA1, CA3 and DG) was assessed by propidium iodide (PI) fluorescence intensity at time-points 24 h (***A***), 48 h (**B**) and 72 h (**C**) after NMDA or OGD treatment. For all hippocampal sub-regions at all time-points NMDA or OGD induced PI fluorescence intensity was not reduced by RO 25-6981 at either concentration. Data are presented as mean ± SEM. n = 4 for all groups.

Furthermore, CP101.606 (10 µM), another antagonist of NR2B containing NMDARs, failed to show any neuroprotective effect (data not shown). CP101.606 has been shown to be more potent than Ro 25-6981 in blocking NR2B-mediated currents in NR2A KO mice (Berberich et al., 2007). Based on my pharmacological data I concluded that the activity of NR2B subunit-containing NMDARs in our model of organotypic slice cultures is not central in mediating neuronal cell death.

5.2 INCREASED SYNAPTIC ACTIVITY AND ATF3 PROTECTS AGAINST DENRITIC

5.2.1 Dendritic beading, subsequent changes in network activity and cell death correlate with lethal NMDA concentrations

With mild or sublethal excitotoxic stimuli formation of dendritic beadings are reversible in cortical and hippocampal *in vitro* preparations (Faddis et al., 1997; Hasbani et al., 1998; Hasbani et al., 2001a; Ikegaya et al., 2001; Park et al., 1996). Dissociated hippocampal neurons display an increased vulnerability to excitotoxic stimuli with age (Brewer et al., 2007). Therefore, I first determined in our hippocampal cultures the dose response relationship between NMDA concentration and the resultant dendritic damage immediately following the insult and the neuronal cell death apparent at a 24 h time point. Hippocampal cultures at DIV14-15 were subjected to NMDA bath application with different NMDA concentrations for 10 min and fixed for morphological evaluation after 0 h, 2 h or 4 h or 24 h recovery period. Cell death was assessed by analysis of nuclear morphological changes visualized with Hoechst staining. Visualization of neurons for dendritic damage (focal dendritic swellings) was achieved by transfection with a plasmid containing an expression cassette for EGFP under the control of a CaMKII promoter. NMDA bath application generated dendritic beadings throughout the whole dendritic arbor (Fig. 12C). Low NMDA concentrations (2.5 to 10 µM) induced pronounced, but transient dendritic

beadings, which partially or fully disappeared during a 4 h recovery period. At higher NMDA concentrations (20-30 µM) the dendritic structure displayed hardly any structural recovery (Fig. 12A). Cell death displayed a similar dose-response pattern; 10 µM NMDA induced a slight increase in cell death whereas higher NMDA concentrations accentuated cell death when compared to control 24 h post-NMDA application (Fig. 12B).

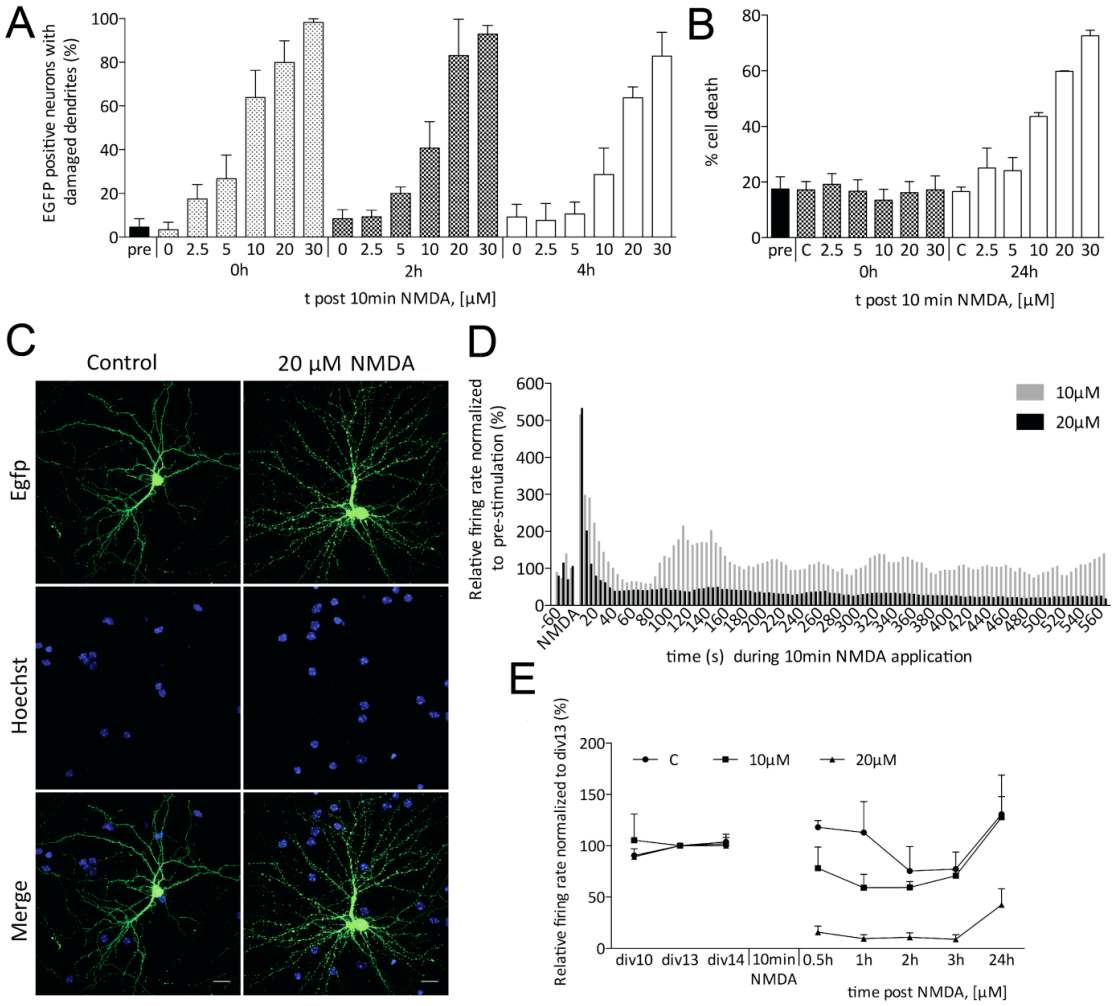

Figure 12. Dendritic damage, cell death and network activity responses are dependent on the magnitude of excitotoxic stimuli. ***A-C,*** Dissociated mouse hippocampal cultures at DIV14-15 were challenged with 2.5, 5, 10, 20 or 30 µM bath-applied NMDA for 10 min, and fixed for morphological evaluation after a recovery period of 0 h, 2 h or 4 h (dendritic damage) or 24 h (cell death). Neuronal cultures were transfected with an EGFP construct for individual cell visualization and nuclei were counterstained with Hoechst33258 for cell death analysis. Cell death and dendritic damage was evaluated based on morphological alterations (for details, see Material and Methods). Dose-response analysis of NMDA-induced dendritic damage presented as a percentage of EGFP positive neurons (***A***). Dose-response analysis of NMDA-induced cell death as a percentage of whole cell population (***B)***.

Representative image of a hippocampal neuron expressing EGFP before and after 20 µM NMDA bath application. Scale bar 20 µm (***C***). ***D***, ***E,*** Microelectrode array (MEA) analysis of network activity in response to 10 and 20 NMDA [µM]. Traces shown are representative of an acute response to 10 min NMDA bath application (***D***). Synaptic transmission measured 24 h post- NMDA application (***E***). Data presented as mean + SEM.

Dendrites are the major postsynaptic structures for synaptic transmission and dendritic beading induces long lasting depression in synaptic transmission in hippocampal slice cultures (Ikegaya et al., 2001). Network activity in dissociated hippocampal cultures reflects synaptic transmission (Arnold et al., 2005). Thus, next microelectrode arrays (MEA) were used to assess the effects of bath application of 10 or 20 µM NMDA on network activity (bursting frequency) in dissociated hippocampal cultures. Application of either concentration of NMDA induced a short-lived ~ 30 s increase in activity. However, while the cultures treated with 10 µM NMDA returned to activity levels slightly above control levels during NMDA treatment, cultures treated with the higher concentration showed a marked reduction in network activity for the remaining period of the NMDA treatment (Fig. 12D). During the 24 h period following washing out of NMDA, cultures that had received 10 µM, displayed slightly reduced or identical activity levels compared to control treatment (medium change). In contrast, cultures treated with 20 µM showed prolonged suppression of activity (Fig. 12E). Similar to the dramatic difference in dendritic swelling and cell death induced by 10 and 20 µM NMDA, network activity 24 h after NMDA application was strongly reduced in cultures treated with 20 µM NMDA whereas cultures treated with 10 µM NMDA displayed normal activity (Fig. 12E). Taken together, 10 µM NMDA bath application results in reversible dendritic beading and a slight increase in cell death but the remaining neuronal population is likely sufficient to re-establish baseline levels of network activity (Fig. 12E). Thus, I concluded that the threshold to induce permanent dendritic damage that precedes pronounced cell death in our model is 20 µM NMDA based on the morphological and functional data (Fig. 12A-B, 12E).

5.2.2 Excitotoxicity induces in hippocampal neurons rapid morphological changes consisting of dendritic beading and rounded mitochondria

Dendritic beading coincides with mitochondrial rounding, another early ultra-structural change during neuronal damage (Greenwood et al., 2007; Rintoul et al., 2003). Under physiological conditions mitochondria display an elongated morphology (Macaskill et al., 2009; Rintoul et al., 2003). Dendritic beading appears within approximately 5 min of the onset of a prolonged depolarization both *in vitro* (Andrew et al., 2007) and *in vivo* in intact mouse cortex and striatum (Li and Murphy, 2008; Murphy et al., 2008), coinciding with the time-frame of mitochondrial rounding *in vitro* (Greenwood et al., 2007; Rintoul et al., 2003). Thus, confocal live time-lapse imaging and electron microscopy (EM) studies were performed to further characterize the time-resolution and morphological alterations of acute neuronal damage in dissociated hippocampal cultures. For simultaneous live imaging of dendrites and mitochondria, hippocampal neurons were co-transfected with plasmids containing expression cassettes for EGFP and mitochondrial targeted mCherry under the control of CaMKII promoter. Time resolution of this imaging was limited to 5 min in order to collect a z-stack of the dendritic arbor at each time-point. This was necessary to ensure the capture of dendritic structures, which change their focal plane during swelling. Imaging was performed according to the time scheme shown in Fig. 13A. I observed that dendritic beading and mitochondrial rounding in general appeared 2-7 min after adding NMDA (Fig. 13B). Dendritic beadings were EGFP dense, but did sometimes display EGFP void structures that overlapped with mitochondrial structures whereas the structures linking the beads had the appearance of thin strings (Fig. 13B). EM studies revealed more detailed information of the dendritic ultra-structure before and after 10 min NMDA bath application (Fig. 13D). The neurons in the control group had intact dendrites with elongated mitochondria, intact microtubules and endoplasmic reticulum. Neurons treated with NMDA displayed focal beadings on dendrites as observed with confocal analysis. Dendritic focal beadings were predominantly empty structures, however, some exhibited fragmented microtubules, rounded mitochondria and swollen endoplasmic reticulum. The structures between the beadings were void of larger organelles, consisting largely of tightly packed microtubuli and filaments. Pre-synaptic terminals in NMDA treated cultures were morphologically similar to the control group.

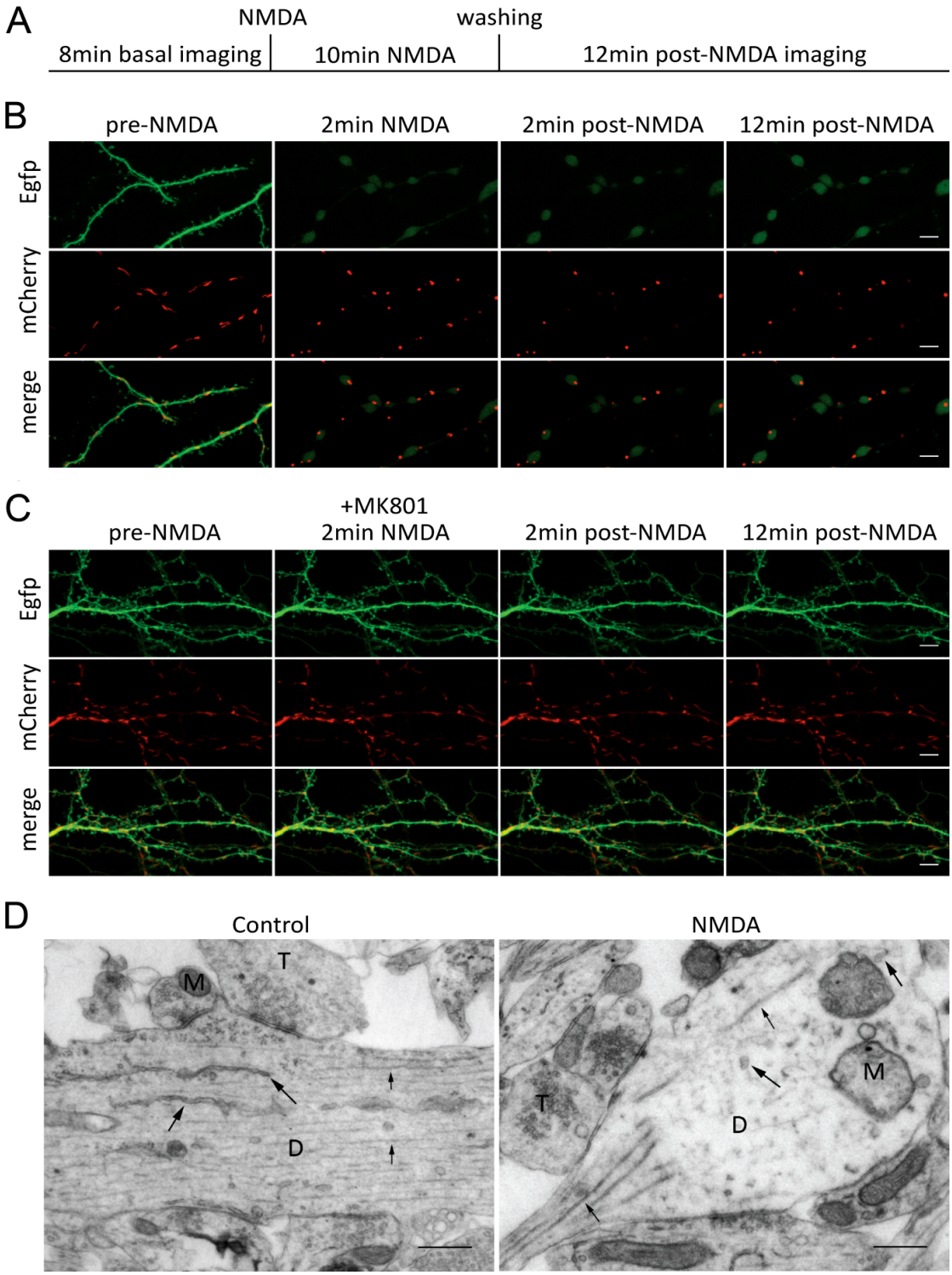

Figure 13. Rapid ultra-structural changes in hippocampal neurons in response to excitotoxic neuronal damage. ***A-C,*** Confocal live time-lapse imaging of hippocampal neurons expressing EGFP and mitochondrial targeted mCherry. Shown is the time-scheme used for live imaging (***A).*** Images are single plane projections of z-stacks at the indicated times before, during and after washout of 10 min NMDA (20 µM) application. Scale bars 5 µm. (***B).*** As in B except that the NMDAR open channel blocker MK-801 (20 µM) was included (***C***). ***D***, Electron microscopy (EM) studies on

dissociated hippocampal neurons ultra-structure. Representative images of neuronal dendrites in control group, and after NMDA (20 µM) treatment. Scale bar 0.5 µm. (D = dendrite, M = mitochondria, T= pre-synaptic terminal, microtubule and filaments are indicated by thin arrows, endoplasmic reticulum by a fat arrow).

Similar microtubule dense string-like dendritic structures linking beads has been observed *in vivo* on ultra-structural level in hippocampal CA1 in an in vivo model of brain ischemia (Petito and Pulsinelli, 1984)

In vitro both morphological alterations are considered to be initiated by NMDAR- mediated prolonged depolarization (Hasbani et al., 2001b; Park et al., 1996; Rintoul et al., 2003). Therefore, I next challenged the cultures with NMDA in combination with the open channel blocker MK-801 (20µM). I found that in the presence of MK-801 both dendritic beading and mitochondrial rounding were blocked (Fig. 13C). Dendritic beading was also abolished in the presence of the competitive NMDAR blocker APV (50 µM; data not shown). During live imaging I came across unexpected quenching of the EGFP signal during NMDA treatment (Fig. 13B). After NMDA washout the signal re-appeared, particularly at the focal dendritic beadings. Similar observations have earlier been reported (Andrew et al., 2007; Risher et al., 2009). For these reasons, it was not possible to analyze the spine structure during the initial steps of the excitotoxic damage. Taken together, the time-resolution of morphological changes in dissociated hippocampal neurons upon a prolonged NMDA exposure are in agreement with other studies using primary hippocampal cultures and with studies both *in vitro* and *in vivo*. I show that dendritic damage in dissociated hippocampal cultures produces similar ultra-structural changes to those occurring *in vivo* and substantiate the use of dissociated hippocampal cultures as a suitable model system when studying acute neuronal damage and dendritic beading.

5.2.3 Synaptic activity protects against acute excitotoxic damage

Increased neuronal activity and consequent activation of synaptic NMDARs has a protective effect against various toxic stimuli including excitotoxcity (Bengtson et al., 2008; Hardingham and Bading, 2010; Hardingham et al., 2002; Lau and Bading, 2009a; Papadia et al., 2008; Papadia et al., 2005; Zhang et al., 2007). Therefore, I investigated the possibility that increased synaptic activity could protect against acute neuronal damage, namely dendritic beading. Synaptic NMDAR activity was increased by treating hippocampal neurons with the $GABA_A$ receptor antagonist

bicuculline (Bic, 50 µM), which removes an inhibitory tone from the neuronal network and leads to bursts of action potentials (AP). AP-bursting leads to an increase in cytoplasmic and nuclear calcium concentrations (Arnold et al., 2005; Hardingham et al., 2002). Bic treatment induced an enlargement of the dendritic spines (Fig. 14A), an indication of synaptic plasticity due to increased synaptic activity (Buchs and Muller, 1996). Sixteen hours after induction of AP-bursting, neurons were challenged with the previously characterized NMDA concentration for 10 min and immediately fixed for morphological evaluation. I observed that groups pre-treated with Bic displayed a lower number of EGFP positive neurons with beaded dendrites compared with non-treated (Fig. 14B). Synaptic activity did not only protect against dendritic damage but also maintained the ATP-levels more stable after an excitotoxic insult (data not shown). These results indicate that increased synaptic activity offers protection against dendritic damage and stabilizes mitochondrial function.

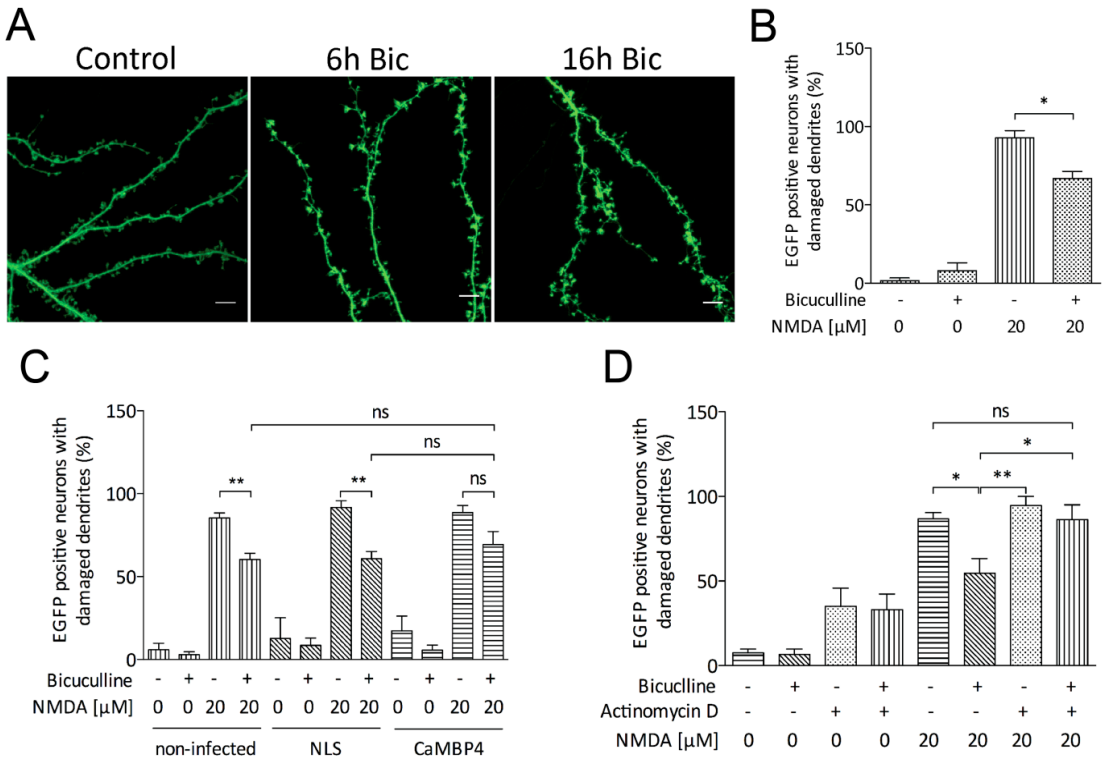

Figure 14. Synaptic activity protects against acute excitotoxic damage in a manner partially dependent upon nuclear calcium signaling. ***A***, Representative confocal images of dendritic spines of EGFP transfected neurons subjected to 6 h and 16 h AP-bursting induced by Bic (50 µM) application. Scale bar 5 µm. ***B-D***, All histograms show the quantification of the percentage of EGFP positive neurons displaying dendritic damage after various treatments. Sixteen h AP-bursting reduces dendritic beading induced by a subsequent exposure for 10 min to 20 µM NMDA ***(B)***.

Analysis of the importance of nuclear calcium signalling for AP-bursting mediated protection against NMDA-induced dendritic damage. Nuclear Ca^{2+}-signaling was blocked by infecting hippocampal neurons at DIV7 with either rAAV-mCherry-CaMBP4 (CaMBP4) or mCherry-NLS (NLS) under CaMKII promoter. Cells were later transfected with EGFP for visual assessment of dendritic damage (***C)***. Analysis of the importance of transcription for AP-bursting mediated protection against NMDA-induced dendritic damage. Transcription was blocked by Actinomycin D (10 µg/ml) incubation prior inducing AP-bursting (***D).*** TTX (1 µM) was included in experiments with CaMBP4 and Actinomycin (***C, D***) during NMDA application to prevent secondary action potential mediated glutamate release. Statistically significant differences are indicated with asterisk; * $p < 0.05$; ** $p < 0.01$, ns = non-significant. Columns represent mean + SEM.

5.2.4 Synaptic activity mediated protection is dependent on gene transcription and partly on nuclear calcium signaling

Synaptic activity mediates long lasting neuroprotection, which is regulated by gene transcription (Hardingham et al., 2002; Papadia et al., 2005; Zhang et al., 2007). Thus, I wanted to investigate if the dendritic protection induced by 16 h preconditioning with AP bursting depended on activity-regulated gene expression. Gene transcription was blocked by incubating neurons with Actinomycin D prior to adding Bic. I observed that the protection was abolished when Bic pre-treatment was done in presence of Actinomycin D (Fig. 14D). However, blocking gene transcription for 16 h with Actinomycin D increased the amount of damaged dendrites in control groups complicating the interpretation of these results and therefore I chose an additional approach to determine the transcription dependency of the activity induced protection. Some of the AP-bursting-induced gene transcription is dependent on nuclear Ca^{2+}-signaling (Hardingham et al., 2002; Papadia et al., 2005; Zhang et al., 2007). Hence, I wanted to investigate if nuclear Ca^{2+}-signaling is involved in AP-bursting-induced protection against dendritic damage. Nuclear Ca^{2+}-regulated events were blocked in neurons by expressing nuclear CaMBP4, a nuclear protein that consists of four repeats of the M13 CaM-binding peptide derived from the myosin light chain kinase; it binds to and inactivates the nuclear calcium/CaM complex (Wang et al., 1995). In all experiments with Actinomycin D and CaMBP4, Bic pre-treatment was terminated with TTX incubation in order to halt all electrical activity to avoid secondary glutamate release following the generation of APs.

I found that by blocking the nuclear Ca^{2+}-mediated signaling with CaMBP4, prior to adding Bic, the protection was partially lost (Fig. 14D). However, no statistical significant difference was found between the Bic pre-treated CaMBP4-

infected group versus the Bic pre-treated group infected with the control virus mCherry-NLS or the non-infected group.

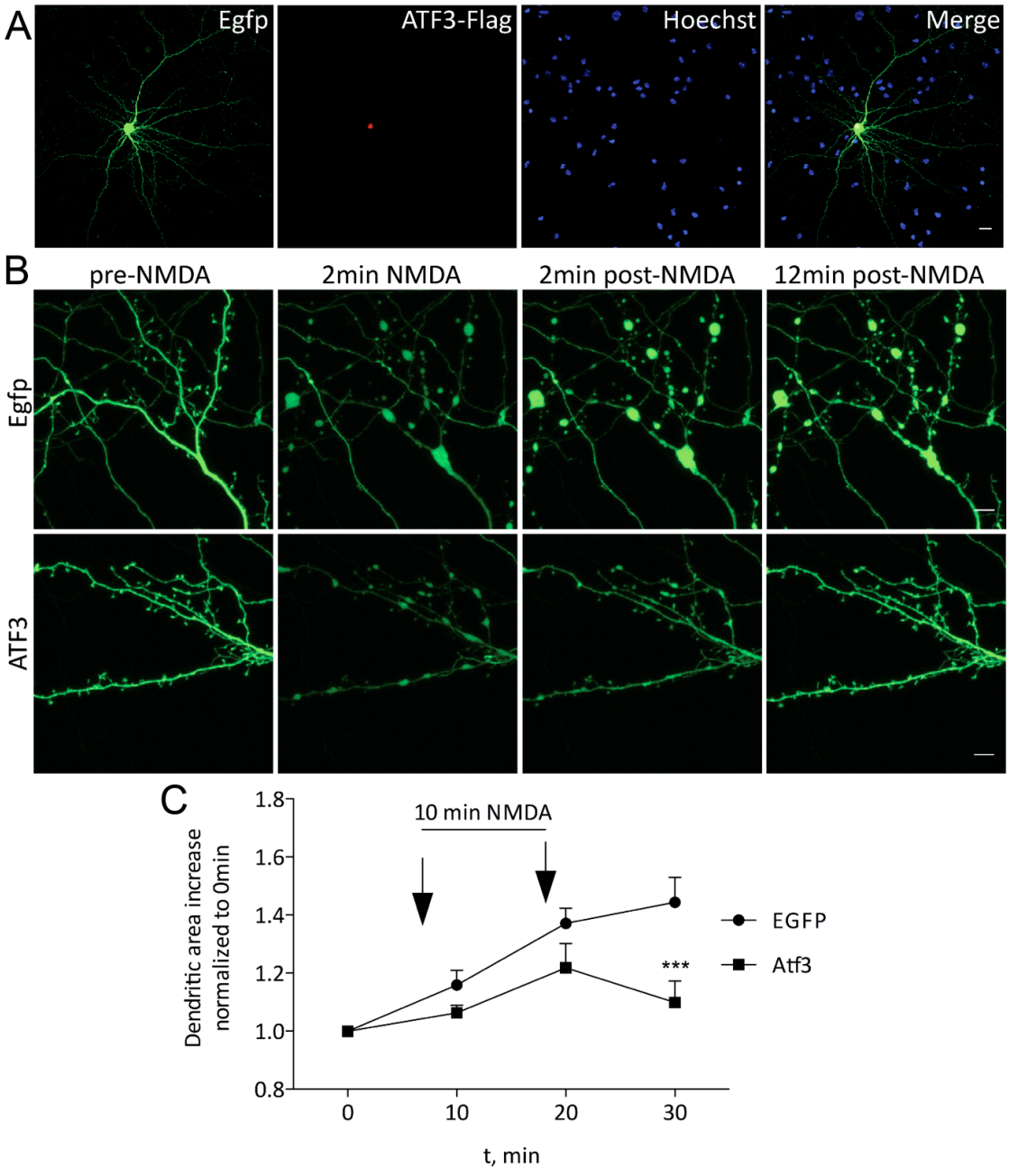

Figure 15. Overexpression of the activity-regulated gene, ATF3, offers protection against the first hallmark of excitotoxic neuronal damage. ***A, B,*** Images are confocal z-stacks projected into one plane showing a representative hippocampal neuronal cultures at DIV14 co-transfected with flag-taged-ATF3 and EGFP at DIV11-12. One hippocampal neuron expressing both EGFP and flag-tagged ATF3 is visible. Scale bar 20 µm ***(A)***. Confocal images showing dendritic beading of an ATF3 overexpressing neuron at the indicated times before and after a 10 min application of 20 µM NMDA. Scale bar 1 µm ***(B). C,*** Quantification of dendritic area of ATF3 overexpressing and control neurons at the indicated time-points after NMDA

treatment. Statistically significant differences are indicated with asterisks; *** $p < 0.001$. Data are presented as mean + SEM.

My results suggest that the synaptic activity induced protection depends on transcription activation mechanisms acting at least in part through a nuclear calcium-dependent process. Thus, the protection is likely dependent on the activation of multiple signalling events, in part of nuclear calcium, that lead to transcription activation.

5.2.5 Overexpression of the activity regulated gene ATF3 offers protection against the first hallmarks of neuronal damage

Activity regulated inhibitors of death (AIDs) are activity regulated genes that suppress neuronal death (Zhang et al., 2009). Among AID transcription factors, ATF3 is known to be upregulated during nerve injuries (Tsujino et al., 2000) and enhances neuronal elongation and proliferation (Seijffers et al., 2006; Seijffers et al., 2007). Most importantly, when over-expressed, it has been shown to be strongly neuroprotective both *in vivo* and in *vitro* (Zhang et al., 2011). Therefore, I wanted to investigate whether ATF3 over-expression would protect against acute neuronal damage. I co-transfected hippocampal neurons with plasmids containing expression cassettes for Flag-tagged ATF3 and EGFP. Immunocytochemical anti-flag staining showed that ATF3 displayed a nuclear localization and co-localized with EGFP expressing neurons (Fig. 15A). I observed during live imaging that ATF3 over-expressed neurons were robustly protected against an excitotoxic challenge (Fig. 15B). Dendritic damage was assessed by measuring an area of 40 µm dendritic length prior and after NMDA bath application. The changes in dendritic area were obtained by normalizing the area after NMDA application to the same area prior NMDA bath application. Overexpression of ATF3 offered a significant reduction in the area increase after NMDA application compared with control group (expressing only EGFP) (Fig. 15C). My results suggest that over-expressing ATF3 makes hippocampal neurons more resilient against excitotoxic damage.

5.2.6 Dendrites protected by ATF3 over-expression are capable of synaptic transmission

A re-establishment of the neuronal network activity after dendritic damage is an important aspect, as many of the synaptic contacts are located on the dendrites and thus may be considered as an indicator of functional and healthy dendrites. Penumbra neurons are believed to exhibit structural and functional properties that contribute to their recovery (Enright et al., 2007). Thus, next the dendrites protected by ATF3 over-expression were assessed if also functional with regard to synaptic transmission after an excitotoxic challenge.

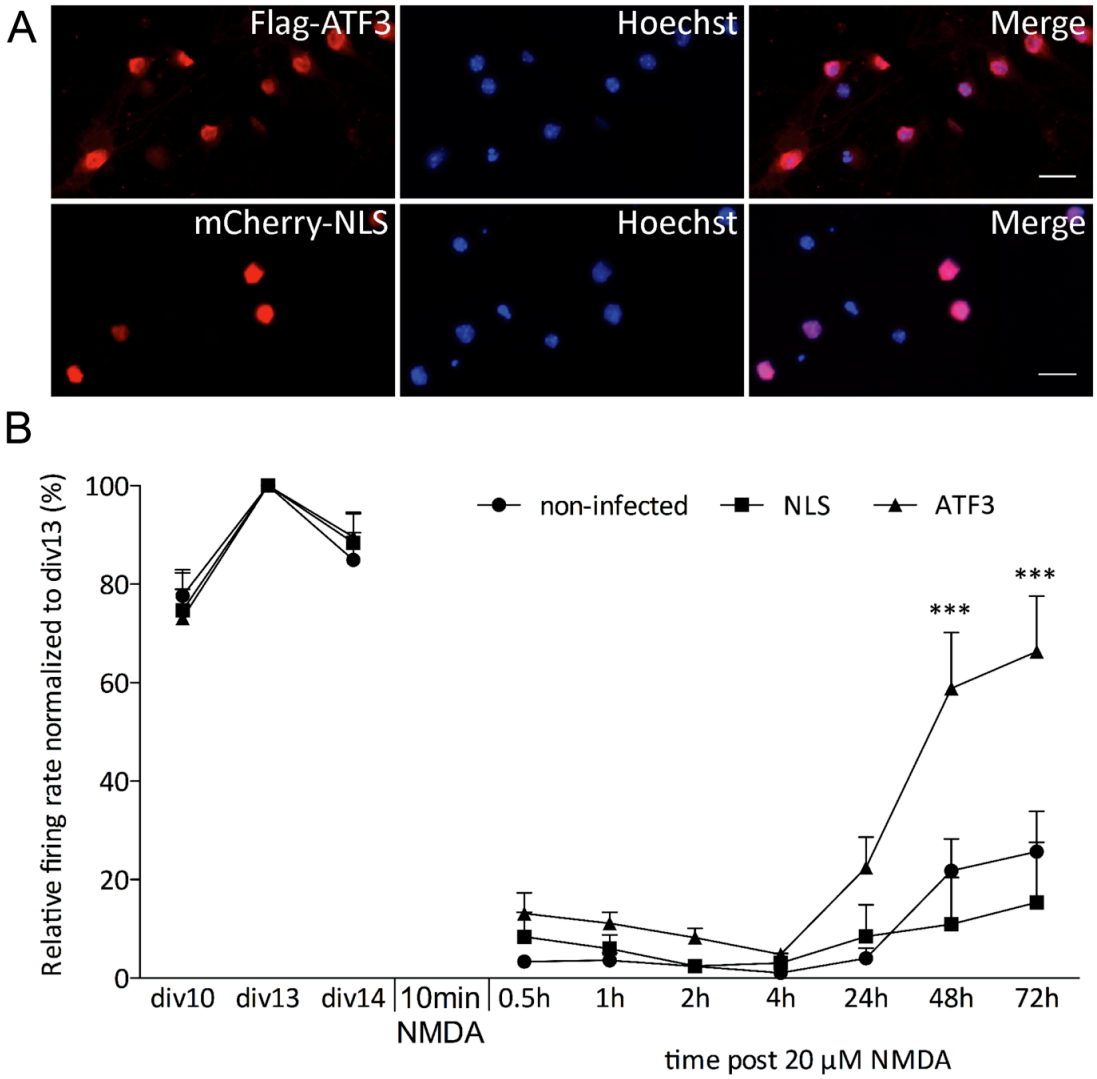

Figure 16. ATF3 protected dendrites regain their network activity within 48 h of NMDA application. ***A-B,*** For MEA analysis, hippocampal neurons were infected at DIV7 with either rAAV-flag-ATF3 or with rAAV-mCherry-NLS. Representative images of rAAV-Flag-ATF3 infected hippocampal neurons labeled with anti-Flag

antibody (upper panels) and rAAV-NLS-mCherry infected hippocampal neurons (lower panels) plated on MEAs. Scale bar 20 µm (***A***). Firing rates normalized to their respective rates at DIV13 of uninfected hippocampal neurons and hippocampal neurons infected with rAAV-Flag-ATF3 or rAAV-mCherry-NLS at the indicated time-points before and after a 10 min application of 20 µM NMDA ***(B)***. Statistically significant differences are indicated with asterisk; *** $p < 0.001$. Data presented as mean + SEM.

Hippocampal neurons plated on MEAs were infected at DIV7 with either rAAV-FLAG-ATF3 or with rAAV-mCherry-NLS for recordings of whole population network activity. Basal activity for infected and non-infected groups was recorded from DIV10 to DIV13 prior an excitotoxic challenge that occurred at DIV14. Infection efficacy was determined immunocytochemically with anti-Flag antibody (around 80 % of the cell populations were infected) (Fig. 16A). The ATF3 overexpressing group was found displaying higher activity immediately after NMDA application and within 48 h post-application these cultures had regained their network activity compared with the mCherry-NLS-infected and the non-infected control groups (Fig. 16B). These observations based on MEA recordings imply that ATF3 over-expressed neuronal dendrites display functional network activity properties that contribute to their ability to recover network activity after neuronal damage.

5.2.7 Expression of certain genes encoding for ion exchangers and channels are down-regulated by increased synaptic activity

Next I wanted to identify synaptic activity regulated genes that could underlie the AP bursting induced dendritic protection. Aside of knowing the ion-dependence, the exact underlying mechanism for dendritic beading is poorly understood and the route for water entry into neurons remains unclear. Hippocampal neurons have low passive water permeability at resting membrane potentials and have no functional water channels on their plasma membrane (Andrew et al., 2007), as aquaporin4 (AQP4) is known to be glia-specific (Amiry-Moghaddam and Ottersen, 2003). Genes thought to be involved in either volume-regulation; dendritic damage and/or excitotoxic ischemic damage were identified from a literature search. Of these I selected the K^+/Cl^--transporter (KCC2), the Na^+/H^+ exchanger isoform 1 (NHE-1), the $Na^+/K^+/Cl^-$-transporter (NKCC1), the transient receptor potential subfamily V member 4 (TRPV4) and the transient receptor potential subfamily M member 7 (TRPM7) for further investigation.

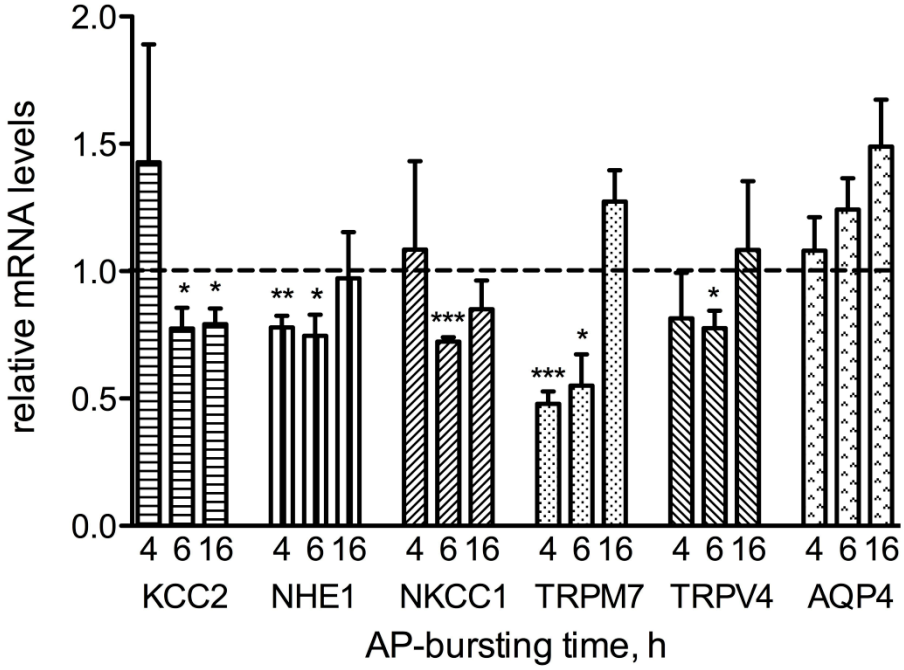

Figure 17. Genomic analysis reveals NHE-1, NKCC1, TRPM7 and TRPV4 .as possible contributors to synaptic activity induced protection against dendritic damage. qPCR analysis of KCC2, NHE-1, NKCC1, TRPV4, RPM7 and AQP4 expression in hippocampal cultures after indicated times of AP bursting induced by bicuculline (50 μM). Statistically significant differences are indicated with asterisks; * $p < 0.05$; **$p < 0.01$, *** $p < 0.001$. All values have been normalized to untreated cultures. Bars present mean ± SEM (4h, n = 3; 6h, n = 4; 16h, n = 4-5).

Their relative gene expression in hippocampal neurons was analyzed by quantitative RT-PCR at 4h, 6h and 16h after AP bursting induced by bicuculline (50 μM). AQP4 was included as a negative control. I observed that after four-hour AP-bursting the NHE-1 and TRPM7 were downregulated and that after an additional 2h of AP-bursting, NKCC1 and TRPV4 were also downregulated (Fig 17). No statistically significant change was noted in AQP4 expression (Fig 17). Taken together, my results suggest that dendritic protection mediated by AP bursting is possibly a multifactorial process and we uncovered potential candidate genes that underlie dendritic protection.

CHAPTER 6 DISCUSSION AND CONCLUSIONS

6.1 VALIDATION OF ORGANOTYPIC HIPPOCAMPAL SLICE CULTURES AS AN *IN VITRO* MODEL TO STUDY NMDAR MEDIATED CELL DEATH

6.1.1 NMDARs are dynamic and central mediators in neurodegenerative conditions

NR2A and NR2B displayed similar developmental protein expression profiles in organotypic hippocampal cultures cultivated with the roller drum technique as in *in situ* material. NR1 was stably expressed throughout the development, whereas NR2A and NR2B subunit expression demonstrated a postnatal age-related change. NR2 subunit age-related changes have previously been described in Stoppini cultures (Wise-Faberowski et al., 2009). Hippocampal organotypic cultures grown as Stoppini cultures develop similar synaptic activity and morphology as acute slices matured in intact ambient *in vivo* (De Simoni et al., 2003). My findings and the observations by de Simoni et al., 2003, suggest that excitatory properties of the postsynaptic compartment are capable to mature *in vitro* in absence of other brain regions or *in vivo* experience. However, my Western blot analysis of the NMDAR subunits revealed some differences between organotypic hippocampal cultures cultivated with the roller drum technique and *in situ* material. I noted a striking down-regulation of NMDAR subunit protein levels 6 h after slice preparation (DIV0). The slices were not collected immediately after the preparation, but in order to treat the slices in exactly the same way as at other time-points, the slices were clotted on a cover slip and allowed 6 h recovery in the incubator; a recovery phase which is in accordance with acute slice preparations. Since the protein levels are so rapidly down regulated after dissection and, more importantly, are down regulated even after the recovery phase, this raises concerns about protein levels in acute slices. Further studies are warranted to measure the time course of protein decay in acute slices, which are typically used over the first few hours after slicing and are prepared and stored in a different manner. This observation may favor the use of organotypic slice cultures instead of acute slices when using young animals (P5-P7). The protein levels in organotypic slices have recovered at DIV14 when the slices are used for experiments.

Moreover, I found that the NR2B subunit displayed an unexpected pattern of three higher MW bands in our Westerns *in situ* material. Throughout the different postnatal days the NR2B subunit displayed a pattern of three higher MW bands, but the dominating band altered from early postnatal day (P6) to later postnatal days (P12-26), a phenomenon that was not hippocampus or species dependent. The most dominating MW band throughout the time-points in my study was the expected ~180 kDa band. This could indicate that under physiological conditions the NR2B subunit is post-translationally modified with age, most probably glycosylated. NR2 subunits are known to undergo post-translational modifications (Hayashi et al., 2009; Li et al., 2002) but no developmental post-translational modifications have been reported. An age-dependent post-translational modification is speculative but would require further investigation with additional tools.

6.1.2 No differential role for NR2 subunits in mediating neuronal cell death after excitotoxcity or OGD

Blocking of NR2B subunits provide neuroprotection *in vitro* in dissociated neuronal cultures (Brewer et al., 2007; Liu et al., 2007; Martel et al., 2009; Stanika et al., 2009 organotypic) and acute slices (Zhou and Baudry, 2007). However, the blockade of NR2B subunit-containing NMDARs at DIV14 failed to prevent excitotoxic or OGD induced cell death in my experiments. A possible explanation is simply that organotypic slice cultures prepared from P5-P6 rat pups at DIV14 correspond to 3-week-old animals where NR2B distribution differs markedly to younger animals used in many studies of NR2B mediated neuroprotection. NR2B mediated neuroprotection has been reported in studies using preparations at DIV14 or earlier which were made from rodent embryos or P0 (at the time of birth), whereas in older neuronal preparations (older than DIV21) neuroprotection achieved by NR2B blockage is only partial (at DIV23, Brewer et al., 2007) or non-existent (at DIV27, Sinor et al., 2000; at DIV21-28, Stanika et al., 2009; 3-month-old acute slices, Zhou and Baudry, 2007). Instead, at DIV21-28 both NR2A and NR2B are reported to mediate excitotoxicity in dissociated cortical (von Engelhardt et al., 2007) and hippocampal cultures (Stanika et al., 2009). At this age NMDAR contribution to neuronal cell death and survival may be independent of NR2 subunit composition and may depend solely on receptor localization. Around this age both NR2A and NR2B

are found at synaptic and extrasynaptic locations shown by postembedding immunogold electron microscopy and fluorescence light microscopy mode (Petralia et al., 2010). Electrophysiological measurements in acute hippocampal slices revealed further that NR2 subunits form stable and uniform pools at both locations (Harris and Pettit, 2007). The contribution of NR2 subunit mediated responses to excitotoxicity appears to depend on the developmental stage of the neuronal preparation. However, an important issue to be taken into consideration is that NMDARs exist in both diheteromeric and triheteromeric (NR1/NR2A/NR2B) constellations making the interpretation of results using 2A and 2B selective antagonists more complicated. Recent electrophysiological data suggest that all NR2Bs in adult CA1 hippocampal synapses (P28) are expressed as part of triheteromeric NR1/NR2A/NR2B constellations (Rauner and Kohr, 2011). We can only speculate whether the amount of triheteromeres expressed in organotypic slice cultures DIV14 (corresponding to P21) is similar. Memantine, the only clinically approved NMDAR antagonist, preferentially acts on extrasynaptic NMDARs in a subunit independent manner, suggesting that the neuroprotective actions of NMDAR antagonists *in vivo* in humans do not depend on receptor subtype selectivity (Leveille et al., 2008). In summary, blocking NR2B in DIV14 organotypic slice cultures failed to attenuate either NMDA- or OGD-induced cell death, implying that cell death is most likely mediated by both subunits. Therefore, NMDAR mediated damaging effects are possibly more dependent on the subcellular localization of NMDA receptors than on their subunit composition.

6.1.3 OGD induced delayed cell death is probably mediated by both NMDA receptor dependent and independent mechanisms

Early OGD-induced neuronal cell death was antagonized with 10 µM MK-801, though, as much as 100 µM was required to obtain cytoprotection after OGD at 72 h. In previous studies of organotypical cultures, 10 or 30 µM MK-801 was reported to offer protection (Bonde et al., 2005; Newell et al., 1995). However, in these studies the pH of the medium was not adjusted to that typical of ischemic tissue CSF (6.5-.6.8) (Nedergaard et al., 1991; Silver and Erecinska, 1992). In earlier studies, only Wieloch´s group used a similar model with mouse Stoppini cultures and obtained significant cytoprotection after OGD with 20 µM MK-801, but presented

data only up to 24h after OGD (Rytter et al. 2003). No previous studies have included observation periods as long as 72 h post-OGD. Therefore, my study suggests that the MK-801 concentration required for protection increases as a function of time.

A reason for the relatively low efficacy of MK-801 post-OGD may be the down-regulation of NMDAR transcription, thus reducing the MK-801 sensitive component of excitotoxic NMDAR activation at later time-points. My qPCR results, however, showed that NMDAR subunit transcription was unchanged following OGD suggesting that efficacy of MK-801 post-OGD was not due to reduced levels of NMDARs. A previous analysis in organotypic hippocampal slice cultures reported an immediate down-regulation of mRNA levels of all NMDAR subunits after OGD, with partial recovery after 3 h (Dos-Anjos et al., 2009). This finding contrasts the present results. However, it is important to take into consideration that these authors prolonged the OGD to 30 min in order to obtain an immediate non-specific cell death, whereas I limited OGD to ~15 min to ensure a delayed and CA1 specific cell death. Hence, the two studies are not directly comparable.

Another explanation for the low MK-801 efficacy could be proton inhibition of the NMDARs as pH in the incubation medium was kept low to mimic the conditions in brain ischemia *in vivo*. NR1 splice variant composition in our slice cultures is unknown, and their differences in pH sensitivity may result in the inactivation of some of the NMDARs (Tang et al., 1990). However, we found that NMDA was able to induce excitotoxic cell death to a similar extent both under ischemic conditions and lowered pH as at physiological pH. Therefore, it seems unlikely that the difference in the time-course of neuroprotection provided by MK-801 was due to proton inhibition of NMDARs.

Taken together, our data indicate that while NMDARs certainly contribute to post-OGD damage, additional mechanisms are also at play. I believe that the significance of these additional mechanisms increases at long observation times and that this must be compensated for by a more complete blockade of NMDA receptors. The lack of MK-801 sensitivity of OGD-induced death at 48 and 72 h but not at 24 h as well as the lack of additive effects of NMDA and OGD on cell death at 48 and 72 h but not at 24 h support NMDAR independent and dependent phases of OGD-induced cell death. The relative significance of other cell death pathways may increase as a consequence of the lowered pH during stimulated ischemia *in vivo* (Nedergaard et al.,

1991; Silver and Erecinska, 1992). Acid sensing calcium channels 1 (ASIC1), which are activated via NMDARs (Gao et al., 2005), and purinergic receptors (P2X) (Runden-Pran et al., 2005) may contribute to delayed damage. Both are activated by parameters, respectively pH and ATP production, that are altered during stimulated ischemia *in vivo* (Nedergaard et al., 1991; Silver and Erecinska, 1992). The ion-channel TRPM7 is as well activated by extracellular pH changes (Bae and Sun, 2011) and is involved in anoxic and delayed ischemic cell death (Aarts et al., 2003; Sun et al., 2009). Common to activation of all these receptors and channels, as well as NMDARs, is their contribution to and increased intracellular level of Ca^{2+}, which can trigger a range of downstream neurotoxic cascades, including mitochondrial uncoupling (Szydlowska and Tymianski, 2010). In conclusion, my findings show differences between the effects of NMDA excitotoxicity and OGD in organotypic hippocampal slice cultures, especially in delayed ischemic cell death. This highlights the need for OGD use in *in vitro* studies when addressing the underlying mechanisms of delayed cell death in brain ischemia, as OGD may more correctly reflect the *in vivo* situation in brain ischemia.

6.1.4 Conclusion for study I

The present investigation is the first comparative evaluation of NMDARs as mediators of NMDA- and OGD-induced cell death in organotypic hippocampal slice cultures. It shows that the organotypic hippocampal slice cultures at DIV14 or 21 offer a valid *in vitro* model to study mechanisms underlying brain ischemia. My data show that the key NMDAR subunits NR1, NR2A, and NRB are expressed in cultured slices and are functional in inducing cell death, both via a chemical agonist and simulated brain ischemia, OGD. Protein levels of NMDAR-subunits are down-regulated after slice preparation, probably an effect of the slice preparation *per se,* necessitating the common practice of allowing slice cultures to mature for ~14 days before experimental manipulations. This offers an advantage over acute slices, as slice cultures have recovered from the stress and damage introduced by slice preparation at the time they are used in experimental settings. *Per se,* the organotypic slice culture is a stable model, although some variability among the cultures occurs after OGD-treatment. The NO OGD control groups displayed very stable gene transcription at different time-points after OGD, indicating that that the observed changes in the OGD

groups reliably reflect the pathological consequences of an OGD insult. The pattern of development of cell death induced by NMDA-and OGD-treatments differs; NMDA evokes an immediate cell death, whereas OGD induces a more gradual one. All in all, based on my pharmacological studies, NMDARs independent on subunit constellations, appear to play a key role in acute OGD responses, initiating delayed cell death mediated through excitotoxicity. The relative significance of other cell death mediators seems to increase as a function of time. The involvement of multiple pathways partly explains why NMDAR antagonists have failed in clinical trials. Taken together, organotypic hippocampal slice cultures represent a good model for studying mechanisms underlying cell death signalling in brain ischemia. The model is independent of systemic parameters and allows full control of the microenvironment and experimental manipulations.

6.2 INCRESED SYNAPTIC ACTIVITY AND ATF3 PROTECTS AGAINST DENDRITIC DAMAGE

6.2.1 Mitochondria- the crossroad for permanent damage

Dendritic beading is accompanied by mitochondrial swelling with a similar temporal progression and Ca^{2+}-dependency. The formation of dendritic beadings is spatially restricted to areas with the highest initial intracellular Ca^{2+} increase (Bindokas and Miller, 1995) as are also Ca^{2+} dependent mitochondrial morphological changes (Macaskill et al., 2009; Pivovarova and Andrews, 2010). Furthermore, permanent dendritic damage coincides with considerable delayed intracellular Ca^{2+} increases (Faddis et al., 1997; Vander Jagt et al., 2008) and breakdown of the mitochondrial membrane potential (Greenwood et al., 2007; Kintner et al., 2010). Although deleterious Ca^{2+} enters mainly via NMDARs (Arundine and Tymianski, 2003; Choi, 1987; Sattler et al., 1998), the NMDAR subpopulations display a differential role in mediating neuronal damage. Extrasynaptic NMDARs mediate cell death whereas the synaptic NMDARs mediate cell survival (Hardingham and Bading, 2010; Hardingham et al., 2002). My findings show that elevated activity of synaptic NMDARs protects against dendritic damage, possibly by stabilizing the mitochondrial membrane potential. Increased synaptic activity is known to delay and reduce the magnitude of NMDA-induced loss of mitochondrial membrane potential

(Lau and Bading, 2009a). It has been shown that Ca^{2+} entry via synaptic NMDARs, such as that activated by bicuculline treatment is detected by mitochondrial Ca^{2+}-sensors triggering the dissociation of mitochondria from microtubuli and their recruitment to synapses (Macaskill et al., 2009). Therefore, a possibility is that increased synaptic activity may cause mitochondria to move physically away from extrasynaptic receptors and give mitochondria a physiological distance to the harmful Ca^{2+} entering via the extrasynaptic NMDARs. The reduced mitochondrial Ca^{2+} overload and subsequent reduced magnitude loss of mitochondrial membrane potential would minimise the ATP loss, pH changes and ion concentration imbalances. I showed that AP-bursting downregulated genes like NHE-1 that are found to aggravate loss of mitochondrial membrane potential and dendritic damage (Kintner et al., 2010). Furthermore, I observed a down-regulation of large pore Na^{+} and Ca^{2+} permeable channels like TRPM7 and TRPV4 (Pedersen et al., 2005) which is expected to reduce intracellular Ca^{2+} overload and mitochondrial Ca^{2+} uptake that is deleterious for neuronal outcome (Stout et al., 1998).

6.2.2 Dendritic beading shuts down the postsynaptic compartment

A lethal NMDA stimulus induced robust dendritic swelling and long-lasting depression in network activity. However, the EM analysis showed that initial neuronal damage was only observed in dendrites and somata whereas axonal terminals were intact. Hence, the NMDA induced morphological changes in the postsynaptic structures most probably renders them non-functional. The most drastic morphological change observed was the microtubule fragmentation, which most likely causes a restriction in microtubule-supported transport. The microtubule cytoskeleton is critical not only for normal structural morphology but also for normal function of neuronal processes (Hoogenraad and Bradke, 2009). Microtubules dissemble when intracellular calcium concentrations increase to the micromolar range (Schliwa et al., 1981), however, the Ca^{2+}-activated protease, calpain, has not been found involved in initial dendritic beading (Faddis et al., 1997; Hoskison and Shuttleworth, 2006). Inhibition of calpain rather reduces the recovery rate from NMDA and glutamate induced dendritic beading indicating that calpain contributes to microtubule degradation at later phases (Faddis et al., 1997; Hoskison and Shuttleworth, 2006). The initial disruption of microtubule morphology may be a result

of an excessive water influx. Dendritic beading and microtubuli fragmentation is prevented by pretreatment with the microtubule-stabilizing compound taxol (Emery and Lucas, 1995; Furukawa and Mattson, 1995; Hoskison and Shuttleworth, 2006; Park et al., 1996). Water influx *per se* may be a factor in generating neurons more vulnerable to ischemic damage.

6.2.3 Potential routes for neuronal water influx during excitotoxic conditions

During ischemia both neurons and astrocytes swell, however, only neurons die (Pekny and Nilsson, 2005; Risher et al., 2009). Astrocytes recover rapidly from swelling, which possibly contributes to their survival (Pekny and Nilsson, 2005; Risher et al., 2009). Their rapid recovery is most likely facilitated by the specific water channels expressed on their plasma membrane, aquaporins (Amiry-Moghaddam and Ottersen, 2003; Nielsen et al., 1997). In contrast, hippocampal neurons are not known to express any functional membrane bound aquaporins (Andrew et al., 2007). The route for water entry into hippocampal neurons is not clear. Hippocampal neurons are largely water impermeable at resting membrane potential and resist volume changes under acute osmotic stress (Somjen et al., 1993) yet swell rapidly during conditions of prolonged depolarization such as during ischemia (Andrew et al., 2007; Risher et al., 2009). Water is generally considered to follow the initial Na^+/Cl^- influx (Hasbani et al., 1998) although no candidate water channels have been suggested for the possible route of entry. The majority of Na^+ and Cl^- ions are stripped from their hydration shell before entering the cell (MacAulay and Zeuthen, 2010). However, during pathophysiological conditions water entry may take place through large pore channels involved in maintaining anoxic depolarization (Anderson et al., 2005, Andrew et al., 2007) such as the transient receptor potential (TRP) family of ion channels. I showed that increased synaptic activity down-regulates TRPM7 and TRPV4, which are Na^+ and Ca^{2+} permeable members of the TRP channel family (Pedersen et al., 2005). Genetic knock down of TRPM7 has been shown to improve functional recovery of neurons, including their dendritic functions, after cerebral ischemia *in vivo* (Sun et al., 2009) Though, as neurons are very resistant to passive water transport under physiological conditions, water entry into neurons possibly occurs via a secondary active transport mechanism, such as ion pumps or exchangers. K^+/Cl^- co-transporters (KCCs) are important for neuronal Cl^- homeostasis (Blaesse et

al., 2009; Delpire, 2000) and transport water against an osmotic gradient (Hamann et al., 2005; Zeuthen, 1994) and are furthermore expressed on pyramidal neurons (Blaesse et al., 2009; Kaila, 1994; Payne et al., 2003). The NKCC1 is believed to transport water into cells (Hamann et al., 2005; Jayakumar et al., 2011; MacAulay and Zeuthen, 2010), including cortical neurons (Jourdain et al., 2011). NKCC1 transports ions (Russell, 2000) and possibly also water into the cell. Hence, a down-regulation of NKCC1 as I observed with increased synaptic activity may lead to reduced inward water transport and reduced dendritic swelling. Protection obtained by increased synaptic activity possibly involves reduced water entry by regulating genes suggested involved in water regulation.

6.2.4 AP-bursting offers a multifactorial protection against dendritic damage

Synaptic activity affords protection against dendritic beading, which is undoubtedly mediated by the regulation of multiple genes. An individual change in each regulated gene is probably not sufficient alone to account for AP-bursting induced protection; more likely the protection is a synergetic phenomenon involving many genes (Lau and Bading, 2009b; Zhang et al., 2007; Zhang et al., 2009). I found several down regulated genes, all of which are thought to aggravate excitotoxic/ischemic damage, and whose down regulation is likely to make neurons more resistant to neuronal damage either via separate or common pathways. Many of the genes have been reported to be activated by common triggers that take place during initial ischemia. NHE-1 is involved in maintenance and regulation of intracellular pH and [Na^+] (Luo and Sun, 2007; Yao et al., 1999) and displays an elevated activity in hippocampal neurons immediately after anoxia (Sheldon et al., 2004; Yao et al., 2001). Genetic (Luo et al., 2005) or pharmacological (Kuribayashi et al., 1999a; Kuribayashi et al., 1999b; Phillis et al., 1999) deletion of NHE-1 reduces infarcted area after simulated ischemia *in vivo*. NKCC1 is involved in maintaining and regulation the intracellular Cl^- homeostasis in neurons (Blaesse et al., 2009; Delpire, 2000) and contributes to excitotoxic damage (Beck et al., 2003) and is functionally upregulated in response to *in vivo* ischemia (Pond et al., 2006). Bumetanide (NKCC1 blocker) or genetic deletion of NKCC1 has shown to reduce final infarct volume after focal cerebral ischemia (Chen et al., 2005; Yan et al., 2003). TRPM7 has been pinpointed to be involved in neuronal cell death (Aarts et al., 2003;

Aarts and Tymianski, 2005), and more recently, the temperature regulated TRPV4 has been suggested to contribute in hypothermia induced protection (Lipski et al., 2006). My finding that the KCC2 is down regulated following AP-bursting seems somewhat of a paradox since excitotoxic events are known to suppress KCC2 expression both *in vitro* (Wake et al., 2007) and *in vivo* (Jaenisch et al., 2010). KCC2 is known to be important for neuronal Cl^- homeostasis (Blaesse et al., 2009; Delpire, 2000) and its expression correlates with the inhibitory action of $GABA_A$ receptors suggesting that its down regulation may lead to excitatory GABA transmission. Furthermore, neurons surviving brain ischemia are reported to display a strong KCC2 expression (Jaenisch et al., 2010; Papp et al., 2008). Taken together, an up-regulation of KCC2 would be more favorable to neuronal outcome than down-regulation, and actually, recently Medina and colleagues presented that down-regulation of KCC2 compromises neuronal survival (Pellegrino et al., 2011).

6.2.5 ATF3 – an intriguing ubiquitously expressed transcription factor protects against neuronal damage

Synaptic activity controls a pool of nuclear calcium- and CREB-regulated genes, among them ATF3 (Nakagomi et al., 2003; Zhang et al., 2009). I show here that ATF3 over-expression protected against dendritic damage, and more importantly, the protected dendrites were functionally sufficient to restore near-normal levels of network activity within 48h of an NMDA insult. Hence, the protected neurons were not only protected on somatic level but were also functional and connected with each other. This kind of intervention to stabilize neuronal function at an early stage of ischemic damage is critical to increases the number of surviving functional penumbra neurons that are crucial for rehabilitation after brain ischemia. Previous *in vivo* studies have shown that ATF3 over-expression reduces the lesion size after MCAO with almost 50% (Zhang et al., 2011), however, functional recovery of model animals still remains to be elucidated. The exact mechanism how ATF3 enhances cell survival is not fully understood. ATF3 does not protect against mitochondrial membrane depolarization (Zhang et al., 2009) but endogenous ATF3 renders mitochondria more resilient against oxidative stress (Kiryu-Seo et al., 2010). As gene repressor ATF3 promotes cell survival in hippocampal neurons, whereas as a transcriptional activator it promotes cell death (Zhang et al., 2011). A possibility is that ATF3 regulated target

genes are involved in microtubule stabilization. It has been shown that upregulated expression of endogenous ATF3 contributes to nerve regeneration by promoting neurite outgrowth both *in vivo* and *in vitro* after nerve injury (Nakagomi et al., 2003; Seijffers et al., 2006; Seijffers et al., 2007). Endogenous ATF3 is upregulated by various stress signals (Chen et al., 1996; Hai et al., 1999), including nerve injury (Hai et al., 1999; Takeda et al., 2000; Tsujino et al., 2000), and ATF3 has been suggested to function as a regulator of intrinsic host defense mechanism in inflammatory responses and cancer (Hai et al., 2010; Thompson et al., 2009). This concept of ATF3 as an intrinsic defense regulator may well apply also in neural cells. ATF3 up-regulation is biphasic after simulated ischemia *in vivo,* MCAO, displaying an immediate early expression in the core area (after 1h) and a later induction in the penumbra area (Ohba et al., 2003). Transient endogenous up-regulation of ATF3 after cell damage raises a possible target for therapeutic intervention. In order to strengthen the intrinsic defensive mechanism of penumbra neurons, ATF3 could be re-supplemented at later time points after ischemia. The BBB that usually prevents the access of any molecules lager than 500 Da, has been shown to be open for weeks after stroke in rodent models (Strbian et al., 2008). This time window of increased BBB permeability could permit access for intravenously administered pharmacological treatments, as ATF3, which offers an ideal cytoprotective agent by increasing the number of healthy neurons with functional network activity. However, in stroke patients the time window during which the BBB is open is not fully defined and requires further work (Blyth et al., 2009).

6.2.6 Conclusion for study II

Over two decades ago Olney described dendritic beading as one of the first hallmarks of neuronal damage in response to intra-peritoneal kainate injections (Olney et al., 1979). This form of dendritic damage is considered to be one of the first ultra-structural changes in pathophysiological conditions like cerebral ischemia (Hori and Carpenter, 1994; Matesic and Lin, 1994). Dendritic beading is linked with ischemic depolarization and excitotoxicity that are the major damaging events associated with stroke (Dirnagl et al., 1999) and are considered to make neurons more susceptible for neuronal damage and to contribute to the development of delayed cell death (Dreier, 2011; Petito and Pulsinelli, 1984). Here I show that increased synaptic

activity offers protection exactly at this key point of events, at the very first stages of neuronal damage, against dendritic beading. My data suggest that this protection is gene transcription and partly nuclear calcium signaling dependent. Over-expression of the activity regulated gene-repressor ATF3 offered both morphological, and more importantly, functional protection against dendritic damage. A genomic approach revealed additional candidate genes possibly contributing to synaptic activity induced protection. I conclude that synaptic activity induced protection against dendritic damage is multifactorial and partly controlled by nuclear calcium and ATF3. ATF3, which as a gene repressor increases the number of functional neurons, could be optimal for future therapeutic treatments of cerebral ischemia. The aim is to treat patients with a neuroprotective agent with multiple targets in combination with tPA (Albers et al., 2011).

6.3 METHODOLOGICAL ASPECTS

To answer a question as complex as the mechanisms underlying excitotoxcity and ischemic cell death requires a thorough characterization of the model used. Knowledge of parameters recognized to be involved in neuronal damage will help us to evaluate, interpret and compare various results from brain ischemia studies. *In vitro* models are essential to unravel mechanisms during neuronal damage and to test possible neuroprotective elements. They offer an easier access to for example genetic manipulations and live imaging without the involvement of systemic parameters.

Classical ischemic cell death seen in the hippocampus is characterized by selective and delayed cell death in the vulnerable CA1 pyramidal cells (Schmidt-Kastner and Freund, 1991). Time course of cell death is important in studies of brain ischemia as it reflects the nature of the underlying signaling mechanisms. The extracellular volume for a slice is very large (750 µl) compared with the interstitial volume in brain *in vivo*, consequently the slice is not able to induce changes in the extracellular fluid composition as seen in ischemia-CSF (Hansen, 1985; Nedergaard et al., 1991; Silver and Erecinska, 1992). To overcome this obstacle the ion-concentrations and pH of the medium were adjusted prior to applying it to slices to induce OGD.

An important aspect to be taken into consideration in studies aimed at discovering possible neuroprotective mechanisms involved in cerebral ischemia is the

parameters used to evaluate neuronal damage. Evaluating neuronal damage solely based on nuclear abnormalities provides an incomplete picture, devoid of information about neuronal function. Restoration of synaptic transmission following an ischemic insult is a critical indicator of functional recovery that is a very important aspect to be taken into consideration in the rehabilitation of stroke patients. A study consisting of cell death analysis in combination with subtler parameters such as dendritic damage and synaptic transmission would give a more complete picture of long term outcomes following ischemic insults. Model characterization and parameters used for evaluation are important, as the only available remediation to date is still the tPa (Goldstein et al., 2011; Green and Shuaib, 2006).

CHAPTER 7 LIST OF ABBREVIATIONS

aCSF	Artificial cerebral spinal fluid
AID	Activity-regulated inhibitors of death
APV	2-amino-5-phosphonovaleric acid
ARA-C	Cytosine d-arabinofuranoside
ATF3	Activating transcription factor 3
AP	Action potential
ASIC1	Acid sensing calcium channels
ATP	Adenosine triphosphate
AQP4	Aquaporin 4
BBB	Blood-brain-barrier
Bic	Bicuculline
BME	Basal medium Eagle
b-ZIP	Basic region-leucine zipper domain
Ca^{2+}	Calcium
CaM	Calmodulin
CaMBP4	Calmodulin-binding peptide 4
CaMK	Ca^{2+}/calmodulin-dependent protein kinase
CA	Cornu Ammonus
CBA	Chicken beta-actin hybrid promoter
CBP	CREB binding protein
Cl^-	Chloride
CMV	Cytomegalovirus enhancer
CNS	Central nervous system
CO2	Carbon dioxide
CREB	cyclic-AMP response element binding protein
DG	Dentate gyrus
DMEM	Dulbecco's Modified Eagle Medium
DMSO	Dimethyl sulfoxide
DNA	Deoxyribonucleic acid
DIV	Days *in vitro*
DOC	Deoxycholic acid

DTT	Dithiothreitol
EGFP	Enhanced green fluorescent protein
EM	Electron microscopy
ERK	Extracellular-signal regulated kinase
ECF	Enhanced Chemi-fluoresence
$GABA_A$	γ-aminobutyric acid
GBSS	Gey's balanced salt solution
h	Hours
H^+	Hydrogen/Protons
HEK293	Human kidney cell line 293
iCSF	Ischemic cerebral spinal fluid
IMDM	Iscove`s Modified Dulbecco Medium
K^+	Potassium
KCC2	K^+/Cl^- -co-transporter
kDa	Kilo Dalton
KO	Knock out
MCAO	Middle cerebral artery occlusion
MEA	Microelectrode array
Mg^+	Magnesium
MK801	Dizocilpine
MSK	Mitogen- and stress-activated protein kinases
MW	Molecular weight
Na^+	Sodium
NGF	Nerve growth factor
NHE-1	Na^+/H^+ exchanger isoform 1
NKCC1	$Na^+/K^+/Cl^-$-transporter
NLS	Nuclear localised signal
NMDA	*N*-Methyl-D-Aspartate
NMDAR/NR	*N*-Methyl-D-Aspartate receptor
NO	Nitric oxide
NOS	Nitric oxide synthase
OGD	Oxygen and glucose depravation
P	Postnatal day

PAGE	Polyacrylamide gel electrophoresis
PCR	Polymerase chain reaction
PI	Propidium iodide
PID	Peri infarct depolarisation
PIK3	Phosphotidylinositide 3'-OH kinase
PVDF	Polyvinylidene difluoride
rAAV	Recombinant adeno-associated virus
RIPA	Radioimmunoprecipitation assay
RNA	Ribonucleic acid
ROI	Region of interest
ROS	Reactive oxygen species
RSK2	p90 ribosomal S6 protein kinase 2
SDS	Sodium dodecyl sulfate
SGG	Salt–glucose–glycine
TEM	Transmission electron microscopy
TM	Transfection medium
tPA	Tissue plasminogen activator
TRPM7	Transient receptor potential subfamily M member 7
TRPV4	Transient receptor potential subfamily V member 4
TTX	Tetrodoxin
Zn^{2+}	Zinc

CHAPTER 8 REFERENCES

Aamodt, S.M., and Constantine-Paton, M. (1999). The role of neural activity in synaptic development and its implications for adult brain function. Adv Neurol *79*, 133-144.

Aarts, M., Iihara, K., Wei, W.L., Xiong, Z.G., Arundine, M., Cerwinski, W., MacDonald, J.F., and Tymianski, M. (2003). A key role for TRPM7 channels in anoxic neuronal death. Cell *115*, 863-877.

Aarts, M.M., and Tymianski, M. (2005). TRPM7 and ischemic CNS injury. Neuroscientist *11*, 116-123.

Albers, G.W., Goldstein, L.B., Hess, D.C., Wechsler, L.R., Furie, K.L., Gorelick, P.B., Hurn, P., Liebeskind, D.S., Nogueira, R.G., and Saver, J.L. (2011). Stroke Treatment Academic Industry Roundtable (STAIR) recommendations for maximizing the use of intravenous thrombolytics and expanding treatment options with intra-arterial and neuroprotective therapies. Stroke; a journal of cerebral circulation *42*, 2645-2650.

Amiry-Moghaddam, M., and Ottersen, O.P. (2003). The molecular basis of water transport in the brain. Nature reviews Neuroscience *4*, 991-1001.

Andrew, R.D., Labron, M.W., Boehnke, S.E., Carnduff, L., and Kirov, S.A. (2007). Physiological evidence that pyramidal neurons lack functional water channels. Cereb Cortex *17*, 787-802.

Arnold, F.J., Hofmann, F., Bengtson, C.P., Wittmann, M., Vanhoutte, P., and Bading, H. (2005). Microelectrode array recordings of cultured hippocampal networks reveal a simple model for transcription and protein synthesis-dependent plasticity. J Physiol *564*, 3-19.

Arthur, J.S., Fong, A.L., Dwyer, J.M., Davare, M., Reese, E., Obrietan, K., and Impey, S. (2004). Mitogen- and stress-activated protein kinase 1 mediates cAMP response element-binding protein phosphorylation and activation by neurotrophins. The Journal of neuroscience : the official journal of the Society for Neuroscience *24*, 4324-4332.

Arundine, M., and Tymianski, M. (2003). Molecular mechanisms of calcium-dependent neurodegeneration in excitotoxicity. Cell Calcium *34*, 325-337.

Bading, H., Ginty, D.D., and Greenberg, M.E. (1993). Regulation of gene expression in hippocampal neurons by distinct calcium signaling pathways. Science *260*, 181-186.

Bading, H., and Greenberg, M.E. (1991). Stimulation of protein tyrosine phosphorylation by NMDA receptor activation. Science *253*, 912-914.

Bae, C.Y., and Sun, H.S. (2011). TRPM7 in cerebral ischemia and potential target for drug development in stroke. Acta Pharmacol Sin *32*, 725-733.

Beck, J., Lenart, B., Kintner, D.B., and Sun, D. (2003). Na-K-Cl cotransporter contributes to glutamate-mediated excitotoxicity. The Journal of neuroscience : the official journal of the Society for Neuroscience *23*, 5061-5068.

Beckman, J.S., and Koppenol, W.H. (1996). Nitric oxide, superoxide, and peroxynitrite: the good, the bad, and ugly. The American journal of physiology *271*, C1424-1437.

Bengtson, C.P., Dick, O., and Bading, H. (2008). A quantitative method to assess extrasynaptic NMDA receptor function in the protective effect of synaptic activity against neurotoxicity. BMC Neurosci *9*, 11.

Benveniste, H., Drejer, J., Schousboe, A., and Diemer, N.H. (1984). Elevation of the extracellular concentrations of glutamate and aspartate in rat hippocampus during transient cerebral ischemia monitored by intracerebral microdialysis. J Neurochem *43*, 1369-1374.

Berberich, S., Jensen, V., Hvalby, O., Seeburg, P.H., and Kohr, G. (2007). The role of NMDAR subtypes and charge transfer during hippocampal LTP induction. Neuropharmacology *52*, 77-86.

Bindokas, V.P., and Miller, R.J. (1995). Excitotoxic degeneration is initiated at non-random sites in cultured rat cerebellar neurons. J Neurosci *15*, 6999-7011.

Blaesse, P., Airaksinen, M.S., Rivera, C., and Kaila, K. (2009). Cation-chloride cotransporters and neuronal function. Neuron *61*, 820-838.

Bliss, T.V., and Collingridge, G.L. (1993). A synaptic model of memory: long-term potentiation in the hippocampus. Nature *361*, 31-39.

Blyth, B.J., Farhavar, A., Gee, C., Hawthorn, B., He, H., Nayak, A., Stocklein, V., and Bazarian, J.J. (2009). Validation of serum markers for blood-brain barrier disruption in traumatic brain injury. J Neurotrauma *26*, 1497-1507.

Bonde, C., Noraberg, J., Noer, H., and Zimmer, J. (2005). Ionotropic glutamate receptors and glutamate transporters are involved in necrotic neuronal cell death induced by oxygen-glucose deprivation of hippocampal slice cultures. Neuroscience *136*, 779-794.

Brewer, L.D., Thibault, O., Staton, J., Thibault, V., Rogers, J.T., Garcia-Ramos, G., Kraner, S., Landfield, P.W., and Porter, N.M. (2007). Increased vulnerability of hippocampal neurons with age in culture: temporal association with increases in NMDA receptor current, NR2A subunit expression and recruitment of L-type calcium channels. Brain research *1151*, 20-31.

Buchs, P.A., and Muller, D. (1996). Induction of long-term potentiation is associated with major ultrastructural changes of activated synapses. Proc Natl Acad Sci U S A *93*, 8040-8045.

Burnashev, N., Zhou, Z., Neher, E., and Sakmann, B. (1995). Fractional calcium currents through recombinant GluR channels of the NMDA, AMPA and kainate receptor subtypes. The Journal of physiology *485 (Pt 2)*, 403-418.

Camacho, A., and Massieu, L. (2006). Role of glutamate transporters in the clearance and release of glutamate during ischemia and its relation to neuronal death. Arch Med Res *37*, 11-18.

Chawla, S., Hardingham, G.E., Quinn, D.R., and Bading, H. (1998). CBP: a signal-regulated transcriptional coactivator controlled by nuclear calcium and CaM kinase IV. Science *281*, 1505-1509.

Chen, B.P., Wolfgang, C.D., and Hai, T. (1996). Analysis of ATF3, a transcription factor induced by physiological stresses and modulated by gadd153/Chop10. Mol Cell Biol *16*, 1157-1168.

Chen, H., Luo, J., Kintner, D.B., Shull, G.E., and Sun, D. (2005). Na(+)-dependent chloride transporter (NKCC1)-null mice exhibit less gray and white matter damage after focal cerebral ischemia. Journal of cerebral blood flow and metabolism : official journal of the International Society of Cerebral Blood Flow and Metabolism *25*, 54-66.

Choi, D.W. (1987). Ionic dependence of glutamate neurotoxicity. The Journal of neuroscience : the official journal of the Society for Neuroscience *7*, 369-379.

Chrivia, J.C., Kwok, R.P., Lamb, N., Hagiwara, M., Montminy, M.R., and Goodman, R.H. (1993). Phosphorylated CREB binds specifically to the nuclear protein CBP. Nature *365*, 855-859.

Clark, A.J., Bissinger, P., Bullock, D.W., Damak, S., Wallace, R., Whitelaw, C.B., and Yull, F. (1994). Chromosomal position effects and the modulation of transgene expression. Reprod Fertil Dev *6*, 589-598.

Dawson, V.L., Dawson, T.M., London, E.D., Bredt, D.S., and Snyder, S.H. (1991). Nitric oxide mediates glutamate neurotoxicity in primary cortical cultures. Proc Natl Acad Sci U S A *88*, 6368-6371.

De Simoni, A., Griesinger, C.B., and Edwards, F.A. (2003). Development of rat CA1 neurones in acute versus organotypic slices: role of experience in synaptic morphology and activity. The Journal of physiology *550*, 135-147.

Delpire, E. (2000). Cation-Chloride Cotransporters in Neuronal Communication. News Physiol Sci *15*, 309-312.

Dirnagl, U., Iadecola, C., and Moskowitz, M.A. (1999). Pathobiology of ischaemic stroke: an integrated view. Trends Neurosci *22*, 391-397.

Dos-Anjos, S., Martinez-Villayandre, B., Montori, S., Perez-Garcia, C.C., and Fernandez-Lopez, A. (2009). Early modifications in N-methyl-D-aspartate receptor subunit mRNA levels in an oxygen and glucose deprivation model using rat hippocampal brain slices. Neuroscience *164*, 1119-1126.

Doyle, K.P., Simon, R.P., and Stenzel-Poore, M.P. (2008). Mechanisms of ischemic brain damage. Neuropharmacology *55*, 310-318.

Dravid, S.M., Erreger, K., Yuan, H., Nicholson, K., Le, P., Lyuboslavsky, P., Almonte, A., Murray, E., Mosely, C., Barber, J.*, et al.* (2007). Subunit-specific mechanisms and proton sensitivity of NMDA receptor channel block. J Physiol *581*, 107-128.

Dreier, J.P. (2011). The role of spreading depression, spreading depolarization and spreading ischemia in neurological disease. Nat Med *17*, 439-447.

Dugan, L.L., Sensi, S.L., Canzoniero, L.M., Handran, S.D., Rothman, S.M., Lin, T.S., Goldberg, M.P., and Choi, D.W. (1995). Mitochondrial production of reactive oxygen species in cortical neurons following exposure to N-methyl-D-aspartate. The Journal of neuroscience : the official journal of the Society for Neuroscience *15*, 6377-6388.

Emery, D.G., and Lucas, J.H. (1995). Ultrastructural damage and neuritic beading in cold-stressed spinal neurons with comparisons to NMDA and A23187 toxicity. Brain Res *692*, 161-173.

Enright, L.E., Zhang, S., and Murphy, T.H. (2007). Fine mapping of the spatial relationship between acute ischemia and dendritic structure indicates selective vulnerability of layer V neuron dendritic tufts within single neurons in vivo. J Cereb Blood Flow Metab *27*, 1185-1200.

Faddis, B.T., Hasbani, M.J., and Goldberg, M.P. (1997). Calpain activation contributes to dendritic remodeling after brief excitotoxic injury in vitro. J Neurosci *17*, 951-959.

Francis, J.S., Dragunow, M., and During, M.J. (2004). Over expression of ATF-3 protects rat hippocampal neurons from in vivo injection of kainic acid. Brain Res Mol Brain Res *124*, 199-203.

Fujimura, M., Morita-Fujimura, Y., Murakami, K., Kawase, M., and Chan, P.H. (1998). Cytosolic redistribution of cytochrome c after transient focal cerebral ischemia in rats. Journal of cerebral blood flow and metabolism : official journal of the International Society of Cerebral Blood Flow and Metabolism *18*, 1239-1247.

Furukawa, H., Singh, S.K., Mancusso, R., and Gouaux, E. (2005). Subunit arrangement and function in NMDA receptors. Nature *438*, 185-192.

Furukawa, K., and Mattson, M.P. (1995). Taxol stabilizes [Ca2+]i and protects hippocampal neurons against excitotoxicity. Brain research *689*, 141-146.

Gahwiler, B.H. (1981). Organotypic monolayer cultures of nervous tissue. J Neurosci Methods *4*, 329-342.

Gahwiler, B.H. (1984). Slice cultures of cerebellar, hippocampal and hypothalamic tissue. Experientia *40*, 235-243.

Gahwiler, B.H., Capogna, M., Debanne, D., McKinney, R.A., and Thompson, S.M. (1997). Organotypic slice cultures: a technique has come of age. Trends in neurosciences *20*, 471-477.

Gao, J., Duan, B., Wang, D.G., Deng, X.H., Zhang, G.Y., Xu, L., and Xu, T.L. (2005). Coupling between NMDA receptor and acid-sensing ion channel contributes to ischemic neuronal death. Neuron *48*, 635-646.

Gilchrist, M., Thorsson, V., Li, B., Rust, A.G., Korb, M., Roach, J.C., Kennedy, K., Hai, T., Bolouri, H., and Aderem, A. (2006). Systems biology approaches identify ATF3 as a negative regulator of Toll-like receptor 4. Nature *441*, 173-178.

Goldstein, L.B., Bushnell, C.D., Adams, R.J., Appel, L.J., Braun, L.T., Chaturvedi, S., Creager, M.A., Culebras, A., Eckel, R.H., Hart, R.G.*, et al.* (2011). Guidelines for the primary prevention of stroke: a guideline for healthcare professionals from the American Heart Association/American Stroke Association. Stroke; a journal of cerebral circulation *42*, 517-584.

Green, A.R., and Shuaib, A. (2006). Therapeutic strategies for the treatment of stroke. Drug Discov Today *11*, 681-693.

Greenwood, S.M., Mizielinska, S.M., Frenguelli, B.G., Harvey, J., and Connolly, C.N. (2007). Mitochondrial dysfunction and dendritic beading during neuronal toxicity. J Biol Chem *282*, 26235-26244.

Groc, L., Bard, L., and Choquet, D. (2009). Surface trafficking of N-methyl-D-aspartate receptors: physiological and pathological perspectives. Neuroscience *158*, 4-18.

Groc, L., Heine, M., Cousins, S.L., Stephenson, F.A., Lounis, B., Cognet, L., and Choquet, D. (2006). NMDA receptor surface mobility depends on NR2A-2B subunits. Proc Natl Acad Sci U S A *103*, 18769-18774.

Hagenston, A.M., and Bading, H. (2011). Calcium Signaling in Synapse-to-Nucleus Communication. Cold Spring Harb Perspect Biol *3*.

Hai, T., and Hartman, M.G. (2001). The molecular biology and nomenclature of the activating transcription factor/cAMP responsive element binding family of transcription factors: activating transcription factor proteins and homeostasis. Gene *273*, 1-11.

Hai, T., Wolfgang, C.D., Marsee, D.K., Allen, A.E., and Sivaprasad, U. (1999). ATF3 and stress responses. Gene Expr *7*, 321-335.

Hai, T., Wolford, C.C., and Chang, Y.S. (2010). ATF3, a hub of the cellular adaptive-response network, in the pathogenesis of diseases: is modulation of inflammation a unifying component? Gene Expr *15*, 1-11.

Hai, T.W., Liu, F., Coukos, W.J., and Green, M.R. (1989). Transcription factor ATF cDNA clones: an extensive family of leucine zipper proteins able to selectively form DNA-binding heterodimers. Genes Dev *3*, 2083-2090.

Hamann, S., Herrera-Perez, J.J., Bundgaard, M., Alvarez-Leefmans, F.J., and Zeuthen, T. (2005). Water permeability of Na+-K+-2Cl- cotransporters in mammalian epithelial cells. The Journal of physiology *568*, 123-135.

Hansen, A.J. (1985). Effect of anoxia on ion distribution in the brain. Physiol Rev *65*, 101-148.

Hardingham, G.E. (2009). Coupling of the NMDA receptor to neuroprotective and neurodestructive events. Biochem Soc Trans *37*, 1147-1160.

Hardingham, G.E., Arnold, F.J., and Bading, H. (2001a). A calcium microdomain near NMDA receptors: on switch for ERK-dependent synapse-to-nucleus communication. Nat Neurosci *4*, 565-566.

Hardingham, G.E., Arnold, F.J., and Bading, H. (2001b). Nuclear calcium signaling controls CREB-mediated gene expression triggered by synaptic activity. Nat Neurosci *4*, 261-267.

Hardingham, G.E., and Bading, H. (2010). Synaptic versus extrasynaptic NMDA receptor signalling: implications for neurodegenerative disorders. Nat Rev Neurosci *11*, 682-696.

Hardingham, G.E., Chawla, S., Cruzalegui, F.H., and Bading, H. (1999). Control of recruitment and transcription-activating function of CBP determines gene regulation by NMDA receptors and L-type calcium channels. Neuron *22*, 789-798.

Hardingham, G.E., Fukunaga, Y., and Bading, H. (2002). Extrasynaptic NMDARs oppose synaptic NMDARs by triggering CREB shut-off and cell death pathways. Nat Neurosci *5*, 405-414.

Harris, A.Z., and Pettit, D.L. (2007). Extrasynaptic and synaptic NMDA receptors form stable and uniform pools in rat hippocampal slices. The Journal of physiology *584*, 509-519.

Hasbani, M.J., Hyrc, K.L., Faddis, B.T., Romano, C., and Goldberg, M.P. (1998). Distinct roles for sodium, chloride, and calcium in excitotoxic dendritic injury and recovery. Exp Neurol *154*, 241-258.

Hasbani, M.J., Schlief, M.L., Fisher, D.A., and Goldberg, M.P. (2001a). Dendritic spines lost during glutamate receptor activation reemerge at original sites of synaptic contact. J Neurosci *21*, 2393-2403.

Hasbani, M.J., Viquez, N.M., and Goldberg, M.P. (2001b). NMDA receptors mediate hypoxic spine loss in cultured neurons. Neuroreport *12*, 2731-2735.

Hayashi, T., Thomas, G.M., and Huganir, R.L. (2009). Dual palmitoylation of NR2 subunits regulates NMDA receptor trafficking. Neuron *64*, 213-226.

Hollmann, M., Boulter, J., Maron, C., Beasley, L., Sullivan, J., Pecht, G., and Heinemann, S. (1993). Zinc potentiates agonist-induced currents at certain splice variants of the NMDA receptor. Neuron *10*, 943-954.

Hoogenraad, C.C., and Bradke, F. (2009). Control of neuronal polarity and plasticity--a renaissance for microtubules? Trends Cell Biol *19*, 669-676.

Hori, N., and Carpenter, D.O. (1994). Functional and morphological changes induced by transient in vivo ischemia. Exp Neurol *129*, 279-289.

Hoskison, M.M., and Shuttleworth, C.W. (2006). Microtubule disruption, not calpain-dependent loss of MAP2, contributes to enduring NMDA-induced dendritic dysfunction in acute hippocampal slices. Experimental neurology *202*, 302-312.

Hossmann, K.A. (1994). Viability thresholds and the penumbra of focal ischemia. Ann Neurol *36*, 557-565.

Iadecola, C. (1997). Bright and dark sides of nitric oxide in ischemic brain injury. Trends in neurosciences *20*, 132-139.

Ikegaya, Y., Kim, J.A., Baba, M., Iwatsubo, T., Nishiyama, N., and Matsuki, N. (2001). Rapid and reversible changes in dendrite morphology and synaptic efficacy following NMDA receptor activation: implication for a cellular defense against excitotoxicity. J Cell Sci *114*, 4083-4093.

Impey, S., Fong, A.L., Wang, Y., Cardinaux, J.R., Fass, D.M., Obrietan, K., Wayman, G.A., Storm, D.R., Soderling, T.R., and Goodman, R.H. (2002). Phosphorylation of CBP mediates transcriptional activation by neural activity and CaM kinase IV. Neuron *34*, 235-244.

Isacsson, A., Kanje, M., and Dahlin, L.B. (2005). Induction of activating transcription factor 3 (ATF3) by peripheral nerve compression. Scand J Plast Reconstr Surg Hand Surg *39*, 65-72.

Jaenisch, N., Witte, O.W., and Frahm, C. (2010). Downregulation of potassium chloride cotransporter KCC2 after transient focal cerebral ischemia. Stroke; a journal of cerebral circulation *41*, e151-159.

Janz, M., Hummel, M., Truss, M., Wollert-Wulf, B., Mathas, S., Johrens, K., Hagemeier, C., Bommert, K., Stein, H., Dorken, B.*, et al.* (2006). Classical Hodgkin lymphoma is characterized by high constitutive expression of activating transcription factor 3 (ATF3), which promotes viability of Hodgkin/Reed-Sternberg cells. Blood *107*, 2536-2539.

Jayakumar, A.R., Panickar, K.S., Curtis, K.M., Tong, X.Y., Moriyama, M., and Norenberg, M.D. (2011). Na-K-Cl cotransporter-1 in the mechanism of cell swelling in cultured astrocytes after fluid percussion injury. J Neurochem *117*, 437-448.

Johnson, J.W., and Ascher, P. (1987). Glycine potentiates the NMDA response in cultured mouse brain neurons. Nature *325*, 529-531.

Jorgensen, M.B., and Diemer, N.H. (1982). Selective neuron loss after cerebral ischemia in the rat: possible role of transmitter glutamate. Acta Neurol Scand *66*, 536-546.

Jourdain, P., Pavillon, N., Moratal, C., Boss, D., Rappaz, B., Depeursinge, C., Marquet, P., and Magistretti, P.J. (2011). Determination of transmembrane water fluxes in neurons elicited by glutamate ionotropic receptors and by the cotransporters KCC2 and NKCC1: a digital holographic microscopy study. The Journal of neuroscience : the official journal of the Society for Neuroscience *31*, 11846-11854.

Kaila, K. (1994). Ionic basis of GABAA receptor channel function in the nervous system. Prog Neurobiol *42*, 489-537.

Katsura, K., Kristian, T., and Siesjo, B.K. (1994). Energy metabolism, ion homeostasis, and cell damage in the brain. Biochemical Society transactions *22*, 991-996.

Kintner, D.B., Chen, X., Currie, J., Chanana, V., Ferrazzano, P., Baba, A., Matsuda, T., Cohen, M., Orlowski, J., Chiu, S.Y.*, et al.* (2010). Excessive Na+/H+ exchange in disruption of dendritic Na+ and Ca2+ homeostasis and mitochondrial dysfunction following in vitro ischemia. J Biol Chem *285*, 35155-35168.

Kirino, T. (1982). Delayed neuronal death in the gerbil hippocampus following ischemia. Brain Res *239*, 57-69.

Kirino, T., Tamura, A., and Sano, K. (1984). Delayed neuronal death in the rat hippocampus following transient forebrain ischemia. Acta Neuropathol *64*, 139-147.

Kiryu-Seo, S., Ohno, N., Kidd, G.J., Komuro, H., and Trapp, B.D. (2010). Demyelination increases axonal stationary mitochondrial size and the speed of axonal mitochondrial transport. The Journal of neuroscience : the official journal of the Society for Neuroscience *30*, 6658-6666.

Klatzo, I. (1994). Evolution of brain edema concepts. Acta Neurochir Suppl (Wien) *60*, 3-6.

Kleckner, N.W., and Dingledine, R. (1988). Requirement for glycine in activation of NMDA-receptors expressed in Xenopus oocytes. Science *241*, 835-837.

Klugmann, M., Symes, C.W., Leichtlein, C.B., Klaussner, B.K., Dunning, J., Fong, D., Young, D., and During, M.J. (2005). AAV-mediated hippocampal expression of short and long Homer 1 proteins differentially affect cognition and seizure activity in adult rats. Mol Cell Neurosci *28*, 347-360.

Kohr, G. (2006). NMDA receptor function: subunit composition versus spatial distribution. Cell Tissue Res *326*, 439-446.

Kristensen, B.W., Noraberg, J., and Zimmer, J. (2001). Comparison of excitotoxic profiles of ATPA, AMPA, KA and NMDA in organotypic hippocampal slice cultures. Brain research *917*, 21-44.

Kristian, T., and Siesjo, B.K. (1998). Calcium in ischemic cell death. Stroke; a journal of cerebral circulation *29*, 705-718.

Kuribayashi, Y., Horikawa, N., Itoh, N., Kitano, M., and Ohashi, N. (1999a). Delayed treatment of Na+/H+ exchange inhibitor SM-20220 reduces infarct size in both transient and permanent middle cerebral artery occlusion in rats. Int J Tissue React *21*, 29-33.

Kuribayashi, Y., Itoh, N., Kitano, M., and Ohashi, N. (1999b). Cerebroprotective properties of SM-20220, a potent Na(+)/H(+) exchange inhibitor, in transient cerebral ischemia in rats. Eur J Pharmacol *383*, 163-168.

Laake, J.H., Haug, F.M., Wieloch, T., and Ottersen, O.P. (1999). A simple in vitro model of ischemia based on hippocampal slice cultures and propidium iodide fluorescence. Brain Res Brain Res Protoc *4*, 173-184.

Lau, D., and Bading, H. (2009a). Synaptic activity-mediated suppression of p53 and induction of nuclear calcium-regulated neuroprotective genes promote survival through inhibition of mitochondrial permeability transition. J Neurosci *29*, 4420-4429.

Lau, D., and Bading, H. (2009b). Synaptic activity-mediated suppression of p53 and induction of nuclear calcium-regulated neuroprotective genes promote survival through inhibition of mitochondrial permeability transition. The Journal of neuroscience : the official journal of the Society for Neuroscience *29*, 4420-4429.

Leveille, F., El Gaamouch, F., Gouix, E., Lecocq, M., Lobner, D., Nicole, O., and Buisson, A. (2008). Neuronal viability is controlled by a functional relation between synaptic and extrasynaptic NMDA receptors. Faseb J *22*, 4258-4271.

Li, B., Chen, N., Luo, T., Otsu, Y., Murphy, T.H., and Raymond, L.A. (2002). Differential regulation of synaptic and extra-synaptic NMDA receptors. Nat Neurosci *5*, 833-834.

Li, P., and Murphy, T.H. (2008). Two-photon imaging during prolonged middle cerebral artery occlusion in mice reveals recovery of dendritic structure after reperfusion. J Neurosci *28*, 11970-11979.

Liang, G., Wolfgang, C.D., Chen, B.P., Chen, T.H., and Hai, T. (1996). ATF3 gene. Genomic organization, promoter, and regulation. J Biol Chem *271*, 1695-1701.

Lin, Y.S., and Green, M.R. (1988). Interaction of a common cellular transcription factor, ATF, with regulatory elements in both E1a- and cyclic AMP-inducible promoters. Proc Natl Acad Sci U S A *85*, 3396-3400.

Lipski, J., Park, T.I., Li, D., Lee, S.C., Trevarton, A.J., Chung, K.K., Freestone, P.S., and Bai, J.Z. (2006). Involvement of TRP-like channels in the acute ischemic response of hippocampal CA1 neurons in brain slices. Brain research *1077*, 187-199.

Lipton, S.A., and Rosenberg, P.A. (1994). Excitatory amino acids as a final common pathway for neurologic disorders. N Engl J Med *330*, 613-622.

Liu, Y., Wong, T.P., Aarts, M., Rooyakkers, A., Liu, L., Lai, T.W., Wu, D.C., Lu, J., Tymianski, M., Craig, A.M.*, et al.* (2007). NMDA receptor subunits have differential roles in mediating excitotoxic neuronal death both in vitro and in vivo. The Journal of neuroscience : the official journal of the Society for Neuroscience *27*, 2846-2857.

Lucas, D.R., and Newhouse, J.P. (1957). The toxic effect of sodium L-glutamate on the inner layers of the retina. AMA Arch Ophthalmol *58*, 193-201.

Luo, J., Chen, H., Kintner, D.B., Shull, G.E., and Sun, D. (2005). Decreased neuronal death in Na+/H+ exchanger isoform 1-null mice after in vitro and in vivo ischemia. The Journal of neuroscience : the official journal of the Society for Neuroscience *25*, 11256-11268.

Luo, J., and Sun, D. (2007). Physiology and pathophysiology of Na(+)/H(+) exchange isoform 1 in the central nervous system. Curr Neurovasc Res *4*, 205-215.

Luo, J., Wang, Y., Yasuda, R.P., Dunah, A.W., and Wolfe, B.B. (1997). The majority of N-methyl-D-aspartate receptor complexes in adult rat cerebral cortex contain at least three different subunits (NR1/NR2A/NR2B). Mol Pharmacol *51*, 79-86.

Macaskill, A.F., Rinholm, J.E., Twelvetrees, A.E., Arancibia-Carcamo, I.L., Muir, J., Fransson, A., Aspenstrom, P., Attwell, D., and Kittler, J.T. (2009). Miro1 is a calcium sensor for glutamate receptor-dependent localization of mitochondria at synapses. Neuron *61*, 541-555.

MacAulay, N., and Zeuthen, T. (2010). Water transport between CNS compartments: contributions of aquaporins and cotransporters. Neuroscience *168*, 941-956.

Malenka, R.C., and Nicoll, R.A. (1999). Long-term potentiation--a decade of progress? Science *285*, 1870-1874.

Martel, M.A., Wyllie, D.J., and Hardingham, G.E. (2009). In developing hippocampal neurons, NR2B-containing N-methyl-D-aspartate receptors (NMDARs) can mediate signaling to neuronal survival and synaptic potentiation, as well as neuronal death. Neuroscience *158*, 334-343.

Martinez-Sanchez, M., Striggow, F., Schroder, U.H., Kahlert, S., Reymann, K.G., and Reiser, G. (2004). Na(+) and Ca(2+) homeostasis pathways, cell death and protection after oxygen-glucose-deprivation in organotypic hippocampal slice cultures. Neuroscience *128*, 729-740.

Matesic, D.F., and Lin, R.C. (1994). Microtubule-associated protein 2 as an early indicator of ischemia-induced neurodegeneration in the gerbil forebrain. J Neurochem *63*, 1012-1020.

Matthews, R.P., Guthrie, C.R., Wailes, L.M., Zhao, X., Means, A.R., and McKnight, G.S. (1994). Calcium/calmodulin-dependent protein kinase types II and IV differentially regulate CREB-dependent gene expression. Mol Cell Biol *14*, 6107-6116.

Mayumi-Matsuda, K., Kojima, S., Nakayama, T., Suzuki, H., and Sakata, T. (1999). Scanning gene expression during neuronal cell death evoked by nerve growth factor depletion. Biochim Biophys Acta *1489*, 293-302.

Meldrum, B., Evans, M., Griffiths, T., and Simon, R. (1985). Ischaemic brain damage: the role of excitatory activity and of calcium entry. Br J Anaesth *57*, 44-46.

Monyer, H., Burnashev, N., Laurie, D.J., Sakmann, B., and Seeburg, P.H. (1994). Developmental and regional expression in the rat brain and functional properties of four NMDA receptors. Neuron *12*, 529-540.

Moriyoshi, K., Masu, M., Ishii, T., Shigemoto, R., Mizuno, N., and Nakanishi, S. (1991). Molecular cloning and characterization of the rat NMDA receptor. Nature *354*, 31-37.

Murphy, T.H., Li, P., Betts, K., and Liu, R. (2008). Two-photon imaging of stroke onset in vivo reveals that NMDA-receptor independent ischemic depolarization is the major cause of rapid reversible damage to dendrites and spines. J Neurosci *28*, 1756-1772.

Mutel, V., Buchy, D., Klingelschmidt, A., Messer, J., Bleuel, Z., Kemp, J.A., and Richards, J.G. (1998). In vitro binding properties in rat brain of [3H]Ro 25-6981, a potent and selective antagonist of NMDA receptors containing NR2B subunits. J Neurochem *70*, 2147-2155.

Nakagomi, S., Suzuki, Y., Namikawa, K., Kiryu-Seo, S., and Kiyama, H. (2003). Expression of the activating transcription factor 3 prevents c-Jun N-terminal kinase-induced neuronal death by promoting heat shock protein 27 expression and Akt activation. The Journal of neuroscience : the official journal of the Society for Neuroscience *23*, 5187-5196.

Nedergaard, M., Kraig, R.P., Tanabe, J., and Pulsinelli, W.A. (1991). Dynamics of interstitial and intracellular pH in evolving brain infarct. Am J Physiol *260*, R581-588.

Newell, D.W., Barth, A., Papermaster, V., and Malouf, A.T. (1995). Glutamate and non-glutamate receptor mediated toxicity caused by oxygen and glucose deprivation in organotypic hippocampal cultures. J Neurosci *15*, 7702-7711.

Nielsen, S., Nagelhus, E.A., Amiry-Moghaddam, M., Bourque, C., Agre, P., and Ottersen, O.P. (1997). Specialized membrane domains for water transport in glial cells: high-resolution immunogold cytochemistry of aquaporin-4 in rat brain. J Neurosci *17*, 171-180.

Noraberg, J. (2004). Organotypic brain slice cultures: an efficient and reliable method for neurotoxicological screening and mechanistic studies. Altern Lab Anim *32*, 329-337.

Noraberg, J., Kristensen, B.W., and Zimmer, J. (1999). Markers for neuronal degeneration in organotypic slice cultures. Brain Res Brain Res Protoc *3*, 278-290.

Nowak, L., Bregestovski, P., Ascher, P., Herbet, A., and Prochiantz, A. (1984). Magnesium gates glutamate-activated channels in mouse central neurones. Nature *307*, 462-465.

Ohba, N., Maeda, M., Nakagomi, S., Muraoka, M., and Kiyama, H. (2003). Biphasic expression of activating transcription factor-3 in neurons after cerebral infarction. Brain Res Mol Brain Res *115*, 147-156.

Olney, J.W. (1969). Brain lesions, obesity, and other disturbances in mice treated with monosodium glutamate. Science *164*, 719-721.

Olney, J.W., Fuller, T., and de Gubareff, T. (1979). Acute dendrotoxic changes in the hippocampus of kainate treated rats. Brain Res *176*, 91-100.

Olney, J.W., Price, M.T., Samson, L., and Labruyere, J. (1986). The role of specific ions in glutamate neurotoxicity. Neuroscience letters *65*, 65-71.

Paoletti, P. (2011). Molecular basis of NMDA receptor functional diversity. Eur J Neurosci *33*, 1351-1365.

Papadia, S., Soriano, F.X., Leveille, F., Martel, M.A., Dakin, K.A., Hansen, H.H., Kaindl, A., Sifringer, M., Fowler, J., Stefovska, V.*, et al.* (2008). Synaptic NMDA receptor activity boosts intrinsic antioxidant defenses. Nat Neurosci *11*, 476-487.

Papadia, S., Stevenson, P., Hardingham, N.R., Bading, H., and Hardingham, G.E. (2005). Nuclear Ca2+ and the cAMP response element-binding protein family mediate a late phase of activity-dependent neuroprotection. J Neurosci *25*, 4279-4287.

Papp, E., Rivera, C., Kaila, K., and Freund, T.F. (2008). Relationship between neuronal vulnerability and potassium-chloride cotransporter 2 immunoreactivity in hippocampus following transient forebrain ischemia. Neuroscience *154*, 677-689.

Park, J.S., Bateman, M.C., and Goldberg, M.P. (1996). Rapid alterations in dendrite morphology during sublethal hypoxia or glutamate receptor activation. Neurobiol Dis *3*, 215-227.

Payne, J.A., Rivera, C., Voipio, J., and Kaila, K. (2003). Cation-chloride co-transporters in neuronal communication, development and trauma. Trends Neurosci *26*, 199-206.

Pedersen, S.F., Owsianik, G., and Nilius, B. (2005). TRP channels: an overview. Cell Calcium *38*, 233-252.

Pekny, M., and Nilsson, M. (2005). Astrocyte activation and reactive gliosis. Glia *50*, 427-434.

Pelzer, A.E., Bektic, J., Haag, P., Berger, A.P., Pycha, A., Schafer, G., Rogatsch, H., Horninger, W., Bartsch, G., and Klocker, H. (2006). The expression of transcription factor activating transcription factor 3 in the human prostate and its regulation by androgen in prostate cancer. J Urol *175*, 1517-1522.

Petito, C.K., and Pulsinelli, W.A. (1984). Delayed neuronal recovery and neuronal death in rat hippocampus following severe cerebral ischemia: possible relationship to abnormalities in neuronal processes. Journal of cerebral blood flow and metabolism :

official journal of the International Society of Cerebral Blood Flow and Metabolism *4*, 194-205.

Petralia, R.S., Wang, Y.X., Hua, F., Yi, Z., Zhou, A., Ge, L., Stephenson, F.A., and Wenthold, R.J. (2010). Organization of NMDA receptors at extrasynaptic locations. Neuroscience *167*, 68-87.

Phillis, J.W., Estevez, A.Y., Guyot, L.L., and O'Regan, M.H. (1999). 5-(N-Ethyl-N-isopropyl)-amiloride, an Na(+)-H(+) exchange inhibitor, protects gerbil hippocampal neurons from ischemic injury. Brain research *839*, 199-202.

Pivovarova, N.B., and Andrews, S.B. (2010). Calcium-dependent mitochondrial function and dysfunction in neurons. Febs J *277*, 3622-3636.

Pond, B.B., Berglund, K., Kuner, T., Feng, G., Augustine, G.J., and Schwartz-Bloom, R.D. (2006). The chloride transporter Na(+)-K(+)-Cl- cotransporter isoform-1 contributes to intracellular chloride increases after in vitro ischemia. The Journal of neuroscience : the official journal of the Society for Neuroscience *26*, 1396-1406.

Rauner, C., and Kohr, G. (2011). Triheteromeric NR1/NR2A/NR2B receptors constitute the major N-methyl-D-aspartate receptor population in adult hippocampal synapses. J Biol Chem *286*, 7558-7566.

Reynolds, E.S. (1963). The use of lead citrate at high pH as an electron-opaque stain in electron microscopy. J Cell Biol *17*, 208-212.

Rintoul, G.L., Filiano, A.J., Brocard, J.B., Kress, G.J., and Reynolds, I.J. (2003). Glutamate decreases mitochondrial size and movement in primary forebrain neurons. J Neurosci *23*, 7881-7888.

Risher, W.C., Andrew, R.D., and Kirov, S.A. (2009). Real-time passive volume responses of astrocytes to acute osmotic and ischemic stress in cortical slices and in vivo revealed by two-photon microscopy. Glia *57*, 207-221.

Rossi, D.J., Oshima, T., and Attwell, D. (2000). Glutamate release in severe brain ischaemia is mainly by reversed uptake. Nature *403*, 316-321.

Rothman, S.M. (1985). The neurotoxicity of excitatory amino acids is produced by passive chloride influx. The Journal of neuroscience : the official journal of the Society for Neuroscience *5*, 1483-1489.

Runden, E., Seglen, P.O., Haug, F.M., Ottersen, O.P., Wieloch, T., Shamloo, M., and Laake, J.H. (1998). Regional selective neuronal degeneration after protein phosphatase inhibition in hippocampal slice cultures: evidence for a MAP kinase-dependent mechanism. J Neurosci *18*, 7296-7305.

Runden-Pran, E., Tanso, R., Haug, F.M., Ottersen, O.P., and Ring, A. (2005). Neuroprotective effects of inhibiting N-methyl-D-aspartate receptors, P2X receptors and the mitogen-activated protein kinase cascade: a quantitative analysis in organotypical hippocampal slice cultures subjected to oxygen and glucose deprivation. Neuroscience *136*, 795-810.

Russell, J.M. (2000). Sodium-potassium-chloride cotransport. Physiol Rev *80*, 211-276.

Rytter, A., Cronberg, T., Asztely, F., Nemali, S., and Wieloch, T. (2003). Mouse hippocampal organotypic tissue cultures exposed to in vitro "ischemia" show selective and delayed CA1 damage that is aggravated by glucose. J Cereb Blood Flow Metab *23*, 23-33.

Sakimura, K., Kutsuwada, T., Ito, I., Manabe, T., Takayama, C., Kushiya, E., Yagi, T., Aizawa, S., Inoue, Y., Sugiyama, H.*, et al.* (1995). Reduced hippocampal LTP and spatial learning in mice lacking NMDA receptor epsilon 1 subunit. Nature *373*, 151-155.

Sattler, R., Charlton, M.P., Hafner, M., and Tymianski, M. (1998). Distinct influx pathways, not calcium load, determine neuronal vulnerability to calcium neurotoxicity. J Neurochem *71*, 2349-2364.

Sattler, R., Xiong, Z., Lu, W.Y., MacDonald, J.F., and Tymianski, M. (2000). Distinct roles of synaptic and extrasynaptic NMDA receptors in excitotoxicity. The Journal of neuroscience : the official journal of the Society for Neuroscience *20*, 22-33.

Schliwa, M., Euteneuer, U., Bulinski, J.C., and Izant, J.G. (1981). Calcium lability of cytoplasmic microtubules and its modulation by microtubule-associated proteins. Proc Natl Acad Sci U S A *78*, 1037-1041.

Schmidt-Kastner, R., and Freund, T.F. (1991). Selective vulnerability of the hippocampus in brain ischemia. Neuroscience *40*, 599-636.

Seijffers, R., Allchorne, A.J., and Woolf, C.J. (2006). The transcription factor ATF-3 promotes neurite outgrowth. Mol Cell Neurosci *32*, 143-154.

Seijffers, R., Mills, C.D., and Woolf, C.J. (2007). ATF3 increases the intrinsic growth state of DRG neurons to enhance peripheral nerve regeneration. The Journal of neuroscience : the official journal of the Society for Neuroscience *27*, 7911-7920.

Sheldon, C., Diarra, A., Cheng, Y.M., and Church, J. (2004). Sodium influx pathways during and after anoxia in rat hippocampal neurons. The Journal of neuroscience : the official journal of the Society for Neuroscience *24*, 11057-11069.

Sheng, M., Cummings, J., Roldan, L.A., Jan, Y.N., and Jan, L.Y. (1994). Changing subunit composition of heteromeric NMDA receptors during development of rat cortex. Nature *368*, 144-147.

Sigler, A., and Murphy, T.H. (2010). In vivo 2-photon imaging of fine structure in the rodent brain: before, during, and after stroke. Stroke *41*, S117-123.

Silver, I.A., and Erecinska, M. (1992). Ion homeostasis in rat brain in vivo: intra- and extracellular [Ca2+] and [H+] in the hippocampus during recovery from short-term, transient ischemia. J Cereb Blood Flow Metab *12*, 759-772.

Siman, R., Noszek, J.C., and Kegerise, C. (1989). Calpain I activation is specifically related to excitatory amino acid induction of hippocampal damage. The Journal of neuroscience : the official journal of the Society for Neuroscience *9*, 1579-1590.

Simard, J.M., Kent, T.A., Chen, M., Tarasov, K.V., and Gerzanich, V. (2007). Brain oedema in focal ischaemia: molecular pathophysiology and theoretical implications. Lancet Neurol *6*, 258-268.

Sinor, J.D., Du, S., Venneti, S., Blitzblau, R.C., Leszkiewicz, D.N., Rosenberg, P.A., and Aizenman, E. (2000). NMDA and glutamate evoke excitotoxicity at distinct cellular locations in rat cortical neurons in vitro. The Journal of neuroscience : the official journal of the Society for Neuroscience *20*, 8831-8837.

Somjen, G.G., Faas, G.C., Vreugdenhil, M., and Wadman, W.J. (1993). Channel shutdown: a response of hippocampal neurons to adverse environments. Brain research *632*, 180-194.

Song, D.Y., Oh, K.M., Yu, H.N., Park, C.R., Woo, R.S., Jung, S.S., and Baik, T.K. (2011). Role of activating transcription factor 3 in ischemic penumbra region following transient middle cerebral artery occlusion and reperfusion injury. Neurosci Res *70*, 428-434.

Soriano, F.X., Papadia, S., Hofmann, F., Hardingham, N.R., Bading, H., and Hardingham, G.E. (2006). Preconditioning doses of NMDA promote neuroprotection by enhancing neuronal excitability. J Neurosci *26*, 4509-4518.

Stanika, R.I., Pivovarova, N.B., Brantner, C.A., Watts, C.A., Winters, C.A., and Andrews, S.B. (2009). Coupling diverse routes of calcium entry to mitochondrial dysfunction and glutamate excitotoxicity. Proc Natl Acad Sci U S A *106*, 9854-9859.

Stanika, R.I., Winters, C.A., Pivovarova, N.B., and Andrews, S.B. (2010). Differential NMDA receptor-dependent calcium loading and mitochondrial dysfunction in CA1 vs. CA3 hippocampal neurons. Neurobiology of disease *37*, 403-411.

Stern, P., Behe, P., Schoepfer, R., and Colquhoun, D. (1992). Single-channel conductances of NMDA receptors expressed from cloned cDNAs: comparison with native receptors. Proc Biol Sci *250*, 271-277.

Stoppini, L., Buchs, P.A., and Muller, D. (1991). A simple method for organotypic cultures of nervous tissue. J Neurosci Methods *37*, 173-182.

Stout, A.K., Raphael, H.M., Kanterewicz, B.I., Klann, E., and Reynolds, I.J. (1998). Glutamate-induced neuron death requires mitochondrial calcium uptake. Nat Neurosci *1*, 366-373.

Strbian, D., Durukan, A., Pitkonen, M., Marinkovic, I., Tatlisumak, E., Pedrono, E., Abo-Ramadan, U., and Tatlisumak, T. (2008). The blood-brain barrier is continuously open for several weeks following transient focal cerebral ischemia. Neuroscience *153*, 175-181.

Suganami, T., Yuan, X., Shimoda, Y., Uchio-Yamada, K., Nakagawa, N., Shirakawa, I., Usami, T., Tsukahara, T., Nakayama, K., Miyamoto, Y*., et al.* (2009). Activating transcription factor 3 constitutes a negative feedback mechanism that attenuates saturated Fatty acid/toll-like receptor 4 signaling and macrophage activation in obese adipose tissue. Circ Res *105*, 25-32.

Sugihara, H., Moriyoshi, K., Ishii, T., Masu, M., and Nakanishi, S. (1992). Structures and properties of seven isoforms of the NMDA receptor generated by alternative splicing. Biochem Biophys Res Commun *185*, 826-832.

Sun, H.S., Jackson, M.F., Martin, L.J., Jansen, K., Teves, L., Cui, H., Kiyonaka, S., Mori, Y., Jones, M., Forder, J.P*., et al.* (2009). Suppression of hippocampal TRPM7 protein prevents delayed neuronal death in brain ischemia. Nat Neurosci *12*, 1300-1307.

Szydlowska, K., and Tymianski, M. (2010). Calcium, ischemia and excitotoxicity. Cell Calcium *47*, 122-129.

Takeda, M., Kato, H., Takamiya, A., Yoshida, A., and Kiyama, H. (2000). Injury-specific expression of activating transcription factor-3 in retinal ganglion cells and its colocalized expression with phosphorylated c-Jun. Invest Ophthalmol Vis Sci *41*, 2412-2421.

Tang, C.M., Dichter, M., and Morad, M. (1990). Modulation of the N-methyl-D-aspartate channel by extracellular H+. Proc Natl Acad Sci U S A *87*, 6445-6449.

Tauskela, J.S., Comas, T., Hewitt, K., Monette, R., Paris, J., Hogan, M., and Morley, P. (2001). Cross-tolerance to otherwise lethal N-methyl-D-aspartate and oxygen-glucose deprivation in preconditioned cortical cultures. Neuroscience *107*, 571-584.

Thomas, C.G., Miller, A.J., and Westbrook, G.L. (2006). Synaptic and extrasynaptic NMDA receptor NR2 subunits in cultured hippocampal neurons. J Neurophysiol *95*, 1727-1734.

Thompson, M.R., Xu, D., and Williams, B.R. (2009). ATF3 transcription factor and its emerging roles in immunity and cancer. J Mol Med *87*, 1053-1060.

Tovar, K.R., and Westbrook, G.L. (1999). The incorporation of NMDA receptors with a distinct subunit composition at nascent hippocampal synapses in vitro. The Journal of neuroscience : the official journal of the Society for Neuroscience *19*, 4180-4188.

Traynelis, S.F., Wollmuth, L.P., McBain, C.J., Menniti, F.S., Vance, K.M., Ogden, K.K., Hansen, K.B., Yuan, H., Myers, S.J., and Dingledine, R. (2010). Glutamate receptor ion channels: structure, regulation, and function. Pharmacol Rev *62*, 405-496.

Tsujino, H., Kondo, E., Fukuoka, T., Dai, Y., Tokunaga, A., Miki, K., Yonenobu, K., Ochi, T., and Noguchi, K. (2000). Activating transcription factor 3 (ATF3) induction by

axotomy in sensory and motoneurons: A novel neuronal marker of nerve injury. Mol Cell Neurosci *15*, 170-182.

Ulbrich, M.H., and Isacoff, E.Y. (2008). Rules of engagement for NMDA receptor subunits. Proc Natl Acad Sci U S A *105*, 14163-14168.

Vander Jagt, T.A., Connor, J.A., and Shuttleworth, C.W. (2008). Localized loss of Ca2+ homeostasis in neuronal dendrites is a downstream consequence of metabolic compromise during extended NMDA exposures. J Neurosci *28*, 5029-5039.

von Engelhardt, J., Doganci, B., Jensen, V., Hvalby, O., Gongrich, C., Taylor, A., Barkus, C., Sanderson, D.J., Rawlins, J.N., Seeburg, P.H., *et al.* (2008). Contribution of hippocampal and extra-hippocampal NR2B-containing NMDA receptors to performance on spatial learning tasks. Neuron *60*, 846-860.

von Lubitz, D.K., and Diemer, N.H. (1983). Cerebral ischemia in the rat: ultrastructural and morphometric analysis of synapses in stratum radiatum of the hippocampal CA-1 region. Acta Neuropathol *61*, 52-60.

Wake, H., Watanabe, M., Moorhouse, A.J., Kanematsu, T., Horibe, S., Matsukawa, N., Asai, K., Ojika, K., Hirata, M., and Nabekura, J. (2007). Early changes in KCC2 phosphorylation in response to neuronal stress result in functional downregulation. The Journal of neuroscience : the official journal of the Society for Neuroscience *27*, 1642-1650.

Wang, J., Campos, B., Jamieson, G.A., Jr., Kaetzel, M.A., and Dedman, J.R. (1995). Functional elimination of calmodulin within the nucleus by targeted expression of an inhibitor peptide. J Biol Chem *270*, 30245-30248.

Watanabe, M., Inoue, Y., Sakimura, K., and Mishina, M. (1992). Developmental changes in distribution of NMDA receptor channel subunit mRNAs. Neuroreport *3*, 1138-1140.

Wolfgang, C.D., Chen, B.P., Martindale, J.L., Holbrook, N.J., and Hai, T. (1997). gadd153/Chop10, a potential target gene of the transcriptional repressor ATF3. Mol Cell Biol *17*, 6700-6707.

Wolfgang, C.D., Liang, G., Okamoto, Y., Allen, A.E., and Hai, T. (2000). Transcriptional autorepression of the stress-inducible gene ATF3. J Biol Chem *275*, 16865-16870.

Wu, G.Y., Deisseroth, K., and Tsien, R.W. (2001). Activity-dependent CREB phosphorylation: convergence of a fast, sensitive calmodulin kinase pathway and a slow, less sensitive mitogen-activated protein kinase pathway. Proc Natl Acad Sci U S A *98*, 2808-2813.

Xing, J., Ginty, D.D., and Greenberg, M.E. (1996). Coupling of the RAS-MAPK pathway to gene activation by RSK2, a growth factor-regulated CREB kinase. Science *273*, 959-963.

Yan, Y., Dempsey, R.J., Flemmer, A., Forbush, B., and Sun, D. (2003). Inhibition of Na(+)-K(+)-Cl(-) cotransporter during focal cerebral ischemia decreases edema and neuronal damage. Brain research *961*, 22-31.

Yao, H., Gu, X.Q., Douglas, R.M., and Haddad, G.G. (2001). Role of Na(+)/H(+) exchanger during O(2) deprivation in mouse CA1 neurons. Am J Physiol Cell Physiol *281*, C1205-1210.

Yao, H., Ma, E., Gu, X.Q., and Haddad, G.G. (1999). Intracellular pH regulation of CA1 neurons in Na(+)/H(+) isoform 1 mutant mice. J Clin Invest *104*, 637-645.

Yin, X., Dewille, J.W., and Hai, T. (2008). A potential dichotomous role of ATF3, an adaptive-response gene, in cancer development. Oncogene *27*, 2118-2127.

Zeuthen, T. (1994). Cotransport of K+, Cl- and H2O by membrane proteins from choroid plexus epithelium of Necturus maculosus. The Journal of physiology *478 (Pt 2)*, 203-219.

Zhang, S., Boyd, J., Delaney, K., and Murphy, T.H. (2005). Rapid reversible changes in dendritic spine structure in vivo gated by the degree of ischemia. J Neurosci *25*, 5333-5338.

Zhang, S.J., Buchthal, B., Lau, D., Hayer, S., Dick, O., Schwaninger, M., Veltkamp, R., Zou, M., Weiss, U., and Bading, H. (2011). A Signaling Cascade of Nuclear Calcium-CREB-ATF3 Activated by Synaptic NMDA Receptors Defines a Gene Repression Module That Protects against Extrasynaptic NMDA Receptor-Induced Neuronal Cell Death and Ischemic Brain Damage. The Journal of neuroscience : the official journal of the Society for Neuroscience *31*, 4978-4990.

Zhang, S.J., Steijaert, M.N., Lau, D., Schutz, G., Delucinge-Vivier, C., Descombes, P., and Bading, H. (2007). Decoding NMDA receptor signaling: identification of genomic programs specifying neuronal survival and death. Neuron *53*, 549-562.

Zhang, S.J., Zou, M., Lu, L., Lau, D., Ditzel, D.A., Delucinge-Vivier, C., Aso, Y., Descombes, P., and Bading, H. (2009). Nuclear calcium signaling controls expression of a large gene pool: identification of a gene program for acquired neuroprotection induced by synaptic activity. PLoS Genet *5*, e1000604.

Zhou, M., and Baudry, M. (2006). Developmental changes in NMDA neurotoxicity reflect developmental changes in subunit composition of NMDA receptors. The Journal of neuroscience : the official journal of the Society for Neuroscience *26*, 2956-2963.

Zimmer, J., and Gahwiler, B.H. (1984). Cellular and connective organization of slice cultures of the rat hippocampus and fascia dentata. J Comp Neurol *228*, 432-446.